Diffusion Kurtosis Imaging of Persistent Developmental Stuttering

by

Ehsan Misaghi

A thesis submitted in partial fulfillment of the requirements for the degree of

Master of Science

Centre for Neuroscience
University of Alberta

Abstract

Stuttering is a developmental speech disorder characterized by prolongations and/or repetitions of speech sounds as well as silent blocks during speech production. It affects about 5% of children and 1% of the general population. Growing evidence shows that white matter connections of the brain show deficiencies in people who stutter. Examples of those connections include the arcuate fasciculus, the frontal aslant tract, the corpus callosum and the corticospinal tract. A widely used method to assess the white matter in vivo is diffusion magnetic resonance imaging. Tractography methods based on Diffusion Tensor Imaging (DTI) are able to isolate the white matter connections of the brain. However, DTI has some limitations. For instance, it is based on the assumption that the diffusion pattern follows a Gaussian distribution, while studies have shown that in specific circumstances, e.g. in complex cell compartments, diffusion can deviate from the Gaussian distribution. Kurtosis metrics are able to quantify this deviation and Diffusion Kurtosis Imaging (DKI) gives us the ability to extract the said metrics. Thus, DKI was used in this study to assess the white matter connections of the brain in a group of adults who stutter and a group of age-, sex-, handedness- and education level-matched controls. Using tractography, I delineated the corpus callosum, arcuate fasciculus, frontal aslant tract and corticospinal tract. The results of this study showed that adults who stutter have higher axial kurtosis in the left frontal aslant tract in comparison to controls and to their right frontal aslant tract. Furthermore, radial kurtosis in the right frontal aslant tract of adults who stutter was negatively correlated with the impact of stuttering on their daily lives. Based on these results, it is suggested that the deficits in the frontal aslant tract are associated with the dysfluency encountered in stuttering.

Preface

This thesis is an original work by Ehsan Misaghi. The research project, of which this thesis is a part, received research ethics approval from the University of Alberta Research Ethics Board, Project Name “Magnetic resonance imaging of the neural network for speech production in adults who stutter”, No. 47990, February, 5, 2015 (Renewed February 11, 2016).

"The human brain, then, is the most complicated organization of matter that we know."

Isaac Asimov

To my beloved parents

And to all the people who share my passion of making this world a better place…

Acknowledgements

I would like to express my sincerest gratitude to my supervisors Dr. Deryk S. Beal and Dr. Jacqueline Cummine for their support, constant guidance, encouragements and helpful advice during the course of my studies and research as a graduate student at the University of Alberta. I'm grateful to have worked under their supervision and I hope that this period was the beginning of a great collaboration that will continue for years to come. I also would like to thank my co-supervisor, Dr. Christian Beaulieu for his help and guidance in the course of this project. I also thank Dr. Donald W. Gross and members of his lab, who taught me so many skills upon my entrance to a field that was almost new to me.

So many people helped me figure things out during this project. Although it won't be possible to thank all of them, I will try my best to acknowledge their help. I appreciate the efforts of Mr. Peter Seres, our kind MRI technician, who helped collect the imaging data needed for this project and even put up with our bad timing issues! I am thankful to my labmates, Sara Laughton and Grace Lee, who helped with both the recruitment of the participants and the collection of the data. I also would like to thank all of the participants that volunteered for this project and helped us reach another finding in our endeavor for a better understanding of the world we live in: our brain!

And last but not least, I want to thank my family, who live almost 10,000 km far from where I'm writing these lines, and my friends, for their constant support. The fact that they were there for me anytime I needed help or a break from sitting in front a computer either writing something (in English or a language computers understand) or drawing green, blue or red colored shapes on people's brain images, was the reason I could manage to do this study and write this document! Special thanks goes to my great friend, soon-to-be-Dr. Farshad Niri, who shared my stress on writing a thesis, while he was writing his own.

Table of Contents

List of Tables

List of Figures

Abbreviations

AWS	Adults Who Stutter
CWS	Children Who Stutter
PWS	People Who Stutter
MRI	Magnetic Resonance Imaging
DTI	Diffusion Tensor Imaging
DKI	Diffusion Kurtosis Imaging
FA	Fractional Anisotropy
MD	Mean Diffusivity
AD	Axial Diffusivity
RD	Radial Diffusivity
MK	Mean Kurtosis
AK	Axial Kurtosis
RK	Radial Kurtosis
BA	Brodmann's Area
FAT	Frontal Aslant Tract
CST	Corticospinal Tract
DIVA	Directions in sensory space Into Velocities of Articulators

1 Introduction

1.1 Speech motor control and the neural correlates of developmental stuttering: A review

Speech is one of the most important and complex activities carried out by humans and sometimes even taken as the line distinguishing humans from other animals. Up to 100 muscles cooperate for speech to be produced and the brain has to control the signals that give rise to these movements (Ackermann & Riecker, 2004; Simonyan & Horwitz, 2011).

In this thesis, I will take the view that development stuttering is primarily a disorder of speech motor control (Ludlow & Loucks, 2003), however it is important to note that linguistic factors have been implicated in the disorder (Ratner, 1995). Section 1.1 will consist of a collective review of the previous findings on the neural correlates of speech motor control and developmental stuttering and section 1.2 will entail information about diffusion imaging as a tool to investigate the connections of the neural network for speech in the brain. I will focus on diffusion kurtosis imaging, which is a newly developed method in diffusion imaging that is proposed to give more information about the structural integrity of the white matter connections in the brain (Jensen, Helpern, Ramani, Lu, & Kaczynski, 2005) and it is the method of choice for this project.

Early studies of speech in the brain were long limited to lesion studies. With the advent of neuroimaging methods and the application of different models, we now have more (advanced) tools available to us in order to investigate the neural correlates of speech and the deficits associated with speech disorders (Borovsky, Saygin, Bates, & Dronkers, 2007; Muller & Knight, 2006; Rorden & Karnath, 2004).

A widely-accepted model of speech motor control in humans is the DIVA model. This model has been proposed by Guenther and colleagues (Guenther, 1995, 2006; Guenther, Ghosh, & Tourville, 2006). The following section describes this model.

1.1.1 The DIVA Model

The DIVA (**D**irections in sensory space **I**nto **V**elocities of **A**rticulators) model is a speech motor control model developed by Guenther and colleagues (Guenther, 1995). Studies investigating its correlation with the neuroimaging data obtained thus far, have given

us an initial sketch of a network of interconnected areas that control the production of speech sounds (Bohland & Guenther, 2006; Guenther, 1995, 2006; Guenther et al., 2006; Guenther, Hampson, & Johnson, 1998). Figure 1.1 shows a diagram of the model and its components.

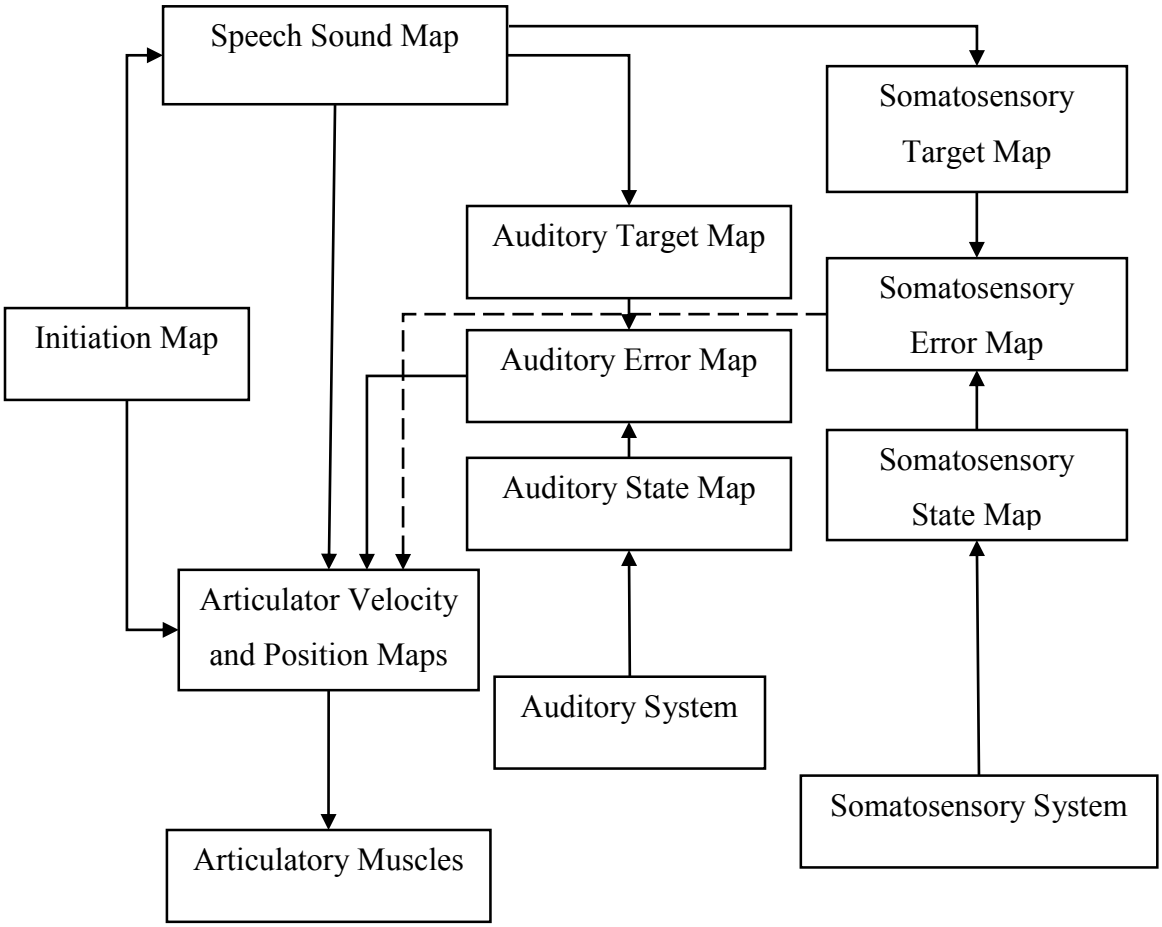

Figure 1.1 – A diagram of the DIVA model.

Adapted from Guenther (2006).

According to the DIVA model, when an infant hears the speech produced in his environment (the first step in learning to speak), cells in an area of his brain known as the 'speech sound map' are activated (Guenther, 1995). These cells learn and represent the speech sounds the infant has just heard. The sounds the infant has heard also help build an 'auditory target map' that will be used in the next phases of speech production. The auditory target map encodes the expected auditory output of the articulators (Guenther, 2006). It is also claimed that each cell in the speech sound map represents one speech sound, which can be a phoneme, syllable, or word that is uttered frequently in the language the infant is

learning, i.e. if a new sound is to be uttered or learned that is not used as frequently, a combination of the previously programmed cells will become activated (Tourville & Guenther, 2011).

The next step in learning to speak is babbling. In this phase, cells in an area of the infant's brain that control the articulation and therefore the movements of the speech-related muscles become activated. This, enables the infant to utter the learned speech sounds (Guenther et al., 2006). These cells in turn, activate the innervated muscles in the articulators and the intended sounds are then produced. At first, random movements of the articulators are produced until the desired output is reached, at which point a 'somatosensory target map' is built. This map consists of cells that encode the expected tactile and proprioceptive signals from the articulators (Guenther, 2008).

It is hypothesized that there is a real-time feedback system in the brain. This system is responsible for monitoring the flow of the signals from the speech sound map to the articulatory musculature and for correcting any errors that may occur (Behroozmand et al., 2015). This is the concept underlying the feedback control system in the DIVA model, which includes two subsystems: the auditory feedback system and the somatosensory feedback system. Each of these subsystems include a target map (discussed above), a state map and an error map (Guenther, 2008). Every time a sound that exists in the speech sound map is uttered, an 'auditory state map' and a 'somatosensory state map' is built. These maps represent the current auditory, and tactile and proprioceptive output, respectively, of the articulators. The state maps along with the maps from the corresponding target areas are compared in the sensory error maps ('auditory error map' and 'somatosensory error map') and corrections are made in the motor output if any discrepancies are identified (Guenther, 1994, 2006; Guenther et al., 2006).

Guenther and colleagues state that the cells that control the position and the velocity of the articulators reside in the lateral motor cortex (precentral gyrus) and they are bundled based on the articulator: tongue, lip, jaw and larynx (Guenther et al., 2006). The speech sound map cells are located in the left posterior inferior frontal gyrus (Broca's area) extending to the neighbouring left ventral premotor cortex (Guenther & Vladusich, 2012). These cells are activated during both the speech learning and the articulation phase (Kohler et

al., 2002). The somatosensory state map is located in postcentral gyrus, posterior to its motor counterpart. Therefore, the tactile and proprioceptive signals coming from the tongue, lip, palate and larynx positions are coded in the postcentral gyrus, with the tongue area being the most ventrolateral part of all and the larynx area being the most dorsomedial one (Penfield & Boldrey, 1937). The somatosensory target and error maps are also claimed to reside in the supramarginal gyrus, posterior to the postcentral gyrus that represents the somatosensory state map (Tourville & Guenther, 2011). Similarly, the auditory state map cells are inside the primary auditory cortex in the superior temporal gyrus and the auditory target and error map cells are located in the planum temporale and the posterior superior temporal gyrus (Guenther et al., 2006). Tourville and Guenther (2011) postulate that the cells in the 'initiation map' are responsible for activating the specific speech sound map cells. They suggest that the initiation map resides in the supplementary motor area (SMA).

The DIVA model does not go into the details of the planning phase for speech production. Consequently, Bohland, Bullock, and Guenther (2010) introduced an advanced version of the model, named GODIVA (**G**radient **O**rder **DIVA**). In this model, the pre-SMA is responsible for the encoding of the 'structural frame' of the syllable, while the SMA (also known as SMA-proper) is hypothesized to be the initiator of the planned speech acts (Bohland et al., 2010).

In the GODIVA model, the inferior frontal sulcus is assumed to encode for the phonological contents of the syllables that one intends to utter, i.e. it fulfils the job of planning the phonemes inside the syllable (Bohland et al., 2010). GODIVA also considers basal ganglia loops that help in the planning and initiation of the speech acts as well. Two loops involving the basal ganglia are present in this model: the planning loop and the motor loop. The former connects the inferior frontal sulcus/pre-SMA to the caudate and the latter connects the SMA/motor cortex to the putamen (Bohland et al., 2010). For more information on the role of basal ganglia in speech, please see Booth, Wood, Lu, Houk, and Bitan (2007); Leh, Ptito, Chakravarty, and Strafella (2007); Lehericy et al. (2004); Pickett, Kuniholm, Protopapas, Friedman, and Lieberman (1998); Tettamanti et al. (2005); Wildgruber, Ackermann, and Grodd (2001) and Murdoch (2001).

1.1.2 Developmental Stuttering

Developmental stuttering is a speech production disorder characterized by speech sound repetitions, prolongations and/or silent blocks that has its onset in children aged 2-6 years old. It affects about 5% of preschool-aged children, 20% of whom continue to struggle with the disorder for their lifetime (Bloodstein & Ratner, 2008). Stuttering is shown to be more prevalent in males than in females, with the ratio being 3:1 in favor of males (Bloodstein & Ratner, 2008). There are many theories about the causes of the disorder: stuttering may be a result of genetics, neurological deficits and/or comorbid developmental speech disorders (Bloodstein & Ratner, 2008; Eling & Whitaker, 2010).

The Overall Assessment of the Speaker's Experience of Stuttering (OASES) is a measure of the impact of stuttering on the person who stutter's (PWS) everyday life (Yaruss & Quesal, 2006). This self-reported paper and pencil questionnaire includes 100 questions in four sections: general information, reactions to stuttering, communication in daily situations and quality of life. Higher scores in this questionnaire means a higher impact of stuttering on the person who stutter's daily life. A study has shown that the overall impact score on the OASES is correlated with stuttering severity (measured using the fluency profile protocol) in children and adolescents (Chun, Mendes, Yaruss, & Quesal, 2010).

Deficiencies in different grey and white matter regions have been shown to exist in PWS. Below, I will introduce the grey and white matter regions pertinent to speech motor control. A report of the findings in the developmental stuttering literature related to the area being introduced will follow under the section for each region, if applicable.

1.1.3 Speech motor control and grey matter

1.1.3.1 Broca's area

Broca's area, also known as the posterior part of the inferior frontal gyrus (pIFG), is comprised of the pars opercularis (Brodmann's area 44) and pars triangularis (Brodmann's area 45) (Dronkers, Plaisant, Iba-Zizen, & Cabanis, 2007). Broca's area is involved in both the storage and the retrieval of speech sounds that are going to be uttered and thus the

readout of the motor program (Ghosh, Tourville, & Guenther, 2008; Golfinopoulos, Tourville, & Guenther, 2010; Guenther et al., 2006). In a recent study using electrocortigography of the peri-sylvian speech production areas (including Broca's area) during overt speech tasks, Flinker and colleagues showed that Broca's area is responsible for associating phonemic structures with motor gestures (Flinker et al., 2015). The repository of these motor gestural scores used in speech production is thought to be included in a mental syllabary that stores the articulation program of the speech sounds (Indefrey & Levelt, 2000; Levelt, Roelofs, & Meyer, 1999) and is the equivalent of the speech sound map in the DIVA model (Papoutsi et al., 2009).

Using functional magnetic resonance imaging, Papoutsi et al. (2009) investigated the functional subunits of Broca's area and ended up dividing this area into two functionally distinct dorsal and ventral parts. The results of this study showed that the dorsal part of the left inferior frontal gyrus, specifically the dorsal pars opercularis, is involved in phonological encoding (breaking the intended message into syllables; syllabification), while the ventral part of the same structure is involved in phonetic encoding (activation of the motor programs related to the utterance of specific syllables), thus elucidating that both of these steps are taking place in the Broca's area.

All in all, BA 44/45 can be considered as a connection between the higher-level language areas and lower-level speech motor control circuit(s) and therefore involved in converting the abstract language codes into articulatory codes and motor programs and transferring them to the motor areas for execution (Golfinopoulos et al., 2010). In other words, Broca's area is involved in higher-order motor aspects of speech production (Ackermann & Ziegler, 2010; Alamia et al., 2016).

Studies have shown that PWS present with structural deficits in Broca's area, both in the left and right hemisphere and both in the grey and white matter underlying this area. A structural imaging study using voxel-based morphometry (VBM) has reported higher density in the grey matter underlying the left inferior frontal gyrus and the white matter underlying the right inferior frontal gyrus of PWS compared to controls (Beal, Gracco, Lafaille, & De Nil, 2007). In another VBM study, Jancke, Hanggi, and Steinmetz (2004) showed that PWS present with higher white matter volume in the right inferior frontal gyrus. In a multimodal

neuroimaging study, Kell et al. (2009) observed lower grey matter volume in the left inferior frontal gyrus of PWS, which was also in a negative correlation with stuttering severity, meaning that the lower the grey matter volume in the left inferior frontal gyrus, the severer the stuttering. Similar results have been reported in studies of children who stutter (CWS). For instance, Chang, Erickson, Ambrose, Hasegawa-Johnson, and Ludlow (2008) reported a lower grey matter volume in the bilateral inferior frontal gyrus of CWS compared to the control group. This result was further corroborated in a VBM study by Beal, Gracco, Brettschneider, Kroll, and De Nil (2013). At first, these results may seem contradictory to the results of the studies on adults who stutter (AWS). However, a recent study done by Beal and colleagues has indicated that the Broca's area develops differently in PWS. In fact, Beal et al. (2015) have shown that the stuttering group shows no signs of change in cortical thickness with age in the area of the left pars opercularis, while cortical thickness in the same region gradually decreases with age in people who do not stutter. That is why CWS have lower grey matter volume in this area, while AWS present with higher grey matter volume in Broca's area, both compared to their control groups (Refer to Figure 3 in Beal et al. (2015)).

1.1.3.2 Supplementary motor area (SMA) and pre-SMA

The SMA is considered to be involved in the starting mechanism of speech (Ackermann & Riecker, 2010) and it is the area of the initiation map in the DIVA model (Guenther et al., 2006). This area is involved in the self-initiation of the speech plans and the motor execution of the speech output (Ghosh et al., 2008; Guenther et al., 2006).

The removal of SMA in monkeys has resulted in slower learning of motor sequences (Halsband, 1987; Passingham, 1987). A case study by Ziegler, Kilian, and Deger (1997) showed that damage to the SMA result in stuttering-like behaviours (dysfluency) and problems transferring the speech sounds to motor components of the speech production network (see also Bohland et al., 2010). The same study concluded that the SMA is involved in initiation of voluntary speech, but not speech triggered as a response to an external stimulation. Blank, Scott, Murphy, Warburton, and Wise (2002) suggested that the SMA is involved in voluntary control of respiration and control of breathing while the person is producing spoken language. Investigations of Penfield and colleagues have shown that stimulation of the SMA do result in stuttering-like behaviours (including sound prolongations

and intermittent vocal utterances) and speech arrest (Penfield & Rasmussen, 1968; Penfield & Roberts, 2014; Penfield & Welch, 1951).

The SMA has direct structural connections with the motor cortex, the brainstem and the spinal cord, while there is no known direct connection between these areas and the pre-SMA (Tremblay & Gracco, 2009; Vergani et al., 2014). This is in agreement with the fact that SMA is more selective to specific movements than the pre-SMA and that pre-SMA is responsible for encoding structural frames (sequencing syllables and phonemes) in the speech output (Bohland et al., 2010). Ghosh et al. (2008) have shown that lexical selection takes place in the anterior pre-SMA, while the posterior pre-SMA is responsible for encoding the sequences of the speech output. Studies have also shown that the pre-SMA is involved in volitional response selections, but not the ones that need external activations or are repetitive (Blank et al., 2002; Ghosh et al., 2008; Tremblay & Gracco, 2009). Therefore, suggesting that the whole dorsal premotor cortex is involved in initiating and planning voluntary movements, including the movements needed for speech to be produced.

Deficits in the SMA and the adjacent structures in the premotor cortex have been implicated in PWS. For example, Cai and colleagues have shown that PWS present with lower fractional anisotropy (FA)* values in the white matter underlying the left premotor cortex (Cai et al., 2014). Connally, Ward, Howell, and Watkins (2014) have reported lower FA values in the white matter of the bilateral superior frontal gyrus, which includes the premotor cortex. Similarly, Watkins, Smith, Davis, and Howell (2008) have reported a lower FA in the white matter underlying the bilateral premotor cortex.

1.1.3.3 Primary motor cortex

Brodmann's area 4 entails the primary motor cortex. This area has a homunculus of the body parts and is involved in controlling their motor activities. It is responsible for the lower level speech motor control functions (Wildgruber et al., 2001). Since breathing and its control is important in speech production, the area that controls the respiratory functions is activated when a person tries to speak (Wildgruber et al., 2001). The parts of the motor cortex that control the vocal tracts and the body parts involved in orofacial movements are

* Please refer to section 1.2 for more information on fractional anisotropy.

located more laterally and ventrally compared to the area that controls the respiratory functions, which sits in the medial and dorsal areas of the precentral gyrus (Penfield & Boldrey, 1937). An fMRI study has also divided the primary motor cortex into two distinct anterior (area 4a) and posterior (4p) parts, with the posterior part responsible for initiative and executive aspects of motor activities, while the area 4a requires feedback from the sensory areas to start motor activities (Fuertinger, Horwitz, & Simonyan, 2015; see also Geyer et al., 1996). Bohland and Guenther (2006) postulate that only the left motor cortex is reliably active when covert speech is produced, whereas both the left and right motor cortex contribute to overt speech production.

Deficits in the motor cortex have been implicated in developmental stuttering. For example, a study by Cai and colleagues showed that PWS present with lower FA values in the white matter underlying the left motor cortex (Cai et al., 2014). Sommer, Koch, Paulus, Weiller, and Buchel (2002) reported a similar result in PWS. Chang et al. (2008) observed a lower grey matter volume in the left motor cortex in CWS and Jancke et al. (2004) showed that the white matter volume underlying the right motor cortex is greater in PWS compared to normal controls.

1.1.3.4 Primary somatosensory and auditory cortices

The primary auditory cortex is the point of entry of the auditory codes into the brain. Also known as Heschl's gyrus and consisting of the BA 41 and 42 (Mendoza, 2011a), it is implicated in listening and learning (acquisition) and in production of speech (Hickok, 2010; Hickok, Houde, & Rong, 2011; Houde, Nagarajan, Sekihara, & Merzenich, 2002; Paus, Perry, Zatorre, Worsley, & Evans, 1996; Seghier et al., 2015). This area is located anterior to the secondary auditory cortex (superior temporal gyrus, BA 22), the posterior part of which is known as the Wernicke's area. As proposed in the DIVA model, the primary and secondary auditory cortices, collectively, represent the auditory state, target and error maps (Guenther et al., 2006; Hickok et al., 2011).

The somatosensory cortex is located in the postcentral gyrus in the parietal lobe and is involved in encoding the sensations received from different parts of the body (Ploner, Schmitz, Freund, & Schnitzler, 2000). This part of the cerebral cortex does represent a homunculus similar to the motor cortex and receives proprioceptive and tactile information

from the orofacial and laryngeal articulators that are involved in speech production (Cheyne, Kristeva, & Deecke, 1991; Penfield & Boldrey, 1937). Gosh and colleagues have reported activations in the somatosensory cortex only when the speech produced is overt, providing more evidence on the involvement of the postcentral gyrus in the proprioceptive and tactile feedback mechanisms (Ghosh et al., 2008).

Both the auditory and the somatosensory cortices are involved in the feedback mechanisms of speech production as mentioned in the description of the DIVA model (Golfinopoulos et al., 2010). Both of these cortices are involved in the auditory and somatic sensations bilaterally (Cogan et al., 2014; Mendoza, 2011b).

1.1.3.5 Wernicke's area

Wernicke's area is the posterior part of the superior temporal gyrus (BA 22). Both left and right posterior superior temporal gyri are implicated in auditory processing (Hickok & Poeppel, 2000), but only the left posterior superior temporal gyrus is involved in speech production (Belin, Zatorre, Lafaille, Ahad, & Pike, 2000; Wise et al., 1991). Functional studies of Wernicke's area have shown its activation during both speech production and speech perception (Buchsbaum, Hickok, & Humphries, 2001). For instance, Hickok et al. (2000) used functional magnetic resonance imaging to show that this area is involved in phonemic facets of speech production and Levelt, Praamstra, Meyer, Helenius, and Salmelin (1998) associated the area with phonological encoding based on the timing of the magnetoencephalography signals they studied in a picture naming task. These results were further confirmed by a case study by Gatignol, Capelle, Le Bihan, and Duffau (2004) and in functional neuroimaging studies by Buchsbaum et al. (2001) and Soros et al. (2006).

Wernicke's area has also been reported to be deficient in PWS. For example, Beal et al. (2007) have shown that the grey matter density underlying the bilateral superior temporal gyri is higher in the stuttering group relative to the control group. Beal et al. (2013) also reported a higher grey matter volume in the right superior temporal gyrus of CWS compared to the normal controls. Furthermore, Jancke et al. (2004) reported a higher volume in the white matter underlying the right superior temporal gyrus of PWS.

1.1.3.6 Geschwind's territory

Geschwind's territory is located at the inferior parietal cortex and is composed of the angular gyrus (BA 39) and the supramarginal gyrus (BA 40). This territory is adjacent to different visual, auditory and somatosensory areas and it has direct connections with them, which makes it a possible candidate to be the set of structures that integrates the information received or constructed at those areas (Stout & Chaminade, 2012).

Geschwind's territory is involved both in speech production and speech comprehension, especially in ideational speech (Awad, Warren, Scott, Turkheimer, & Wise, 2007; Geschwind, 1965a, 1965b). It is thought to be the link between speech perception and speech production (Wise et al., 2001). This territory is implicated in somatosensory feedback during speech production (Tremblay, Shiller, & Ostry, 2003) and in combining the sensory information received from the speech produced, comparing the target and state maps and building error maps if applicable (Golfinopoulos et al., 2010; Guenther et al., 2006). Additionally, it is postulated that this area is responsible for the selection of articulatory gestures needed for speech production (Tremblay & Gracco, 2010) along with the integration of the information in the speech perceived over time, which may translate to it being involved in composition of the connected speech that is going to be produced (Lerner, Honey, Silbert, & Hasson, 2011). Semantic processing of the speech to-be-produced and/or the speech perceived has also been associated with this territory (Geranmayeh et al., 2012).

CWS have been shown to present with higher volume in the grey matter of the right Geschwind's territory (Beal et al., 2013). Watkins et al. (2008) reported that while the white matter underlying the left supramarginal gyrus has lower FA values in PWS, the right counterpart of this area has higher FA values in PWS.

Collectively, the cortical grey matter regions described above comprise the neural network for speech motor control. Although the association of each region with specific aspects of the speech motor control process is both important and well supported, speech would not be possible without the underlying network of white matter pathways connecting these regions and facilitating signaling among them. With this sentiment in mind, I now turn

the focus of my writing to the important white matter connections that are investigated in this study.

1.1.4 White matter connections of the speech related brain areas

Methods based on magnetic resonance imaging have been used to identify the white matter connections in the brain. These methods (for instance, tractography*) have given us more insight as per the location and the termination/origination/projections of these white matter connections. Here I will focus on the white matter connections that facilitate the information flow between the speech related brain areas.

1.1.4.1 Arcuate Fasciculus

Thought to be involved in mapping sound to articulation (Axer, Klingner, & Prescher, 2013; Baker, Blumstein, & Goodglass, 1981; Hart & Gordon, 1990; Hickok & Poeppel, 2004), the arcuate fasciculus is composed of two pathways: direct and indirect. The direct pathway (also known as the long segment) connects the Broca's area to the Wernicke's area, or as Catani and Thiebaut de Schotten (2012) suggest, the Broca's territory to the Wernicke's territory (in the sense that the regions that are connected by the arcuate fasciculus are broader than the classically known Broca's and Wernicke's areas). This pathway is suggested to be engaged in phonological information transfer (Duffau, 2008; Duffau et al., 2002). It is worth mentioning that the stimulation of the direct pathway has shown to cause dysarthria (incoordination of the muscles involved in speech articulation) or anarthria (total loss of articulation ability) (Duffau, Gatignol, Denvil, Lopes, & Capelle, 2003; Duffau, Peggy Gatignol, Mandonnet, Capelle, & Taillandier, 2008; Fridriksson et al., 2010; Yagmurlu, Middlebrooks, Tanriover, & Rhoton, 2016).

Studies based on histology and virtual dissection (tractography) have shown that the indirect pathway connects the Wernicke's and Broca's territories to the Geschwind's territory (Catani, Jones, & ffytche, 2005; Catani & Thiebaut de Schotten, 2012; Parker et al., 2005). This pathway is thus composed of two segments: the anterior segment and the posterior segment. The anterior segment connects the Broca's territory to the Geschwind's territory and is involved in speech articulation (Duffau, 2008; Duffau et al., 2003). The evidence for

* Please refer to section 1.2 for more information.

this comes from a study by Duffau et al. (2003) in which intraoperative stimulation of this pathway elicited articulatory disorders. The posterior segment connects the Geschwind's territory to the Wernicke's territory and is implicated in speech perception (Duffau et al., 2003; Parker et al., 2005). The evidence for this comes from a study by Vandermosten et al. (2012). This study concluded that the FA in the posterior segment of the left arcuate fasciculus is significantly correlated with measures of speech perception.

It is of note that other classification systems of the arcuate fasciculus also exist. For example, some researchers believe that the arcuate fasciculus only connects the Broca's and Wernicke's areas directly and that it is a part of the bigger Superior Longitudinal Fasciculus (SLF) system (Bernal & Altman, 2010; Kamali, Flanders, Brody, Hunter, & Hasan, 2014). Others have proposed that the arcuate fasciculus and the SLF refer to the same tract (Dejerine, 1895). However, in this study, I will take the view that the SLF has three segments and only the third segment corresponds to the anterior segment of the arcuate fasciculus (Catani & Thiebaut de Schotten, 2012; Schmahmann & Pandya, 2006).

Arcuate fasciculus has been shown to be deficient in PWS. For example, Connally et al. (2014) reported a lower FA in the arcuate fasciculus in both hemispheres in PWS. Cai et al. (2014) observed lower FA only in the right arcuate fasciculus of PWS. However, Sommer et al. (2002) and Cykowski, Fox, Ingham, Ingham, and Robin (2010) showed that FA is lower only in the left arcuate fasciculus of PWS relative to controls and Chang et al. (2008) observed the same pattern in CWS. These studies do not explicitly state which parts of the arcuate fasciculus are deficient in PWS and they still are not in agreement whether it is the right or the left arcuate fasciculus or both that contributes to stuttering. Therefore, additional investigations are required to assess the arcuate fasciculus in PWS.

1.1.4.2 Frontal Aslant Tract

The frontal aslant tract (FAT) connects the SMA and pre-SMA to the Broca's area and is a left-lateralized tract in right-handed people (Catani et al., 2012). The areas this tract connects have been implicated in speech production as described above. However, there are also direct evidences for the involvement of this tract in speech production (Aziz-Zadeh, Cattaneo, Rochat, & Rizzolatti, 2005; Knecht, Deppe, et al., 2000; Rinne et al., 1999; Sussman, 2015). For instance, studies have shown that deficits to the fibers connecting the

mesiofrontal cortex, encompassing the SMA, to the Broca's area (possibly the FAT) result in symptoms similar to reduced instantaneous verbal behaviour and transcortical motor aphasia (Ackermann & Riecker, 2010; Freedman, Alexander, & Naeser, 1984; Ziegler et al., 1997). A study by Catani and colleagues showed that the FAT is impaired in patients with primary progressive aphasia (PPA) (Catani et al., 2013). The FAT is postulated to be immersed in selection and ordering of the verbal working memory cues during speech production (Dick, Bernal, & Tremblay, 2014; Rizio & Diaz, 2016). Studies have also shown that stimulation of the FAT results in speech arrest and/or problems initiating speech (Fujii et al., 2015; Vassal, Boutet, Lemaire, & Nuti, 2014), the same symptoms associated with the stimulation of the SMA by Penfield and colleagues, mentioned above. Damages to the FAT have also been associated with oral dyspraxia (inability to produce voluntary movements) (Dhakar, Ilyas, Jeong, Behen, & Chugani, 2016; Gibbs, Appleton, & Appleton, 2007), inability to initiate speech (Duffau et al., 2002; Kinoshita et al., 2015) and verbal dysfluencies (Catani et al., 2013; Kinoshita et al., 2015; Kronfeld-Duenias, Amir, Ezrati-Vinacour, Civier, & Ben-Shachar, 2016; Mandelli et al., 2014; Sierpowska et al., 2015).

A recent DTI study showed that AWS present with higher axial (AD) and radial diffusivity (RD) and thus higher mean diffusivity (MD) in the bilateral FAT. Furthermore, the same researchers reported that the higher the MD values in the left FAT, the less fluent AWS were (Kronfeld-Duenias et al., 2016). A previous study from our own lab has shown that FA is higher in the right FAT of CWS in comparison with both the FA in the left FAT of the same group and FA in the right FAT of the control group (Misaghi et al., in preparation). The same study showed a similar trend for AD, with the addition of a higher AD in the left FAT of normal children compared to their right FAT, i.e. in the opposite direction of the trend observed in the stuttering group. A study by Connally and colleagues is also in agreement with these results as they report that the white matter underlying the superior frontal gyrus and the inferior frontal gyrus, both bilaterally, have lower FA and lower AD in PWS compared to controls (Connally et al., 2014) and we already know that the FAT connects these two gyri (Catani et al., 2012). Although these studies have reported deficiencies in the FAT of PWS, there still is no agreement in the type of deficiency (i.e. whether, for example, higher AD contributes to stuttering or is it lower AD that is associated

with this dysfluency) and the hemisphere of the brain that presents with these deficiencies and this calls for more studies.

1.1.4.3 Corticospinal tract

As mentioned previously, both the ventral and the dorsal primary motor cortex are involved in speech production, since the ventral parts have areas that control the respiratory system and thus the breathing needed while speaking and the dorsal parts have areas that control the orofacial and laryngeal muscles that are involved in articulation (Penfield & Rasmussen, 1968; Takai, Brown, & Liotti, 2010). The corticospinal tract (CST) is a tract connecting the dorsal and medial parts of the motor cortex, i.e. the parts involved in respiration, to the spinal cord (Jurgens, 2002; Rogic Vidakovic et al., 2016).

Studies have reported deficits in the CST of both adults and CWS. Cai et al. (2014) have shown that PWS present with lower FA in the CST, bilaterally. Chang et al. (2008) reported a similar observation in CWS. However, these studies have only shown focal differences in the CST and a recent study using tractography found that, compared to normal adults, AWS present with elevated levels of MD only in the left CST (Kronfeld-Duenias et al., 2016). This calls for more investigations of this tract.

1.1.4.4 Corpus Callosum

Corpus callosum is the largest white matter fiber bundle in the brain, is a commissural pathway that connects the two hemispheres of the brain and it consists of different areas and projects to the occipital, parietal, temporal and frontal lobes (Hofer & Frahm, 2006). It is conventionally divided into three parts: the genu (anterior-most part of the tract), the splenium (the posterior-most part) and the body or trunk (the area in between) (Andrade et al., 2014; Witelson, 1989). A study by Chao and colleagues has shown that corpus callosum connects various brain areas, including those that are important for speech production (Chao et al., 2009).

There is growing evidence that the corpus callosum transmits information between the two hemispheres in the sense that it suppresses a structure in the non-dominant hemisphere so that the contralateral structure becomes active (Banich & Belger, 1990; Clarke, Lufkin, & Zaidel, 1993; Cook, 1984; Denenberg, Gall, Berrebi, & Yutzey, 1986;

Dennis, 1976; Hynd et al., 1995). This is in addition to its involvement in combining the information received in both hemispheres separately, e.g. in the visual system (Pietrasanta, Restani, & Caleo, 2012).

Studies of people with primary progressive apraxia of speech have shown that the body of the corpus callosum is damaged (loss of white matter) in this disorder (Josephs et al., 2012; Whitwell et al., 2013). However, abnormalities in the corpus callosum are not limited to the loss of white matter. Involvement of bilateral structures in functions that are normally unilateral may lead to greater white matter volume in the corpus callosum, since it has to facilitate more data transfer between the hemispheres (e.g. see Preston et al., 2014). Morphological and white matter deficits have also been found in the corpus callosum of people with dyslexia (for a review, see Elnakib et al., 2014). In an investigation of patients with corpus callosum infarctions, Li and colleagues showed that damages to the corpus callosum may result in very broad symptoms, including (but not limited to) clumsy and slurred speech (Li et al., 2015). These results provide even more evidence that the corpus callosum is involved in data transfer related to speech and that deficits in this white matter fiber bundle have been observed in people with different communication disorders.

Studies have also assessed the corpus callosum in PWS. Beal et al. (2013) reported that the white matter volume is lower in the fibers of the genu of the corpus callosum in CWS in comparison with their fluent peers. While Choo, Chang, Zengin-Bolatkale, Ambrose, and Loucks (2012) did not find any differences between the volume of the corpus callosum in CWS versus normal controls, a study from the same research group on AWS did report higher area in the overall corpus callosum and in the genu and body of the corpus callosum, in addition to increased white matter volume in the genu of corpus callosum (Choo et al., 2011). DTI studies have also shown that PWS present with lower FA in the white matter fibers of the body (Cykowski et al., 2010) and the genu (Cai et al., 2014; Civier, Kronfeld-Duenias, Amir, Ezrati-Vinacour, & Ben-Shachar, 2015) of the corpus callosum in PWS. Although many of these studies have indicated the genu of corpus callosum as a potential contributor to overt stuttering characteristics, they are not in agreement in terms of the direction of the differences they have found (e.g. we are not sure whether lower white matter

volume in this area is contributing to the stuttering behaviour in PWS or higher white matter volume).

As already discussed, a few studies on neural correlates of stuttering have reported an increased density of white matter and/or grey matter underlying the right hemisphere homologues of the speech related structures in the left hemisphere. This may be the result of those areas taking over the functions of the components of the speech network that are normally left-lateralized (Frost et al., 1999; Knecht, Deppe, et al., 2000; Knecht, Drager, et al., 2000). This is an indication of the compensatory mechanisms carried out by the right hemisphere (Beal et al., 2007; Xing et al., 2016; Zipse, Norton, Marchina, & Schlaug, 2012). For instance, Beal et al. (2013) showed that there is a negative correlation between stuttering severity and the grey matter volume in the right inferior frontal gyrus of CWS. This is in agreement with the above statement in the sense that as the right hemisphere counterpart of Broca's area takes over the responsibilities of the Broca's area, the stuttering becomes less severe.

Table 1.1 below summarizes the results of the studies discussed above:

Table 1.1 - Summary of the structural imaging results in developmental stuttering.

All comparisons are PWS vs. controls; PrCG: precentral gyrus, AF: arcuate fasciculus, VBM: Voxel-Based Morphometry. STG: superior temporal gyrus, IFG: inferior frontal gyrus, SMA: supplementary motor area, CST: corticospinal tract, CBT: corticobulbar tract, ROI: Region of Interest, vPMC: ventral premotor cortex, PoCG: postcentral gyrus, SMG: supramarginal gyrus, TBSS: Tract-Based Spatial Statistics, gCC: genu of the corpus callosum, RO: rolandic operculum, IPL: inferior parietal lobule, pdPMC: posterior dorsal premotor cortex, SFG: supeior frontal gyrus, bCC: body of the corpus callosum, POp: pars opercularius, FAT: Frontal Aslant Tract.

Study	White Matter Results (Methods)	Grey Matter Results (Methods)
Sommer et al. (2002)	Lower FA in left dorsal PrCG and left AF (VBM)	N/A
Jancke et al. (2004)	Greater white matter volume in right STG, IFG and PrCG (VBM)	N/A
Beal et al. (2007)	Increased white matter density in right IFG (VBM)	Increased grey matter density in bilateral STG and left IFG (VBM)
Chang et al. (2008)	Lower FA in bilateral CST/CBT and left AF (VBM)	Lower grey matter volume in bilateral IFG, bilateral SMA, left PrCG (VBM, ROI Analysis)
Watkins et al. (2008)	Lower FA in bilateral IFG, PrCG, and vPMC, left SMG and right CST Higher FA in left IFG, right PoCG and right SMG (TBSS)	N/A
Kell et al. (2009)	N/A	Lower grey matter volume in left IFG (VBM)
Cykowski et al. (2010)	Lower FA in left AF (TBSS)	N/A
Choo et al. (2011)	Increased white matter volume in gCC (VBM)	N/A
Beal et al. (2013)	Decreased white matter volume in gCC (VBM)	Decreased grey matter volume in bilateral IFG Increased grey matter volume in the right RO, PoCG, STG and IPL (VBM)
Cai et al. (2014)	Lower FA in right AF, bilateral CST, left pdPMC and left gCC (TBSS)	N/A
Connally et al. (2014)	Lower FA in bilateral SFG and IFG Lower FA in bilateral AF and bCC (TBSS, Probabilistic Tractography)	N/A
Beal et al. (2015)	N/A	Thinner grey matter in left POp in younger PWS and thicker grey matter in the same area in older PWS (ROI Analysis)
Civier et al. (2015)	Lower FA in gCC (TBSS)	N/A
Kronfeld-Duenias et al. (2016)	Higher AD, RD and MD in bilateral FAT (Tractography)	N/A

1.2 From diffusion in the brain to diffusion kurtosis images: a review

Although researchers were using the diffusion properties of materials in the nuclear magnetic resonance (NMR) studies for a long time, it wasn't until the mid-80's that diffusion MRI was born (Le Bihan et al., 1986) and used for the studies of humans and animal models. In this section, I will first explore diffusion imaging in general and will then go into the particulars of diffusion tensor imaging (DTI) and one of its successors, diffusion kurtosis imaging (DKI).

1.2.1 Diffusion

Diffusion is the transfer of molecules down the concentration gradient (from area(s) of higher concentration to area(s) of lower concentration) (Basser & Özarslan, 2011). In liquids, including water, this transfer is fulfilled via random motions due to the thermal energy, called Brownian motion (Hagmann et al., 2006). Barriers can alter the way molecules travel when they are following a random path, which is the case in a cellular environment (Basser & Özarslan, 2011). There are various hindrances that molecules may encounter during diffusion, e.g. cellular membranes or organelles (Alexander, Lee, Lazar, & Field, 2007; Beaulieu, 2002; Hagmann et al., 2006). In environments where diffusion is not limited by barriers, diffusion is isotropic, i.e. the molecules diffuse equally in different directions. Conversely, if the movement of the molecules are hindered by different barriers and their diffusion is direction-dependent, diffusion is known as anisotropic, meaning it is greater in one direction (e.g. in the direction parallel to the main axis of the neural filaments) (Beaulieu, 2002). Isotropic diffusion can be modeled using a sphere, while anisotropic diffusion needs to be modeled using more complex shapes such as an ellipsoid (more on the ellipsoidal model below) (Jellison et al., 2004).

1.2.2 Diffusion-weighted magnetic resonance imaging

MR images can be diffusion-sensitized or weighted using a dephasing and rephasing gradient before and after the 180° radiofrequency (RF) pulse and measuring the signal loss that is generated based on the distance traveled by certain molecules (Sivapatham & Melhem, 2012). This is based on the Stejskal-Tanner (Pulsed Gradient Spin Echo; PGSE) method of

diffusion MRI, in which there are two RF pulses: a 90° pulse followed by an 180° pulse (Stejskal & Tanner, 1965). In case the molecules are stationary, the dephasing and rephasing pulses cancel out and there won't be any salient signal losses, whereas if there is a bulk motion (i.e. the net diffusion of the particles in the environment is not zero), there will be a relative signal attenuation that is pertinent to the b-value, the diffusion sensitization factor (Sivapatham & Melhem, 2012). For a Gaussian motion, the relation between the b-value and the signal intensities before and after the application of the diffusion-weighted gradients is governed by the following (Stejskal-Tanner) equation (Stejskal & Tanner, 1965):

$$S = S_0 e^{-bD_{app}} \tag{1.1}$$

Where S is the signal intensity if diffusion weighting is applied and S_0 is the signal intensity when there is no diffusion weighting ($b = 0$). D_{app} is the diffusion coefficient, or the apparent diffusion coefficient (ADC), and b is the diffusion weighting that is determined using the following equation:

$$b = \gamma^2 G^2 \delta^2 (\Delta - \delta/3) \tag{1.2}$$

Here, γ is the gyromagnetic ratio, G is the gradient strength, Δ is the time between and δ is the length of the two pulsed gradients (Melhem et al., 2002).

1.2.3 Diffusion Tensor Imaging (DTI)

Diffusion is normally direction-independent in isotropic media, such as the brain grey matter. In this case, a simple scalar diffusion coefficient, D_{app}, is sufficient to characterize the diffusional behaviour of the tissue. However, in the brain white matter, where diffusion is anisotropic, no scalar value alone can describe the mentioned behaviour (Sivapatham & Melhem, 2012). Thus, the tensor **D**, here a 3x3 covariance matrix of diffusion displacements in 3D, was proposed to replace the scalar D_{app} (Basser, Mattiello, & LeBihan, 1994; Dhollander, 2016). This tensor is symmetrical with respect to the diagonal elements:

$$\mathbf{D} = \begin{bmatrix} D_{xx} & D_{xy} & D_{xz} \\ D_{yx} & D_{yy} & D_{yz} \\ D_{zx} & D_{zy} & D_{zz} \end{bmatrix}; \begin{cases} D_{yx} = D_{xy} \\ D_{zx} = D_{xz} \\ D_{zy} = D_{yz} \end{cases} \tag{1.3}$$

As can be seen above, the tensor has 9 elements in total, but because of the symmetry, only 6 elements need to be calculated in order to obtain the full tensor. Therefore, a minimum of 6 non-collinear diffusion directions (along with a non-diffusion-weighted image, i.e. the $b = 0$ image) are needed for the tensor to be fully reconstructed (a system of six equations with six variables) (Alexander et al., 2007). The diffusion tensor is modeled using an ellipsoid (Figure 1.2), with the major, medium and minor principal axes described by the three eigenvectors ε_1, ε_2 and ε_3 with values equal to the eigenvalues λ_1, λ_2 and λ_3, respectively (Jellison et al., 2004).

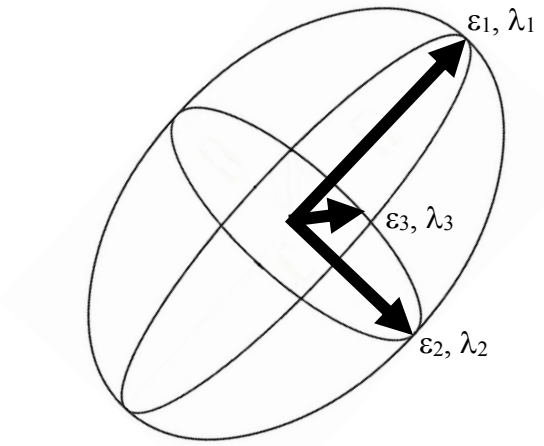

Figure 1.2 – The diffusion tensor ellipsoid.

Pathological conditions alter the architecture and microstructure of the tissues (e.g. demyelination, ischemia, axonal damage, edema and inflammation). Diffusion patterns change as a result of those alterations. For instance, demyelination may induce more diffusion in the direction perpendicular to the main axis of the axons or axonal damage may decrease diffusion in the parallel direction (Lin, Tench, Morgan, Niepel, & Constantinescu, 2005). Thus, diffusion-based imaging can help assess the microstructure of the tissue and any pathological conditions they may have been affected by as well as the extent of the deficit (Alexander et al., 2007).

Some of the measures that are normally used in the diffusion imaging studies of normal and abnormal brains are as follows:

a) Trace (Tr): is the sum of the diagonal elements of the diffusion tensor and shows the magnitude of diffusion (Soares, Marques, Alves, & Sousa, 2013):

$$\mathrm{Tr} = D_{xx} + D_{yy} + D_{zz} = \lambda_1 + \lambda_2 + \lambda_3 \quad (1.4)$$

b) Mean diffusivity (MD): Sometimes referred to as the apparent diffusion coefficient (ADC), MD is the Trace divided by 3, i.e. the average of the eigenvalues (Alexander et al., 2007):

$$\mathrm{MD} = \frac{\mathrm{Tr}}{3} = \frac{D_{xx} + D_{yy} + D_{zz}}{3} = \frac{\lambda_1 + \lambda_2 + \lambda_3}{3} \quad (1.5)$$

c) Fractional anisotropy (FA): is a measure of diffusion anisotropy. It's the most commonly reported measure in diffusion imaging studies, but it is of note that this measure does not completely describe the pattern of diffusion or the extent and type of the changes, as it cannot describe the orientation of diffusion and thus the shape of the whole tensor (Alexander et al., 2007; Mukherjee, Berman, Chung, Hess, & Henry, 2008; Soares et al., 2013):

$$\mathrm{FA} = \frac{\sqrt{3}\sqrt{(\lambda_1 - \mathrm{MD})^2 + (\lambda_2 - \mathrm{MD})^2 + (\lambda_3 - \mathrm{MD})^2}}{\sqrt{2}\sqrt{\lambda_1^2 + \lambda_2^2 + \lambda_3^2}} \quad (1.6)$$

d) Radial diffusivity (RD): is the average of the medium and minor eigenvalues and appears to be specific to myelin in white matter and may change as a result of dysmyelination or demyelination (Alexander et al., 2011; Alexander et al., 2007; Feldman, Yeatman, Lee, Barde, & Gaman-Bean, 2010):

$$\mathrm{RD} = \frac{\lambda_2 + \lambda_3}{2} \quad (1.7)$$

e) Axial diffusivity (AD): is the major eigenvector, is aligned parallel to the axonal main axis, and may be modulated by axonal degeneration. Better myelination also results in greater AD values (Alexander et al., 2007; Feldman et al., 2010):

$$\mathrm{AD} = \lambda_1 \quad (1.8)$$

1.2.4 Tractography

In the tensors with high anisotropy, the major eigenvector is assumed to be parallel to the white matter tract direction in that voxel. This is the concept underlying white matter tractography. In fact, to obtain the white matter connections using the Fiber Assignment by Continuous Tracking (FACT) algorithm (Mori, Crain, Chacko, & van Zijl, 1999), steps in the flowchart below are taken (Figure 1.3):

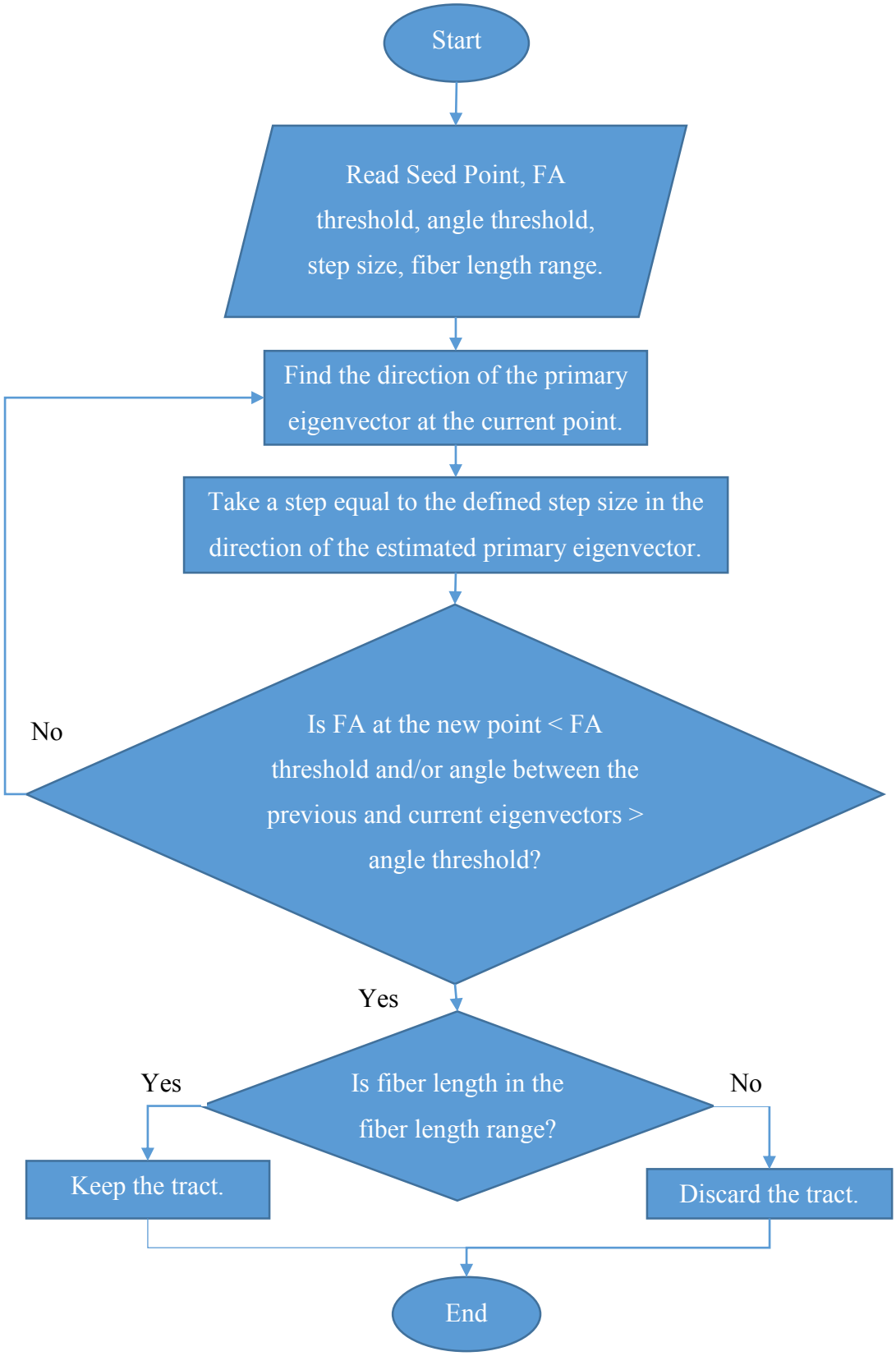

Figure 1.3 – Flowchart showing the steps taken in white matter tractography.

In case the seed points are not based on specific regions of interest (ROIs), but rather based on the entire brain, the method (known as whole brain tractography) requires more computational load and thus is called the brute-force approach (Huang, Zhang, van Zijl, & Mori, 2004). In the brute-force approach, first the white matter tracts of the whole brain are reconstructed. The rater, then places specific region of interest (ROI) 'gates' on the locations of interest. If the rater wants to include fibers that pass through a specific location, they draw an AND ROI there. In case they need fibers passing through either of the two locations, OR ROIs are used (A SEED ROI used after whole brain tractography fulfils the same role as an OR ROI). NOT ROIs are normally used to edit/prune the tracts, i.e. if the rater doesn't want to include fibers passing through a certain location, they place a NOT ROI there. This is called the deterministic tractography method (Mori & van Zijl, 2002; Mukherjee et al., 2008; Wakana et al., 2007; Zhang, Olivi, Hertig, van Zijl, & Mori, 2008).

As mentioned above, DTI tractography is capable of identifying only one dominant fiber direction, while one- to two-thirds of the voxels in the brain white matter are thought to contain more than one tract streamline (crossing fibers) and thus multiple fiber orientations (Behrens, Berg, Jbabdi, Rushworth, & Woolrich, 2007; Qiu, Mori, & Miller, 2015). Additionally, the DTI model is based on the assumption that the diffusion in white matter follows a Gaussian distribution. However, this is only the case when a molecule is diffusing inside a homogeneous liquid and not the brain white matter, in which the cellular membranes and spaces between and inside the cells hinder the normal movement of the molecules and as such render the diffusion probability distribution non-Gaussian (Hori et al., 2012; Jensen & Helpern, 2010). The non-Gaussianity of the diffusion distribution has also been confirmed by observations in higher b-values (Cohen & Assaf, 2002; Steven, Zhuo, & Melhem, 2014). Both of these limitations demand the usage of a better method to model the diffusion more accurately in white matter and to delineate the tracts of interest more robustly (Mori & Zhang, 2006).

Different high angular resolution diffusion imaging (HARDI) methods have been proposed to mitigate these problems. Examples of these methods are diffusion spectrum imaging (DSI) and q-ball imaging (QBI) (Tuch, Reese, Wiegell, & Wedeen, 2003). However,

these methods require very long scanning times (more than 30 minutes), a large number of gradient directions (over 40 directions) and high b-values (typically $3000 - 8000\ s/mm^2$) (Lazar, Jensen, Xuan, & Helpern, 2008; Steven et al., 2014). Although higher b-values enable the representation of the interactions occurring in the intracellular space and the membrane interactions and thus a clearer visualization of the tissue structure and fiber directions (Le Bihan, 2013; Wisnowski, Ceschin, & Schmithorst, 2013), they also decrease the signal-to-noise ratio (SNR) of the acquired images (Tournier & Mori, 2014). Diffusion kurtosis imaging (DKI), which makes use of a HARDI sequence, conversely, requires lower, but still multiple, b-values and smaller number of gradient directions (thus shorter scan times) and yet is capable of resolving the problems associated with the limitations of DTI (Lazar et al., 2008; Steven et al., 2014; Tournier & Mori, 2014). Shorter scan times decrease the possibility of subject movements inside the MRI scanner and thus the possibility of acquiring distorted images. The lower b-values used in the DKI sequence also resolve the problem of lower SNR in DSI and QBI.

1.2.5 Diffusion Kurtosis Imaging (DKI)

Statistically, kurtosis is defined as the amount of deviation of a certain distribution from the Gaussian pattern (the well-known bell curve), more specifically, the peakedness of the curve representing the distribution (DeCarlo, 1997; Steven et al., 2014). Therefore, a distribution with a positive kurtosis (leptokurtic) has a higher peak and heavier tails, whereas a negative kurtosis (platykurtic) represents a lower peak and lighter tails in a distribution (DeCarlo, 1997). Figure 1.4 shows this concept.

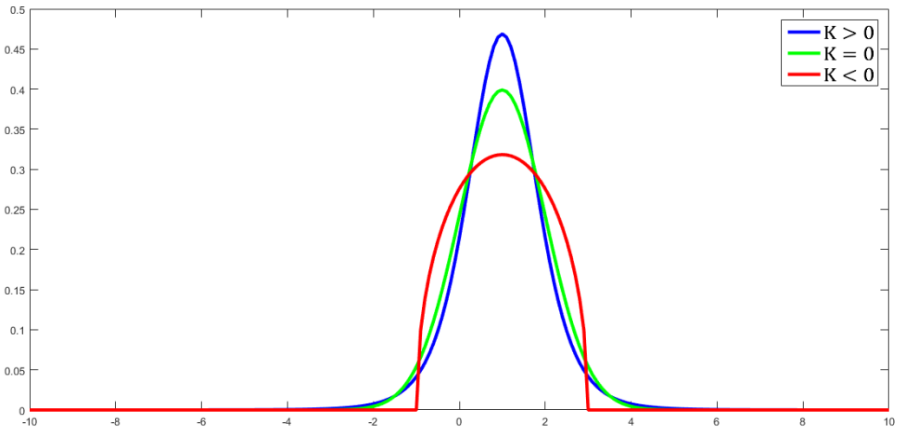

Figure 1.4 – A graph showing different probability distribution functions based on the degree of kurtosis (K).

As discussed above, DKI is capable of resolving, at least partially, the limitations of DTI. Mathematically, the DKI model includes higher order terms in the formulation of $\ln(S)$, which effects a more accurate estimation of the signal:

$$\ln(\mathrm{S}) = \ln(S_0) - bD_{app} + \frac{1}{6}b^2 D_{app}^2 K_{app} \quad (1.9)$$

Here, K_{app} is the excess apparent diffusional kurtosis, or kurtosis for short, and D_{app} is the apparent diffusion coefficient.

The measures normally extracted from DKI include the mean kurtosis (MK), axial kurtosis (AK) and radial kurtosis (RK). The following equations show the derivations of those values (Hui, Cheung, Qi, & Wu, 2008; Marrale et al., 2015):

$$K_i = \frac{\mathrm{MD}^2}{\lambda_i^2} W_{iiii} \quad (1.10)$$

$$\mathrm{MK} = \frac{1}{N}\sum_{i=1}^{N} K_i \quad (1.11)$$

$$\mathrm{AK} = K_1 \quad (1.12)$$

$$\mathrm{RK} = \frac{K_2 + K_3}{2} \quad (1.13)$$

MD is the mean diffusivity, W_{iiii}s are the diagonal components of the kurtosis tensor, $\mathbf{W}$, and λ_is are the eigenvalues of the diffusion tensor. K_is are the kurtosis values along different directions and N is the total number of gradient directions.

A few studies have reported regional values of the kurtosis metrics in the human brain (Das, Wang, Bing, Bhetuwal, & Yang, 2016; Jensen et al., 2005; Latt et al., 2013; Paydar et al., 2014). Table 1.2 below shows some of the reported measures pertinent to the study at hand. Note that the differences in the values could be due to the selection of ROIs, number of participants and chosen methods of analysis (Jensen et al., 2005).

Table 1.2 – Regional values of the kurtosis measures in the human brain.

Mean ± SD. MK: Mean Kurtosis, AK: Axial Kurtosis, RK: Radial Kurtosis, SLF: Superior Longitudinal Fasciculus, CC: Corpus Callosum, CST: Corticospinal Tract.

Area	Study	MK	AK	RK
SLF	Das et al. (2016)	1.03 ± 0.05	0.67 ± 0.01	0.95 ± 0.01
	Latt et al. (2013)	1.11 ± 0.04	N/A	1.84 ± 0.13
Body of CC	Das et al. (2016)	0.91 ± 0.1	0.46 ± 0.01	1.01 ± 0.02
	Latt et al. (2013)	1.17 ± 0.07	N/A	2.54 ± 0.34
Genu of CC	Das et al. (2016)	0.90 ± 0.05	0.41 ± 0.05	0.90 ± 0.07
	Latt et al. (2013)	1.06 ± 0.11	N/A	2.07 ± 0.45
Splenium of CC	Das et al. (2016)	1.07 ± 0.08	0.45 ± 0.03	1.05 ± 0.07
	Latt et al. (2013)	1.32 ± 0.09	N/A	2.72 ± 0.41
CST	Das et al. (2016)	1.07 ± 0.07	0.52 ± 0.01	0.98 ± 0.02
	Latt et al. (2013)	1.23 ± 0.07	N/A	2.04 ± 0.28

Growing evidence shows that the kurtosis metrics are more sensitive to the exchanges occurring between the cell compartments in vivo than the values extracted from the diffusion tensor alone, suggesting a better sensitivity to the integrity of white matter (De Santis, Assaf, & Jones, 2012; Fieremans, Jensen, & Helpern, 2011; Fieremans, Novikov, Jensen, & Helpern, 2010; Jensen & Helpern, 2010). This sensitivity makes DKI more specific to the tissue microstructure than DTI (Mohammadi et al., 2014). Comparisons of different measures extracted using DTI (e.g. FA and MD) and the measures extracted using DKI (e.g. MK) have shown a clinical advantage of DKI to DTI in terms of diagnoses and the extent of change determined using diffusion maps and values (See Kamagata et al., 2013; Kazumata et al., 2016; Wang et al., 2011 for examples). Jensen et al. (2005) postulated that the kurtosis metrics are more specific measures of tissue complexity and the heterogeneity of the

diffusion environment including cellular membranes and compartments, than their conventional diffusion counterparts (Latt et al., 2013).

1.3 Hypotheses

As described in section 1.1, different studies have already shown white matter deficits in the brains of PWS. These deficits seem to be seen in a distributed set of structures and tracts, specifically, the arcuate fasciculus, the CST, the FAT and the corpus callosum. These studies are inconclusive in nature and they have mostly used the conventional DTI to study the brains of PWS. Our lab has been the first group to extract these tracts in a single study of a group of CWS (Misaghi et al., in preparation), but still using DTI tractography. In order to assess these tracts in a population of AWS and given the discussed advantages of DKI over DTI, I decided to use tractography on a DKI dataset of AWS in this study. More specifically, I hypothesized that:

1. AWS will have higher AK in the (left) FAT, the CST (bilaterally), the (at least left) arcuate fasciculus and the genu and body of corpus callosum. The lower FA and AD observed in these tracts in the previous studies may be due to a failure of these areas to properly develop neurons or myelinate the existing ones (Alexander et al., 2011; Feldman et al., 2010). Since AK is an indicator of the integrity of the cell membrane and surrounding myelin sheaths (Steven et al., 2014), while being negatively correlated with AD (Falangola et al., 2014; Hui et al., 2008; Pang et al., 2015), this hypothesis is in line with the results of the previous studies.
2. There will be a negative correlation between the OASES impact score and RK in both the left and the right FAT, since the OASES impact score is a measure of the impact of stuttering on the daily lives of PWS and it is correlated with stuttering severity (Chun et al., 2010). This is expected based on the results of studies by Kronfeld-Duenias et al. (2016) and Catani et al. (2013).
3. Both groups will have a left-lateralized arcuate fasciculus and FAT (Catani et al., 2007; Catani et al., 2012; Catani et al., 2005).

2 Materials and Methods

2.1 Participants

Sixteen right-handed men, who were fluent speakers of English, participated in this research study. Eight were adults who stutter and the other eight were normal healthy controls matched with the first group based on their age, years of education and the other languages spoken. The sample was drawn from the greater Edmonton area. The AWS were recruited through the Institute for Stuttering Treatment and Research (ISTAR) at the University of Alberta and through online advertisements via university mailing lists. The controls were also recruited through online university mailing lists, online advertising websites and word of mouth. The study was approved by the Biomedical Health Panel of the Research Ethics Office at the University of Alberta. The participants provided signed consent before participating in the study. Table 2.1 summarizes the demographic information of the participants (age, handedness and years of education). At the end of the experiment, the participants were given a gift card as a token of appreciation for their participation in the study.

Table 2.1 – Study participants' demographic information.

** Handedness has been quantified based on the Edinburgh Handedness Inventory (Oldfield, 1971). Values less than -40 correspond to left-handedness, while values greater than 40 correspond to right-handedness. Values between -40 and 40 correspond to ambidextrous people.*

AWS	Age when scanned	Handedness*	Years of Education	Matched Control	Age when scanned	Handedness	Years of Education
P01	28	83.3	17	C01	27	100	20
P02	21	45.4	15	C02	21	100	13
P03	20	81.8	13	C03	20	83.3	13
P04	24	73.9	17	C04	25	91.7	13
P05	22	89.5	15	C05	21	83.3	16
P06	34	58.3	18	C06	35	91.3	15
P07	27	91.7	17	C07	27	100	21
P08	26	100	18	C08	25	77.8	17

2.2 Materials

The tests administered in this study included a revised version of the Edinburgh Handedness Inventory (Oldfield, 1971) to assess the participants' handedness, the Peabody Picture Vocabulary Test (PPVT) - version 4 (Dunn & Dunn, 2007) to assess their receptive vocabulary and the Digit Span task from the Wechsler Adult Intelligence Scale (WAIS) - version 4 (Wechsler, 2008) to assess their cognitive abilities in working memory, attention and encoding. Additionally, AWS filled out the OASES form to self-report their experience of stuttering (Yaruss & Quesal, 2008). Participants of both groups also played the Towers of Hanoi video game that was implemented in a MATLAB program developed by Brian Moore (http://www.mathworks.com/MATLABcentral/fileexchange/38202-towers-of-hanoi). The purpose was to determine the performance of AWS in non-speech motor tasks and match it

with that of normal controls. They were then scanned using a 4.7T Varian Inova Scanner (Palo Alto, CA, USA) at the MR Research Centre at the University of Alberta.

2.3 Procedures

Prior to their participation in the study, volunteers were screened to ensure that they met the inclusion and exclusion criteria of our study, including eligibility for safe entry into the MRI scanner. The specific screening questions are included in Appendix A. Eligible volunteers were scheduled for behavioural assessment and an MRI scan. The experiment was completed either in one 3-hour session inclusive of behavioural assessment and the MRI scan or in two 1.5 hour sessions in which case the participant came in for the behavioural assessment on one day and returned for the scan on the following day. Participants were assessed in a quiet room with no distractions in the Clinical Sciences Building at the University of Alberta and the MRI scan took place at the Peter S. Allen MR Research Centre at the University of Alberta.

At the beginning of the screening session, the participants were given some information regarding the study. Then, they signed the consent form (Appendices A2 & A3) in accordance with the ethics approval secured for the study. As per the MR Research Centre and ethics guidelines, they were also given some information about the scanning phase and they were asked to fill out and sign the MRI screening form (Appendix A4). Their handedness was assessed using a revised version of the Edinburgh Handedness Inventory (Appendix A5). The participants were then administered the PPVT and the Digit Span task. They also played the Towers of Hanoi video game. AWS also filled out the OASES form.

The code for the Towers of Hanoi game was edited to record the number of moves the player made and the time it took to complete a level. The game had three pegs with 3 and 5 blocks in the leftmost peg for level 1 and level 2, respectively. The aim of the game was to move all of the blocks from the leftmost peg to the rightmost peg using the number keys 1, 2 and 3, with 1 representing the leftmost peg, 2, the middle peg and 3, the rightmost peg. The rules of the game dictate that only the block at the top of a peg can be moved at a time and that the player cannot place a larger block on top of a smaller block. The participants were taught the rules of the game (without the game being played) before they were asked to play

the game with 3 and 5 blocks. The time it took them to move all of the blocks from the far left peg to the far right peg was recorded along with the number of moves. A move was counted only if it was allowed based on the rules of the game. Figure 2.1 shows a screenshot of the game with 5 blocks.

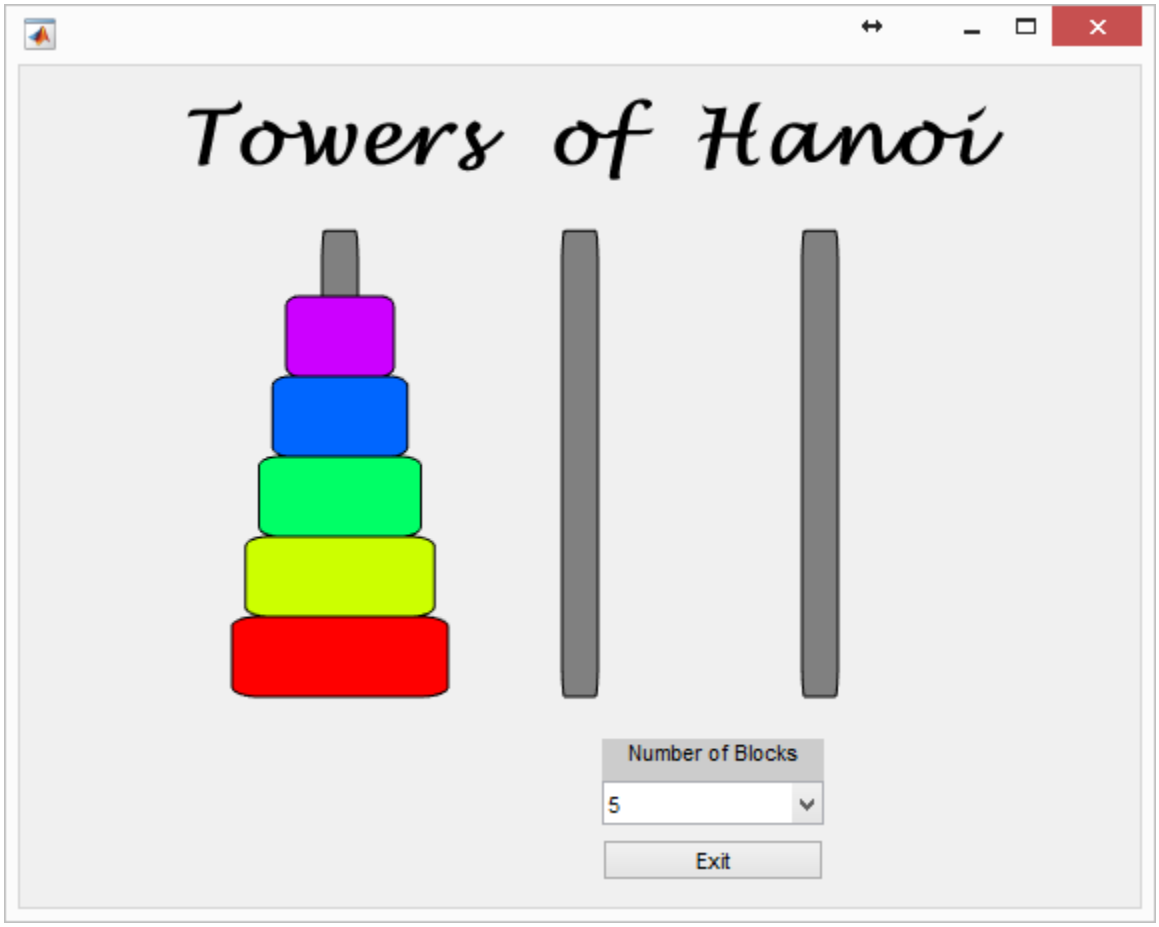

Figure 2.1 – The Towers of Hanoi game with 5 blocks.

Following the screening session, participants were scanned using a series of sequences including a T1-weighted Magnetization Prepared Rapid Gradient Echo (MPRAGE), a Resting-State Functional Magnetic Resonance Imaging (rs-fMRI), a Susceptibility-Weighted Imaging (SWI) and a DKI sequence. The sequences other than the DKI sequence were collected for a purpose beyond the scope of the current study and thus the DKI sequence will only be discussed in this document. The scanning parameters for the DKI sequence were as follows:

TR: 9 s, TE: 68 ms, Resolution: 1x1x2 mm^3 (upsampled; no interslice gap), Matrix size:

256x224x60 (upsampled), Field-of-view: 256x224 mm^2, flip angle: 90°, Number of slices: 60, Number of volumes: 70 (10 $b = 0$ and 60 diffusion-weighted images with b-values: 1000 and 3000 s/mm^2, 30 gradient directions each).

2.4 Data analysis

The raw data used for (pre-) processing were saved in the nifti file format, with ten $b = 0$ images at the beginning of the nifti files followed by thirty $b = 1000\ s/mm^2$ and thirty $b = 3000\ s/mm^2$ images. The nifti files were numbered using a code written in MATLAB to make sure that the tractographer (myself) was blind to the groups the images belonged to. The images were first checked for motion and Echo-Planar Imaging (EPI) distortions using the FSLView tool. None of the images showed signs of salient distortions. The images were then skull and scalp stripped using the Brain Extraction Tool (BET) module in the FMRIB Software Library (FSL) program (Jenkinson, Beckmann, Behrens, Woolrich, & Smith, 2012; Smith, 2002). The resultant images were imported into ExploreDTI version 4.8.6 (Leemans, Jeurissen, Sijbers, & Jones, 2009) for further processing. First, the diffusion and kurtosis tensors were estimated and the images were converted into MATLAB files (mat). Then, whole brain (deterministic) tractography was carried out on the data based on the diffusion tensor with the FA threshold of 0.2, a maximum angle threshold of 30° and a minimum tract length of 20 mm. The FA threshold of 0.2 is a common threshold used in tractography studies (Wakana et al., 2007). The conservative angle threshold of 30° was chosen so as to minimize the number of erroneous streamlines and the minimum tract length of 20 mm was chosen to include the smaller tracts such as the FAT and the posterior segment of the arcuate fasciculus. These thresholds have also been used in tractography studies before (Andrade et al., 2014; Kronfeld-Duenias et al., 2016; Liu, Concha, Beaulieu, & Gross, 2011).

2.4.1 Tractography and extraction of the metrics

Using different sets of ROIs discussed below, three parts of the corpus callosum (genu, body and splenium), three parts of the arcuate fasciculus (anterior, posterior and long segments), the FAT and the CST were delineated (on both hemispheres). The methods used to isolate these tracts are as follows:

2.4.1.1 Corpus Callosum

I divided the corpus callosum into three parts, the genu, the body and the splenium (based on Hofer and Frahm (2006)). First, the midline of the brain was identified using the FA- and diffusion direction-based color coded axial and sagittal images. The width of the corpus callosum was calculated using the number of pixels on the sagittal image. The anterior ⅙ of the width was identified as the genu of corpus callosum, the posterior ¼ as the splenium and the part in between was considered the body of corpus callosum. This method has previously been used by Andrade et al. (2014). Sets of ROIs drawn for each of these parts are discussed below separately.

2.4.1.1.1 Delineation of the genu of corpus callosum

An AND ROI* was drawn to entail the anterior ⅙ of the width of the corpus callosum in the midline. Two SEED ROIs were drawn four sagittal slices (4 mm) in either side of the midline. Two NOT ROIs were also drawn just lateral to the CSTs sagittally, to exclude the fibers that may travel more laterally and thus might not be a part of the fibers of the genu. Another NOT ROI was drawn in the coronal slice in the middle of the corpus callosum width to exclude any fibers that may go backwards because of the potential problems in the calculation of the directions in voxels. Figure 2.2 shows the set of ROIs that I drew to isolate the fibers passing through the genu of corpus callosum in a representative subject.

* For more information about the different ROIs and tractography itself, please refer to part 1.2.4.

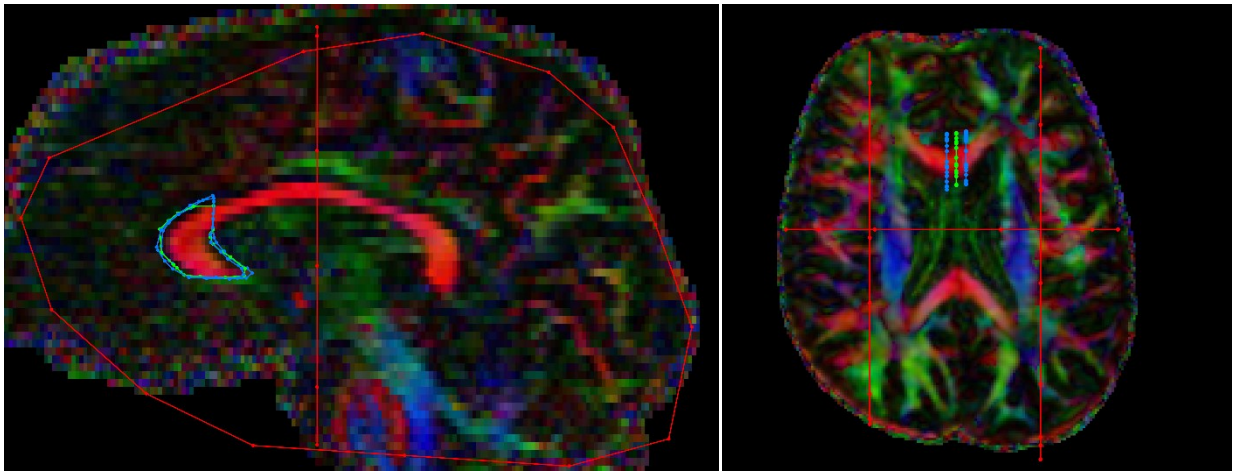

Figure 2.2 – ROIs used to delineate genu of corpus callosum on a representative subject's color-coded brain image.

The red ROIs are NOT gates, the blue ROIs are SEED (OR) gates and the green ones are AND gates. (left) sagittal view. (right) axial view (radiological convention).

2.4.1.1.2 Delineation of the body of corpus callosum

An AND ROI was drawn in the midline such that its anterior boundary touched the posterior boundary of the AND ROI used to isolate the genu fibers and its posterior boundary touched the anterior boundary of the splenium ROI, the delineation method of which will be discussed in the next section. Two SEED ROIs were drawn 4 slices parasagittal to the midline on either side to encompass the AND ROI drawn in the midline. Two NOT ROIs were also drawn just lateral to the CSTs in the sagittal plane. Another NOT ROI was drawn just under the AND ROI in the axial plane to exclude any fibers that may be travelling in the inferior direction and thus may not be a part of the fibers of the body of the corpus callosum. Figure 2.3 shows the ROIs on an image of a representative subject.

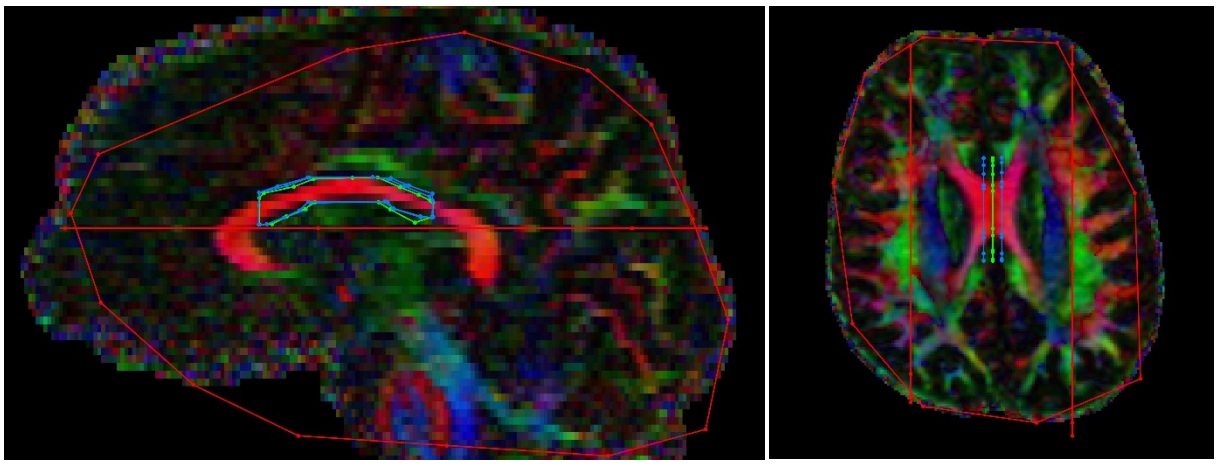

Figure 2.3 – ROIs used to isolate the body of corpus callosum on a representative subject's brain image.

(left) sagittal view. (right) axial view.

2.4.1.1.3 Delineation of the splenium of corpus callosum

In order to delineate the splenium of corpus callosum, an AND ROI was drawn encompassing the posterior ¼ of the corpus callosum width. Two SEED ROIs were drawn in the sagittal plane 4 slices parasagittal to the midline on either side. Two NOT ROIs were also drawn just lateral to the optic radiations to exclude fibers that may travel more laterally and thus may not be a part of the fibers of the splenium. Figure 2.4 shows the ROIs used to delineate the splenium.

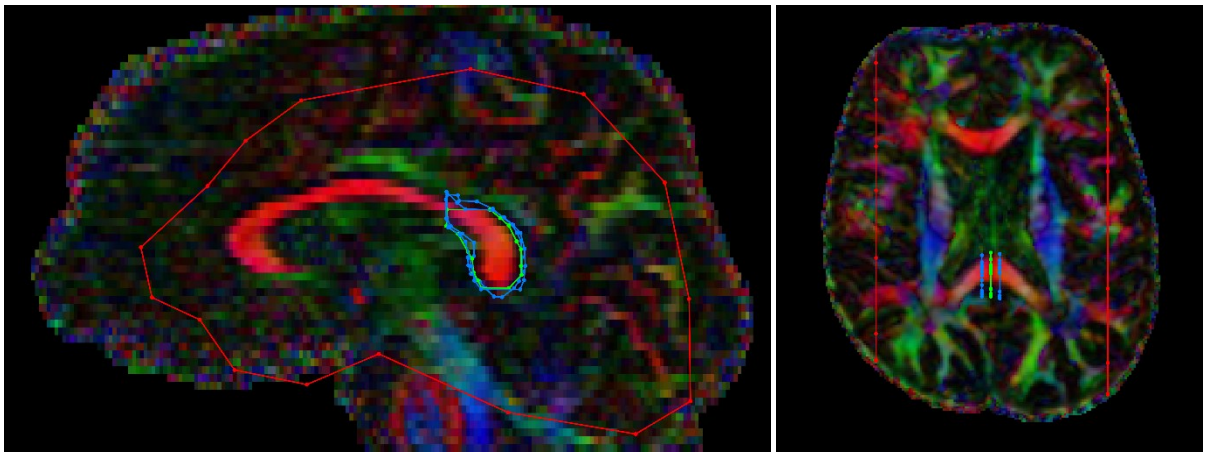

Figure 2.4 – ROIs used for virtually dissecting the fibers of the splenium of corpus callosum.

(left) sagittal view. (right) axial view.

Figure 2.5 and Figure 2.6 show the complete corpus callosum delineated in the control group and in AWS, respectively.

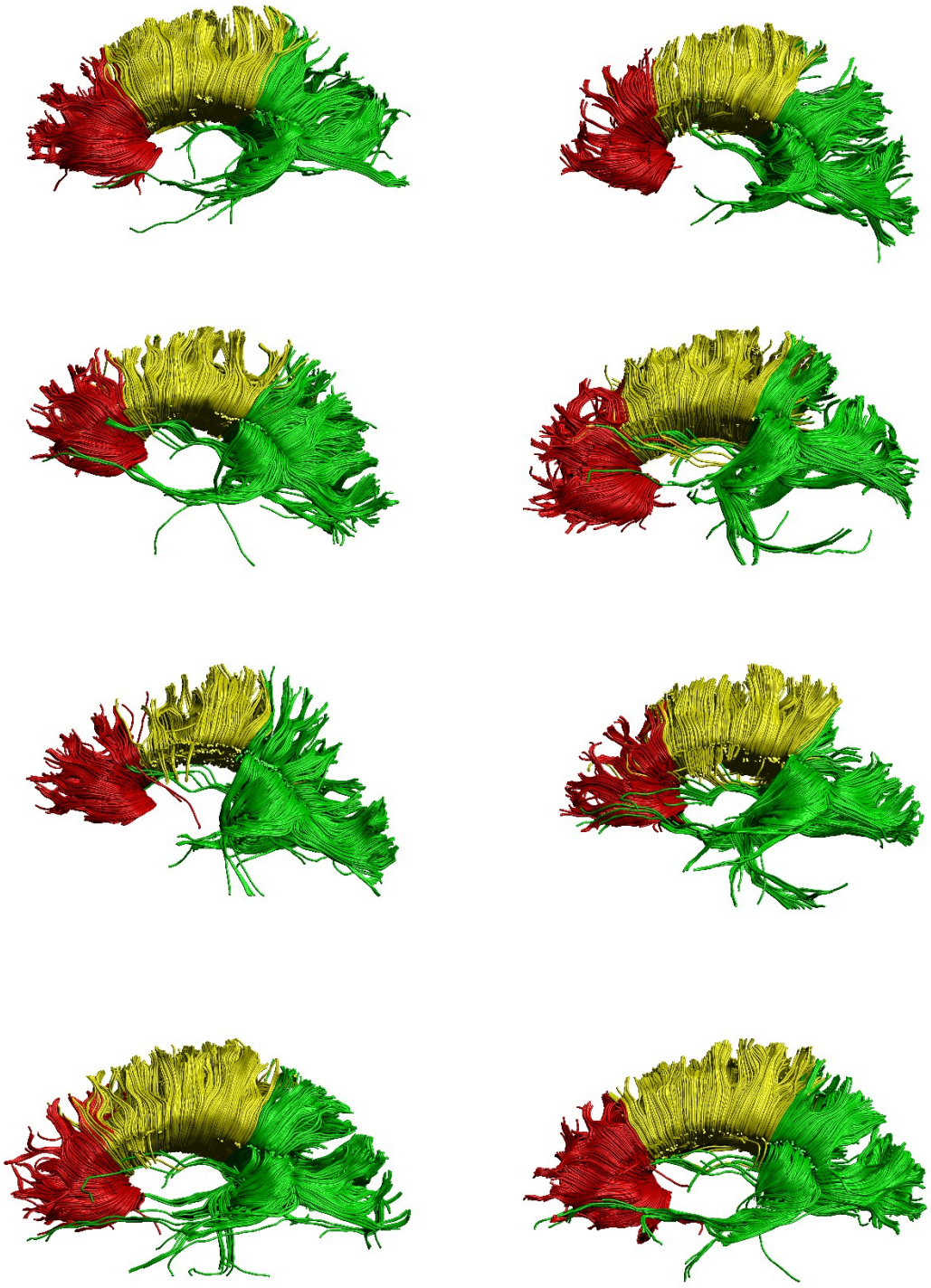

Figure 2.5 – The fibers of corpus callosum extracted in the control group.

The red fibres (anterior part) represent genu, the yellow fibers represent body and the green fibers (posterior part) represent the splenium of corpus callosum.

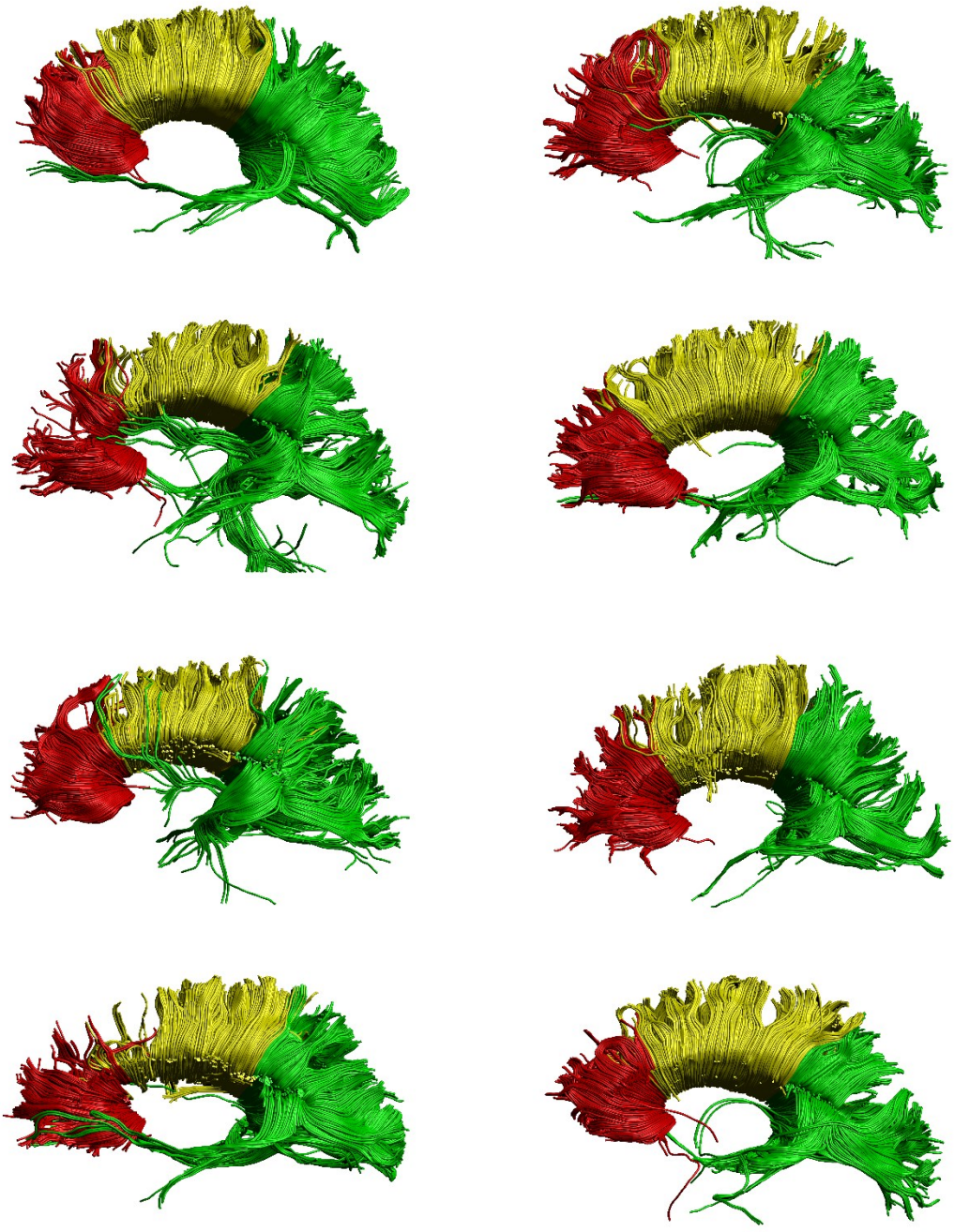

Figure 2.6 – The fibers of corpus callosum extracted in AWS.

The red fibres (anterior part) represent genu, the yellow fibers represent body and the green fibers (posterior part) represent the splenium of corpus callosum.

2.4.1.2 Arcuate Fasciculus

As discussed previously, the arcuate fasciculus is composed of three parts: anterior segment, posterior segment and long segment. The first two entail the indirect pathway,

while the long segment is the direct pathway* (Catani & Thiebaut de Schotten, 2012). I used the same method as Catani et al. (2013) to delineate the three segments of this fasciculus. First, two AND ROIs were drawn over Broca's and Geschwind's territories. These ROIs helped me obtain the anterior segment in each hemisphere. Using an AND ROI on Wernicke's territory and deleting the one encompassing Geschwind's territory, I delineated the long segment of arcuate fasciculus. The posterior segment of the fasciculus was obtained using the ROI encompassing Geschwind's territory and the ROI on Wernicke's territory, i.e. a combination of two out of three identical ROIs were used to isolate the different segments of arcuate fasciculus each time. This method was used for both hemispheres. Figure 2.7 shows the ROIs used for the delineation of these segments in a representative subject. Figure 2.8, Figure 2.9, Figure 2.10 and Figure 2.11 show the complete delineation of the left and the right arcuate fasciculus in the control and the AWS groups, respectively.

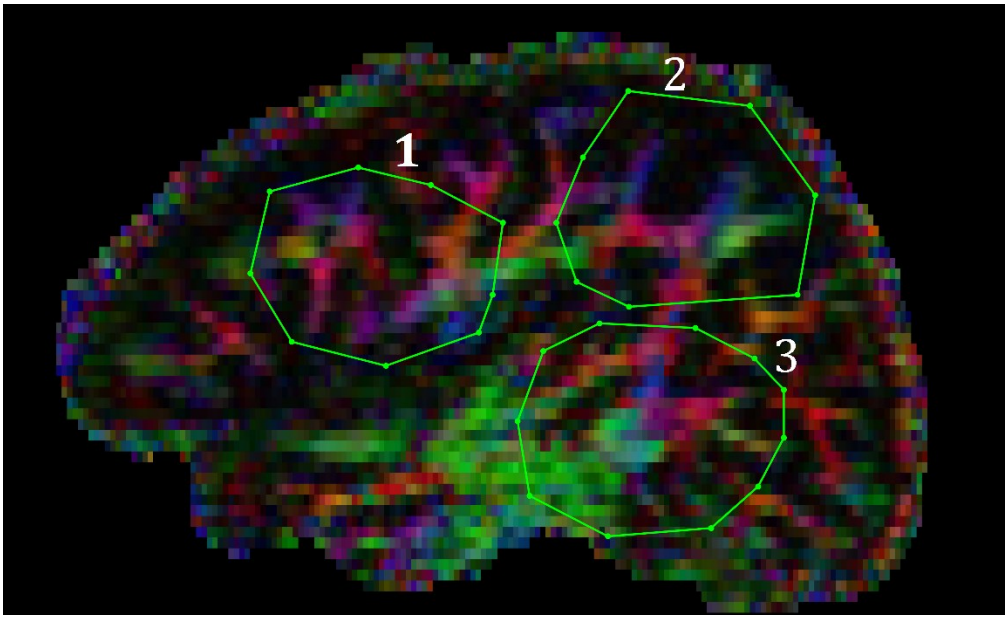

Figure 2.7 – ROIs used to isolate the segments of the arcuate fasciculus.

ROI 1 represents the Broca's territory. ROI 2 encompasses Geschwind's territory. ROI 3 is located over the Wernicke's territory. The anterior segment of the arcuate fasciculus runs between ROIs 1 and 2. The posterior segment runs between ROIs 2 and 3 and the long segment passes through ROIs 1 and 3.

* For a description of the direct and indirect pathways, please refer to section 1.1.4.1 of this thesis.

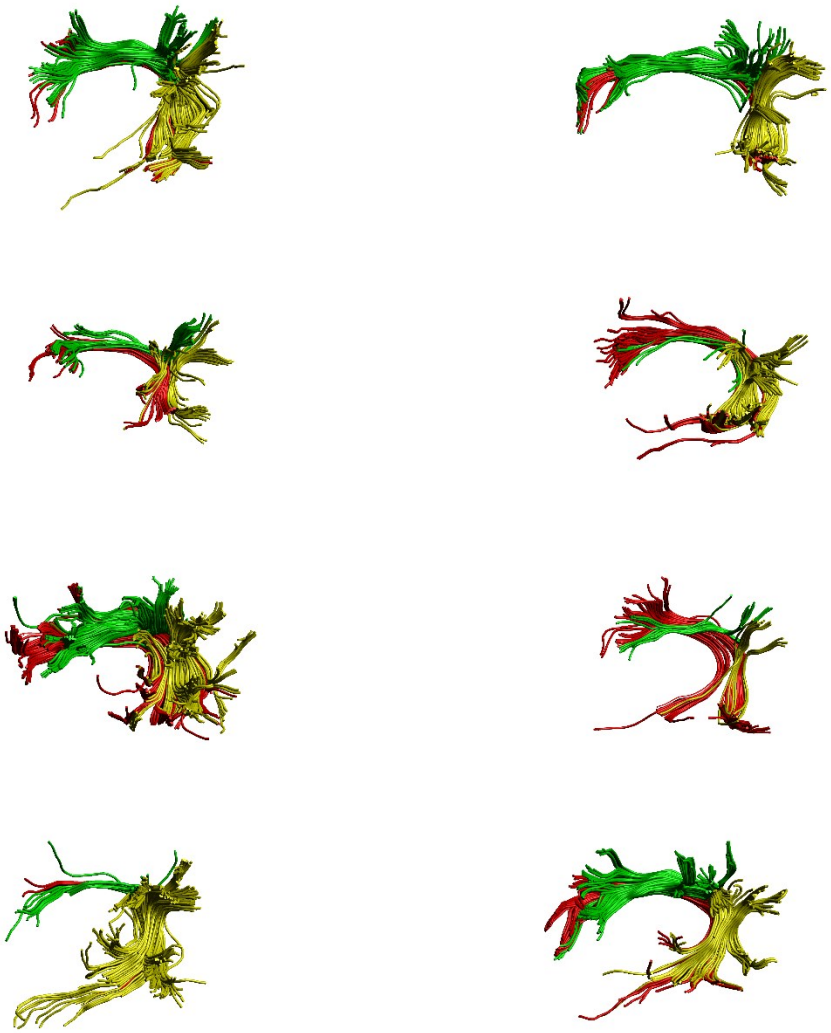

Figure 2.8 – The left arcuate fasciculus in the control group.

The fibers shown in red are the fibers of the long segment. The yellow fibers represent the posterior segment and the green ones the anterior segment.

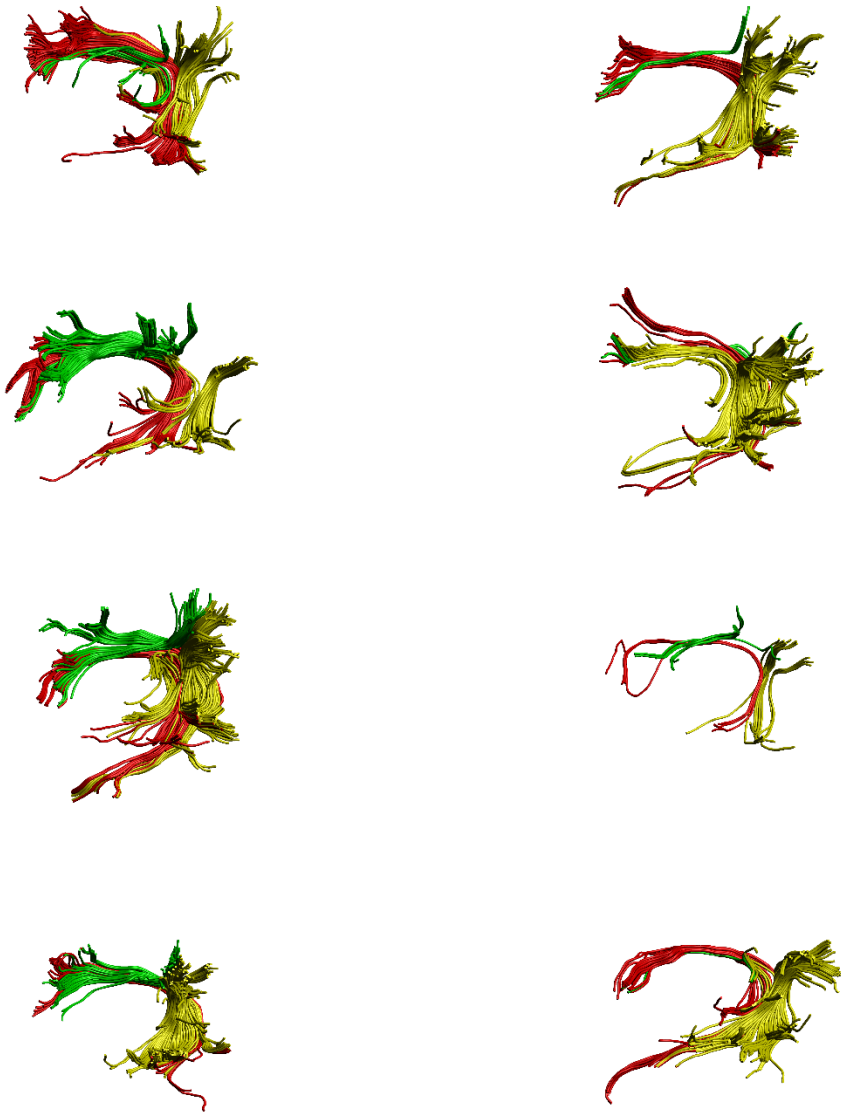

Figure 2.9 – The left arcuate fasciculus in AWS.

The fibers shown in red are the fibers of the long segment. The yellow fibers represent the posterior segment and the green ones the anterior segment.

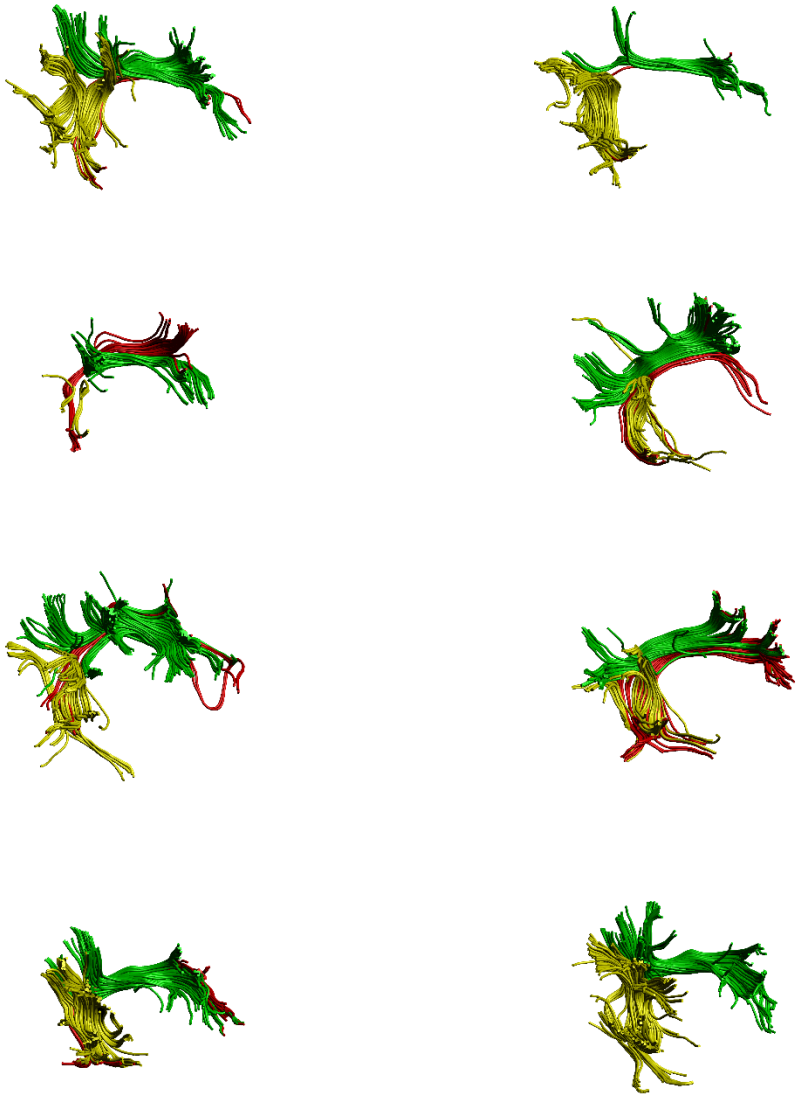

Figure 2.10 – The right arcuate fasciculus in the control group.

The fibers shown in red are the fibers of the long segment. The yellow fibers represent the posterior segment and the green ones the anterior segment.

Figure 2.11 – The right arcuate fasciculus in AWS.

The fibers shown in red are the fibers of the long segment. The yellow fibers represent the posterior segment and the green ones the anterior segment.

2.4.1.3 FAT

As discussed above, the FAT is a tract connecting the SMA and pre-SMA in the medial superior frontal gyrus to Broca's area in the inferior frontal gyrus*. I was able to isolate this tract in both hemispheres using two AND ROIs for each hemisphere, one of them encompassing the SMA and pre-SMA in the superior frontal gyrus and the other encompassing the inferior frontal gyrus (Kronfeld-Duenias et al., 2016). Figure 2.12 shows the ROIs in a representative subject. Figure 2.13 is a demonstration of the FAT in the control group, while Figure 2.14 shows this tract in AWS.

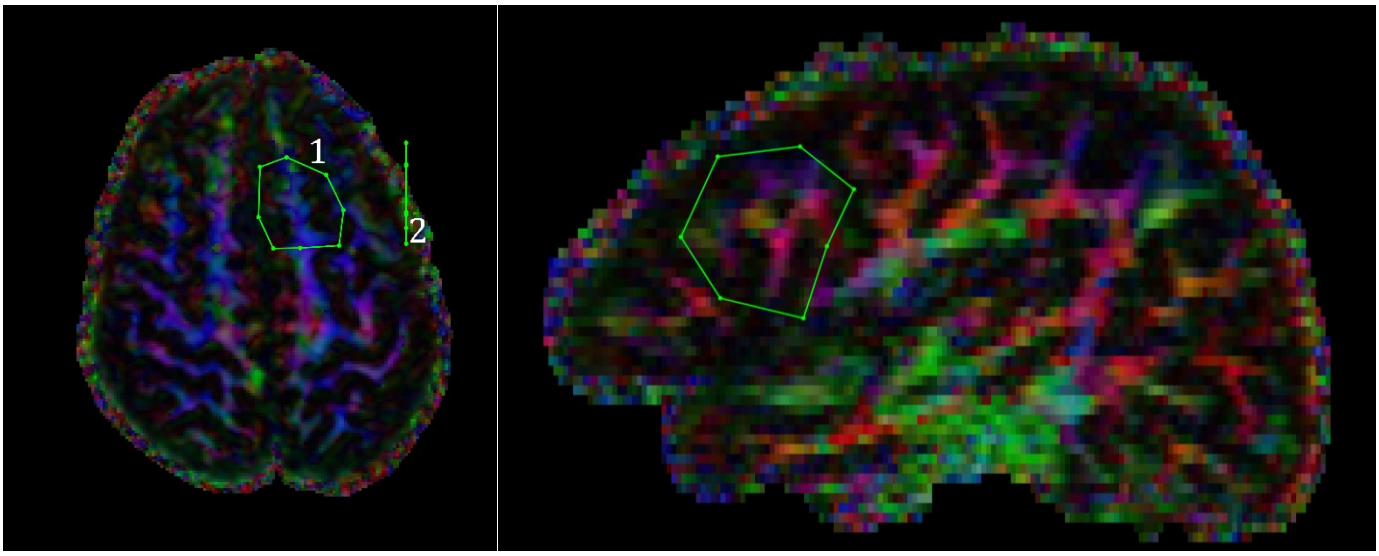

Figure 2.12 – ROIs used to isolate the frontal aslant tract.

(left) axial view showing the ROI on the superior frontal gyrus (ROI 1) and the inferior frontal gyrus (ROI 2). (right) sagittal view showing the ROI on the inferior frontal gyrus.

* Please refer to section 1.1.4.2 for a detailed description of the FAT.

Figure 2.13 – The bilateral FAT as delineated in the control group.

Figure 2.14 – The bilateral FAT in adults who stutter.

2.4.1.4 CST

In order to extract the CST, I used the method proposed by Wakana et al. (2007). An AND ROI was drawn in the level of the pons to encircle the cerebral peduncle. Another ROI was drawn in the level of the cerebral cortex upon careful observation of the fibers passing through the pons ROI to isolate only the fibers that reach the motor cortex. NOT ROIs were used in the sagittal and/or coronal planes as needed to prune the fibers and exclude fibers that

may not be a part of the CST. Figure 2.15, Figure 2.16 and Figure 2.17 show the ROIs used to extract this tract and the extracted tract in the control and AWS groups, respectively.

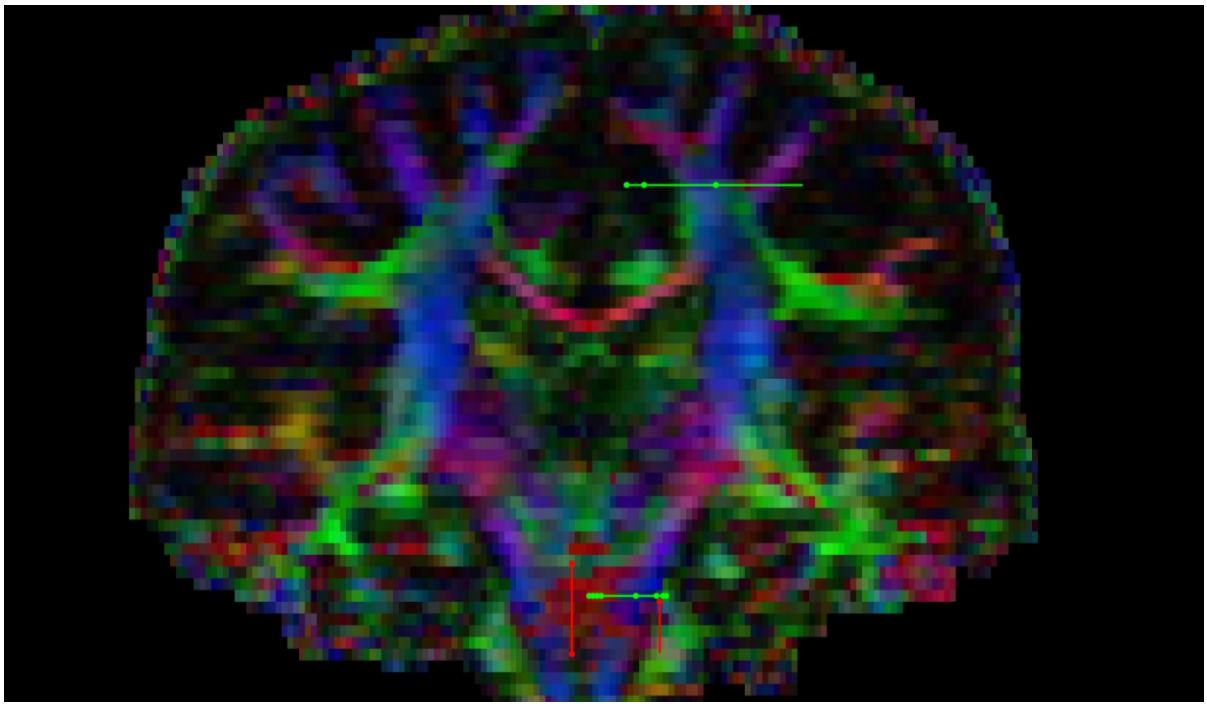

Figure 2.15 – ROIs used to isolate the corticospinal tract.

The superior ROI encompasses the medial aspects of the motor cortex and the inferior ROI encompasses the projections of the corticospinal tract through the pons. The NOT ROIs are used for pruning the resultant tract.

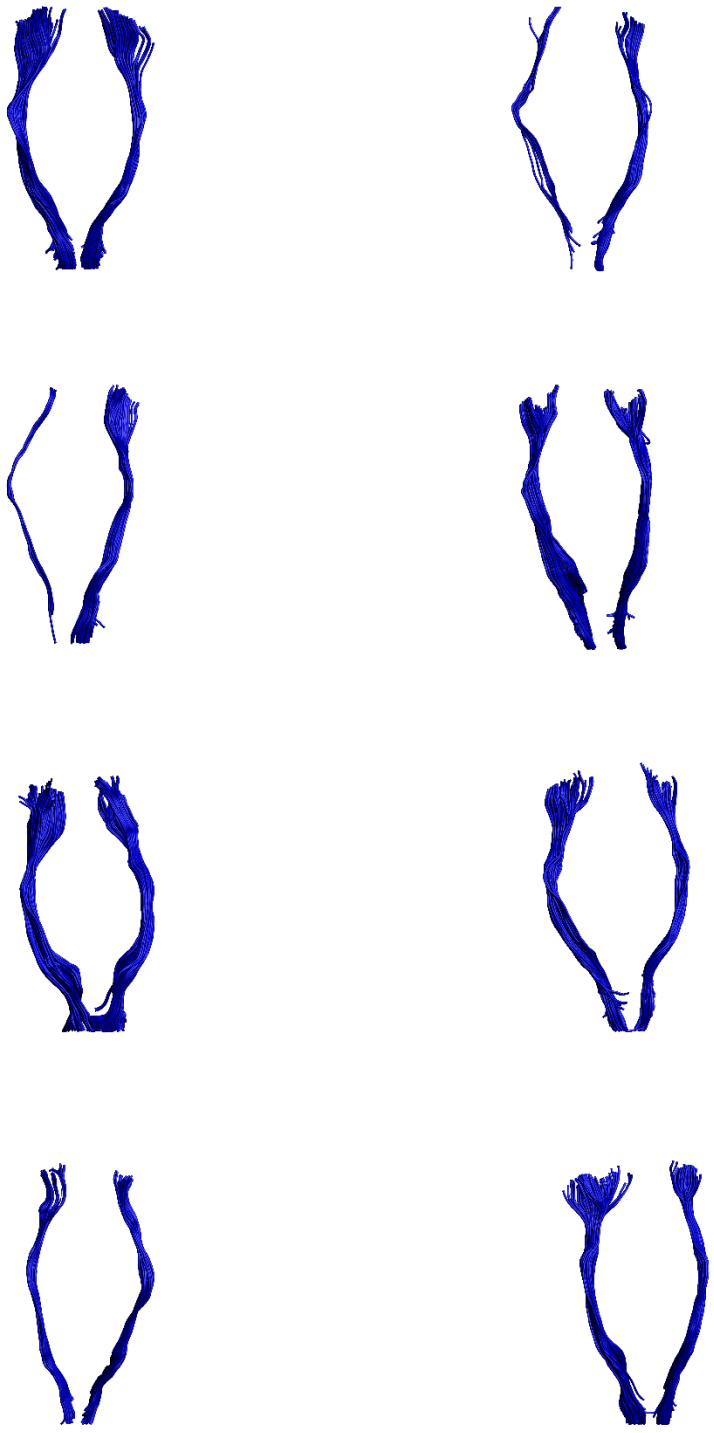

Figure 2.16 – The delineated bilateral corticospinal tract in the control group.

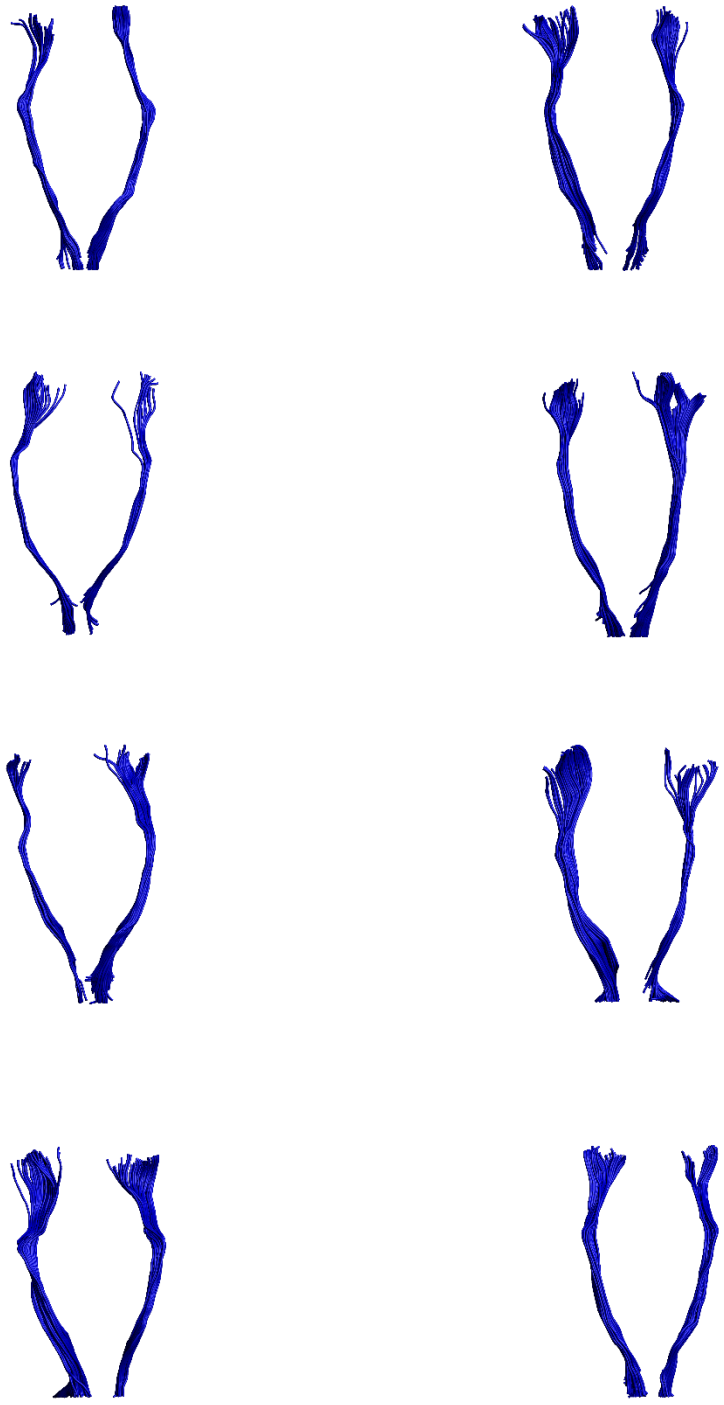

Figure 2.17 – The CST delineated in AWS.

All of the tracts in all of the participants were successfully traced, except for the long segment of the right arcuate fasciculus in one control and one AWS subject.

After isolating all the tracts, the diffusion tensor-based measures (FA, MD, AD and RD) and tract morphology-based measures (tract length and tract volume) were extracted using ExploreDTI. In order to extract the kurtosis tensor-based measures (MK, AK and RK), I created the MK, AK and RK maps using the United DKI (DKIu) MATLAB toolbox (Neto-Henriques, Ferreira, & Correia, 2015; Neto Henriques, Correia, Nunes, & Ferreira, 2015) and then, using a MATLAB script that I developed myself, overlaid the maps onto the tract masks extracted from ExploreDTI and then calculated the kurtosis tensor-based measures of the tracts as much the same way as one can extract diffusion tensor-based measures using ExploreDTI. The measures were then combined in a spreadsheet for all of the participants.

In order to further measure the laterality of the tracts of interest, I used the laterality index (LI) calculation using the following equation (Jansen et al., 2006; Sreedharan, Menon, James, Kesavadas, & Thomas, 2015):

$$\mathrm{LI} = \frac{\mathrm{L} - \mathrm{R}}{\mathrm{L} + \mathrm{R}} \qquad (2.1)$$

In this equation, L is the value of the measure (e.g. tract volume) in the left hemisphere and R is the value of the same measure in the right hemisphere. The tract is considered left-lateralized if $LI >= 0.1$ and right-lateralized if $LI =< -0.1$ and bilateral in between (Sreedharan et al., 2015; Szaflarski, Holland, Schmithorst, & Byars, 2006).

As per the behavioural data, the PPVT standard scores, the digit span scores and the time per each movement on the 5 block task of the Towers of Hanoi game (time divided by the number of movements the participant made during playing the second level of the game) were also added to the spreadsheet.

2.4.2 Statistical Analysis

IBM SPSS Statistics for Windows, version 23 (IBM Corp. 2015. Armonk, NY) was used for statistical analysis. The diffusion- and the kurtosis-tensor-based measures for the five tracts on each hemisphere of the brain (anterior segment of arcuate fasciculus, posterior

segment of arcuate fasciculus, long segment of arcuate fasciculus, FAT and CST) were separately compared using 20 and 15 (respectively) mixed analysis of variance (ANOVA) with hemisphere being the within-subjects measure and group as the between-subjects measure. Therefore, the results were adjusted using the Bonferroni correction ($p = \frac{.05}{20} = .0025$ for diffusion-tensor-based measures and $p = \frac{.05}{15} = .0033$ for kurtosis-tensor-based measures). The conservative approach of correction for multiple comparisons was chosen in order to decrease the possibility of making type I errors. The tract morphology related measures were also compared using a set of 10 mixed ANOVAs (five tracts and two measures). The Bonferroni correction dictated that the significance level be at $p = \frac{.05}{10} = .005$ in this case. Any interactions observed in the results were followed up with post-hoc *t*-tests between groups and hemispheres. The measures extracted from the genu, body and splenium of corpus callosum were separately compared using student's t-tests and thus the significance level was set to be at $p = \frac{.05}{3} = .017$. The behavioural data (the PPVT, Towers of Hanoi and digit span task scores) were also analyzed using a set of three student's t-tests. Therefore, the significance level for these analyses were also set to $p = \frac{.05}{3} = .017$. Pearson's correlations were investigated between the OASES impact scores and RK in the left and the right FAT.

3 Results

3.1 Behavioural data results

The behavioural data analysis showed no significant differences between the two groups and thus, Table 3.1 only shows the mean and the standard deviation of the PPVT, the digit span task and the Towers of Hanoi game scores for AWS and for controls.

Table 3.1 – Mean and standard deviation of the scores for the PPVT, Digit Span Task and Towers of Hanoi game scores.

Mean ± Standard deviation

	PPVT Standard Score	Digit Span Task Score	Towers of Hanoi Game Score
Control	113.75 ± 9.48	29.12 ± 3.83	2.12 ± 0.51
AWS	105.25 ± 5.28	28.75 ± 7.70	2.69 ± 0.57

3.2 Tractography results

3.2.1 Diffusion tensor based measures

The mean and standard deviation of the diffusion tensor based measures are reported below in Table 3.2 thru Table 3.9, separated by tracts. It is noteworthy that the unit for the reported MD, AD and RD is $\mu m^2/ms$. Results of the mixed ANOVAs used for the diffusion-tensor-based measures are summarized in Table 3.10. Since this study included only two conditions for the ANOVAs, the sphericity assumption is met. There was a hemispheric effect in the AD and MD of the long segment of the arcuate fasciculus and the CST and the MD of the anterior segment of the arcuate fasciculus. More specifically, AD and MD were higher in the long segment of the left arcuate fasciculus and the left CST compared to their right counterpart in the combined AWS and control group. Also, MD was found to be higher in the anterior segment of the left arcuate fasciculus relative to its right counterpart in the combined AWS and control group. The t-tests applied to the measures extracted from all the three parts of the corpus callosum (genu, splenium and body) did not show any differences between the groups.

Table 3.2 – The Mean ± Standard Deviation of the diffusion measures in the long segment of the arcuate fasciculus.

Measure	Group	Hemisphere	
		Left	Right
FA	AWS	0.526 ± 0.030	0.517 ± 0.031
	Control	0.523 ± 0.024	0.509 ± 0.025
MD	AWS	0.877 ± 0.023	0.831 ± 0.033
	Control	0.877 ± 0.023	0.829 ± 0.033
AD	AWS	1.435 ± 0.050	1.354 ± 0.039
	Control	1.437 ± 0.049	1.346 ± 0.036
RD	AWS	0.598 ± 0.027	0.569 ± 0.039
	Control	0.596 ± 0.026	0.570 ± 0.039

Table 3.3 – The Mean ± Standard Deviation of the diffusion measures in the anterior segment of the arcuate fasciculus.

Measure	Group	Hemisphere	
		Left	Right
FA	AWS	0.498 ± 0.032	0.501 ± 0.024
	Control	0.495 ± 0.024	0.506 ± 0.021
MD	AWS	0.860 ± 0.026	0.825 ± 0.033
	Control	0.860 ± 0.025	0.822 ± 0.032
AD	AWS	1.369 ± 0.054	1.317 ± 0.052
	Control	1.378 ± 0.041	1.312 ± 0.050
RD	AWS	0.606 ± 0.030	0.578 ± 0.031
	Control	0.602 ± 0.029	0.577 ± 0.031

Table 3.4 – The Mean ± Standard Deviation of the diffusion measures in the posterior segment of the arcuate fasciculus.

Measure	Group	Hemisphere	
		Left	Right
FA	AWS	0.485 ± 0.025	0.478 ± 0.032
	Control	0.478 ± 0.020	0.468 ± 0.033
MD	AWS	0.886 ± 0.025	0.883 ± 0.032
	Control	0.886 ± 0.025	0.882 ± 0.032
AD	AWS	1.406 ± 0.029	1.387 ± 0.043
	Control	1.405 ± 0.030	1.378 ± 0.039
RD	AWS	0.626 ± 0.031	0.631 ± 0.043
	Control	0.627 ± 0.031	0.634 ± 0.041

Table 3.5 – The Mean ± Standard Deviation of the diffusion measures in the FAT.

Measure	Group	Hemisphere	
		Left	Right
FA	AWS	0.490 ± 0.016	0.455 ± 0.045
	Control	0.469 ± 0.030	0.447 ± 0.028
MD	AWS	0.814 ± 0.024	0.812 ± 0.037
	Control	0.813 ± 0.023	0.812 ± 0.037
AD	AWS	1.288 ± 0.026	1.243 ± 0.037
	Control	1.282 ± 0.019	1.242 ± 0.037
RD	AWS	0.576 ± 0.030	0.597 ± 0.053
	Control	0.578 ± 0.030	0.597 ± 0.053

Table 3.6 – The Mean ± Standard Deviation of the diffusion measures in the CST.

Measure	Group	Hemisphere	
		Left	Right
FA	AWS	0.585 ± 0.018	0.574 ± 0.021
	Control	0.577 ± 0.021	0.563 ± 0.019
MD	AWS	0.859 ± 0.011	0.842 ± 0.019
	Control	0.860 ± 0.011	0.845 ± 0.017
AD	AWS	1.514 ± 0.029	1.474 ± 0.049
	Control	1.518 ± 0.027	1.481 ± 0.043
RD	AWS	0.532 ± 0.018	0.526 ± 0.019
	Control	0.530 ± 0.017	0.527 ± 0.020

Table 3.7 – The Mean ± Standard Deviation of the diffusion measures in the body of corpus callosum.

Measure	Group	
	AWS	Control
FA	0.568 ± 0.014	0.565 ± 0.010
MD	0.911 ± 0.036	0.918 ± 0.030
AD	1.586 ± 0.060	1.595 ± 0.052
RD	0.574 ± 0.030	0.579 ± 0.026

Table 3.8 – The Mean ± Standard Deviation of the diffusion measures in the genu of corpus callosum.

Measure	Group	
	AWS	Control
FA	0.543 ± 0.023	0.533 ± 0.016
MD	0.956 ± 0.029	0.961 ± 0.026
AD	1.614 ± 0.043	1.622 ± 0.037
RD	0.626 ± 0.034	0.630 ± 0.034

Table 3.9 – The Mean ± Standard Deviation of the diffusion measures in the splenium of corpus callosum.

Measure	Group	
	AWS	Control
FA	0.566 ± 0.013	0.571 ± 0.017
MD	1.027 ± 0.036	1.026 ± 0.037
AD	1.776 ± 0.065	1.780 ± 0.063
RD	0.652 ± 0.027	0.649 ± 0.026

Table 3.10 – Results of the diffusion-tensor-based measures' comparisons.

*lAF: long segment of the arcuate fasciculus, aAF: anterior segment of the arcuate fasciculus, pAF: posterior segment of the arcuate fasciculus, CST: corticospinal tract, FAT: frontal aslant tract, bCC: body of corpus callosum, gCC: genu of corpus callosum, sCC: splenium of corpus callosum, n. s.: not significant at the level of the adjusted p-value, *: significant at the adjusted p-value level, the p-values without any symbols are not significant at the level of p<.05.*

Tract	Measure	Hemispheric Effect Statistics	Group Effect Statistics	Interaction Statistics
lAF	**FA**	$p = .377$ $F(1,12) = 0.840$	$p = 0.818$ $F(1,12) = 0.055$	$p = .547$ $F(1,12) = 0.384$
	MD	$p < .001*$ $F(1,12) = 19.70$	$p = .271$ $F(1,12) = 1.331$	$p = .891$ $F(1,12) = 0.020$
	AD	$p < .001*$ $F(1,12) = 41.950$	$p = .129$ $F(1,12) = 2.658$	$p = .869$ $F(1,12) = 0.029$
	RD	$p = .026\ (n.s.)$ $F(1,12) = 6.495$	$p = .560$ $F(1,12) = 0.359$	$p = .795$ $F(1,12) = 0.070$
aAF	**FA**	$p = .438$ $F(1,14) = 0.636$	$p = .919$ $F(1,14) = 0.011$	$p = .710$ $F(1,12) = 0.144$
	MD	$p < .001*$ $F(1,14) = 21.98$	$p = .142$ $F(1,14) = 2.423$	$p = .663$ $F(1,14) = 0.198$
	AD	$p = .016\ (n.s.)$ $F(1,14) = 7.540$	$p = .120$ $F(1,14) = 2.735$	$p = .522$ $F(1,14) = 0.430$
	RD	$p = .006\ (n.s.)$ $F(1,14) = 10.262$	$p = .272$ $F(1,14) = 1.305$	$p = .967$ $F(1,14) = 0.002$

Tract	Measure	Hemispheric Effect Statistics	Group Effect Statistics	Interaction Statistics
pAF	FA	$p = .296$ $F(1, 14) = 1.176$	$p = .464$ $F(1, 14) = 0.567$	$p = .841$ $F(1, 14) = 0.042$
	MD	$p = .315$ $F(1, 14) = 1.087$	$p = .242$ $F(1, 14) = 1.494$	$p = .495$ $F(1, 14) = 0.490$
	AD	$p = .110$ $F(1, 14) = 2.908$	$p = .027\ (n.s.)$ $F(1, 14) = 6.098$	$p = .659$ $F(1, 14) = 0.203$
	RD	$p = .925$ $F(1, 14) = 0.009$	$p = .696$ $F(1, 14) = 0.160$	$p = .602$ $F(1, 14) = 0.285$
FAT	FA	$p = .003\ (n.s.)$ $F(1, 14) = 13.18$	$p = .315$ $F(1, 14) = 1.087$	$p = .454$ $F(1, 14) = 0.593$
	MD	$p = .705$ $F(1, 14) = 0.149$	$p = .674$ $F(1, 14) = 0.185$	$p = .868$ $F(1, 14) = 0.029$
	AD	$p = .006\ (n.s.)$ $F(1, 14) = 10.578$	$p = .831$ $F(1, 14) = 0.047$	$p = .725$ $F(1, 14) = 0.129$
	RD	$p = .062$ $F(1, 14) = 4.101$	$p = .501$ $F(1, 14) = 0.477$	$p = .648$ $F(1, 14) = 0.217$
CST	FA	$p = .090$ $F(1, 14) = 3.314$	$p = .181$ $F(1, 14) = 1.977$	$p = .797$ $F(1, 14) = 0.069$
	MD	$p = .002 *$ $F(1, 14) = 15.249$	$p = .118$ $F(1, 14) = 2.780$	$p = .402$ $F(1, 14) = 0.747$
	AD	$p < .001 *$ $F(1, 14) = 16.244$	$p = .839$ $F(1, 14) = 0.043$	$p = .312$ $F(1, 14) = 1.101$
	RD	$p = .467$ $F(1, 14) = 0.558$	$p = .117$ $F(1, 14) = 2.791$	$p = .986$ $F(1, 14) = 0.0003$
bCC	FA	N/A	$p = .710$ $t(14) = -0.379$	N/A
	MD	N/A	$p = .840$ $t(14) = -0.205$	N/A

Tract	Measure	Hemispheric Effect Statistics	Group Effect Statistics	Interaction Statistics
bCC	**AD**	N/A	$p = .864$ $t(14) = -0.174$	N/A
	RD	N/A	$p = .838$ $t(14) = -0.208$	N/A
gCC	**FA**	N/A	$p = .373$ $t(14) = -0.921$	N/A
	MD	N/A	$p = .537$ $t(14) = 0.632$	N/A
	AD	N/A	$p = .660$ $t(14) = 0.450$	N/A
	RD	N/A	$p = .519$ $t(14) = 0.662$	N/A
sCC	**FA**	N/A	$p = .524$ $t(14) = 0.654$	N/A
	MD	N/A	$p = .293$ $t(14) = -1.093$	N/A
	AD	N/A	$p = .436$ $t(14) = -0.802$	N/A
	RD	N/A	$p = .249$ $t(14) = -1.202$	N/A

3.2.2 Kurtosis tensor based measures

The mean and standard deviation of the kurtosis measures are reported below in Table 3.11 thru Table 3.18, separated by the tract. Results of the mixed ANOVAs carried out on the kurtosis-tensor-based measures are summarized in Table 3.19. The results of these investigations showed that there was a hemisphere by group interaction in the AK of the FAT (Figure 3.1). Post-hoc t-tests showed that the left FAT had higher AK in AWS compared to controls ($t(14) = -2.18$, $p = .024$, one-tailed, adjusted) and that the AWS had higher AK

in their left FAT compared to their right FAT ($t(7) = 3.91$, $p = .006$, two-tailed, adjusted) (Figure 3.2). Hemispheric effects were also observed in the RK of FAT. The t-tests applied to the measures extracted from the corpus callosum did not yield any significant differences between the two groups.

Table 3.11 – The Mean ± Standard Deviation of the kurtosis measures in the long segment of the arcuate fasciculus.

Measure	Group	Hemisphere	
		Left	Right
MK	AWS	1.141 ± 0.537	1.058 ± 0.175
	Control	0.966 ± 0.045	0.969 ± 0.047
AK	AWS	0.704 ± 0.079	0.740 ± 0.047
	Control	0.730 ± 0.015	0.747 ± 0.026
RK	AWS	1.358 ± 0.100	1.419 ± 0.059
	Control	1.376 ± 0.099	1.374 ± 0.070

Table 3.12 – The Mean ± Standard Deviation of the kurtosis measures in the anterior segment of the arcuate fasciculus.

Measure	Group	Hemisphere	
		Left	Right
MK	AWS	1.057 ± 0.346	0.961 ± 0.080
	Control	0.961 ± 0.054	0.960 ± 0.019
AK	AWS	0.717 ± 0.027	0.737 ± 0.020
	Control	0.723 ± 0.021	0.746 ± 0.020
RK	AWS	1.260 ± 0.166	1.337 ± 0.163
	Control	1.319 ± 0.126	1.375 ± 0.044

Table 3.13 – The Mean ± Standard Deviation of the kurtosis measures in the posterior segment of the arcuate fasciculus.

Measure	Group	Hemisphere	
		Left	Right
MK	AWS	0.988 ± 0.254	0.940 ± 0.093
	Control	0.881 ± 0.045	0.910 ± 0.051
AK	AWS	0.660 ± 0.030	0.675 ± 0.020
	Control	0.672 ± 0.016	0.677 ± 0.024
RK	AWS	1.187 ± 0.106	1.213 ± 0.112
	Control	1.151 ± 0.087	1.206 ± 0.096

Table 3.14 – The Mean ± Standard Deviation of the kurtosis measures in the FAT.

Measure	Group	Hemisphere	
		Left	Right
MK	AWS	0.950 ± 0.099	0.926 ± 0.104
	Control	0.932 ± 0.055	0.904 ± 0.031
AK	AWS	0.736 ± 0.027	0.714 ± 0.022
	Control	0.705 ± 0.031	0.726 ± 0.029
RK	AWS	1.196 ± 0.113	1.122 ± 0.085
	Control	1.232 ± 0.080	1.147 ± 0.072

Table 3.15 – The Mean ± Standard Deviation of the kurtosis measures in the CST.

Measure	Group	Hemisphere	
		Left	Right
MK	AWS	1.120 ± 0.353	1.168 ± 0.500
	Control	0.968 ± 0.041	0.953 ± 0.034
AK	AWS	0.641 ± 0.070	0.639 ± 0.074
	Control	0.659 ± 0.012	0.662 ± 0.018
RK	AWS	1.435 ± 0.125	1.451 ± 0.067
	Control	1.412 ± 0.067	1.373 ± 0.098

Table 3.16 – The Mean ± Standard Deviation of the kurtosis measures in the body of corpus callosum.

Measure	Group	
	AWS	**Control**
MK	1.019 ± 0.326	0.911 ± 0.042
AK	0.602 ± 0.049	0.619 ± 0.016
RK	1.444 ± 0.100	1.482 ± 0.091

Table 3.17 – The Mean ± Standard Deviation of the kurtosis measures in the genu of corpus callosum.

Measure	Group	
	AWS	**Control**
MK	1.031 ± 0.478	0.849 ± 0.023
AK	0.604 ± 0.044	0.619 ± 0.013
RK	1.294 ± 0.151	1.257 ± 0.057

Table 3.18 – The Mean ± Standard Deviation of the kurtosis measures in the splenium of corpus callosum.

Measure	Group	
	AWS	**Control**
MK	1.090 ± 0.561	0.880 ± 0.023
AK	0.542 ± 0.053	0.562 ± 0.010
RK	1.411 ± 0.043	1.368 ± 0.050

Table 3.19 – Results of the comparisons on kurtosis-tensor-based measures.

*lAF: long segment of the arcuate fasciculus, aAF: anterior segment of the arcuate fasciculus, pAF: posterior segment of the arcuate fasciculus, CST: corticospinal tract, FAT: frontal aslant tract, bCC: body of corpus callosum, gCC: genu of corpus callosum, sCC: splenium of corpus callosum, n. s.: not significant at the level of the adjusted p-value, *: significant at the adjusted p-value level, the p-values without any symbols are not significant at the level of p<.05.*

Tract	Measure	Hemispheric Effect Statistics	Group Effect Statistics	Interaction Statistics
lAF	MK	$p = .445$ $F(1, 12) = 0.624$	$p = .309$ $F(1, 12) = 1.129$	$p = .430$ $F(1, 12) = 0.666$
	AK	$p = .041\ (n.s.)$ $F(1, 12) = 5.237$	$p = .441$ $F(1, 12) = 0.635$	$p = .356$ $F(1, 12) = 0.923$
	RK	$p = .387$ $F(1, 12) = 0.804$	$p = .622$ $F(1, 12) = 0.256$	$p = .299$ $F(1, 12) = 1.177$
aAF	MK	$p = .374$ $F(1, 14) = 0.842$	$p = .514$ $F(1, 14) = 0.448$	$p = .386$ $F(1, 14) = 0.802$
	AK	$p = .007\ (n.s.)$ $F(1, 14) = 9.937$	$p = .416$ $F(1, 14) = 0.702$	$p = .864$ $F(1, 14) = 0.031$
	RK	$p = .068$ $F(1, 14) = 3.916$	$p = .415$ $F(1, 14) = 0.706$	$p = .760$ $F(1, 14) = 0.097$
pAF	MK	$p = .757$ $F(1, 14) = 0.099$	$p = .289$ $F(1, 14) = 1.215$	$p = .238$ $F(1, 14) = 1.523$
	AK	$p = .132$ $F(1, 14) = 2.562$	$p = .497$ $F(1, 14) = 0.487$	$p = .435$ $F(1, 14) = 0.646$
	RK	$p = .085$ $F(1, 14) = 3.440$	$p = .646$ $F(1, 14) = 0.220$	$p = .523$ $F(1, 14) = 0.430$
FAT	MK	$p = .048\ (n.s.)$ $F(1, 14) = 4.684$	$p = .595$ $F(1, 14) = 0.296$	$p = .868$ $F(1, 14) = 0.029$
	AK	$p = .937$ $F(1, 14) = 0.007$	$p = .438$ $F(1, 14) = 0.637$	$p = .001 *$ $F(1, 14)$ $= 15.982$
	RK	$p = .003 *$ $F(1, 14) = 13.137$	$p = .439$ $F(1, 14) = 0.633$	$p = .802$ $F(1, 14) = 0.066$

Tract	Measure	Hemispheric Effect Statistics	Group Effect Statistics	Interaction Statistics
CST	**MK**	$p = .579$ $F(1, 14) = 0.322$	$p = .245$ $F(1, 14) = 1.473$	$p = .286$ $F(1, 14) = 1.231$
	AK	$p = .904$ $F(1, 14) = 0.015$	$p = .442$ $F(1, 14) = 0.626$	$p = .569$ $F(1, 14) = 0.340$
	RK	$p = .715$ $F(1, 14) = 0.139$	$p = .175$ $F(1, 14) = 2.040$	$p = .368$ $F(1, 14) = 0.867$
bCC	**MK**	N/A	$p = .368$ $t(14) = -0.930$	N/A
	AK	N/A	$p = .378$ $t(14) = 0.911$	N/A
	RK	N/A	$p = .440$ $t(14) = 0.795$	N/A
gCC	**MK**	N/A	$p = .299$ $t(14) = -1.078$	N/A
	AK	N/A	$p = .360$ $t(14) = 0.946$	N/A
	RK	N/A	$p = .522$ $t(14) = -0.657$	N/A
sCC	**MK**	N/A	$p = .308$ $t(14) = -1.057$	N/A
	AK	N/A	$p = .315$ $t(14) = 1.042$	N/A
	RK	N/A	$p = .090$ $t(14) = -1.818$	N/A

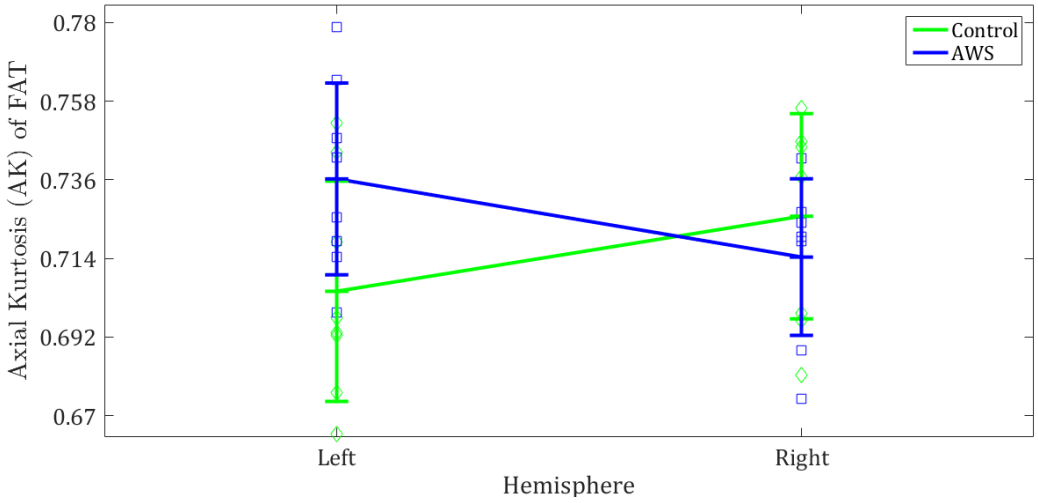

Figure 3.1 – Graph showing the hemisphere by group interaction in the AK of the FAT.

The green diamonds are the data points showing the AK of FAT in controls and the blue squares represent the data points for the AK in AWS. The central line represents the mean and the upper and lower lines demonstrate the standard deviation.

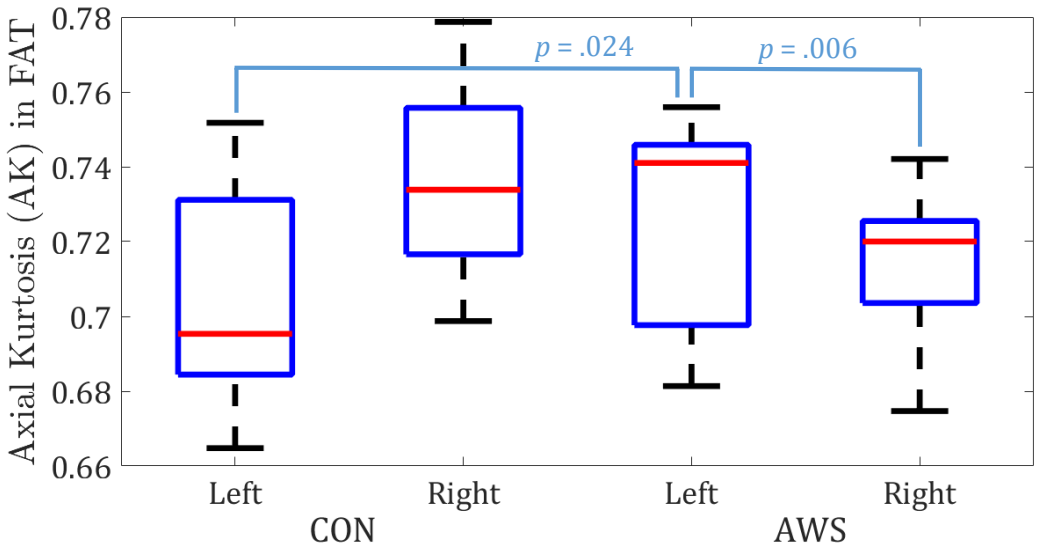

Figure 3.2 – Boxplot demonstrating the post-hoc t-test results of the AK in FAT hemisphere by group interaction.

On each box, the central mark (red) is the median, the edges of the box are the 25th and 75th percentiles and the whiskers extend to the extreme data points. There are no outliers here.

3.2.3 Results pertaining to tract morphology

The mean and standard deviation of the tract morphology measures are reported below in Table 3.20 thru Table 3.27, separated by tracts. Results of the investigations on tract length and tract volume are summarized in Table 3.28. Hemispheric effects were observed in the tract volume of both the anterior and the long segments of the arcuate fasciculus. Again, t-tests on the three parts of the corpus callosum did not show any significant results.

Table 3.20 – The Mean ± Standard Deviation of the tract morphology measures in the long segment of the arcuate fasciculus.

Measure	Group	Hemisphere	
		Left	Right
Tract Volume	AWS	6793 ± 2627	2844 ± 1919
	Control	7101 ± 3579	4079 ± 2327
Tract Length	AWS	119.486 ± 9.409	112.938 ± 9.108
	Control	114.807 ± 10.255	110.238 ± 5.028

Table 3.21 – The Mean ± Standard Deviation of the tract morphology measures in the anterior segment of the arcuate fasciculus.

Measure	Group	Hemisphere	
		Left	Right
Tract Volume	AWS	3577 ± 2568	6352 ± 2487
	Control	5649 ± 3314	8275 ± 2981
Tract Length	AWS	81.503 ± 8.917	74.940 ± 10.386
	Control	75.840 ± 10.395	78.202 ± 4.080

Table 3.22 – The Mean ± Standard Deviation of the tract morphology measures in the posterior segment of the arcuate fasciculus.

Measure	Group	Hemisphere	
		Left	Right
Tract Volume	AWS	9866 ± 2948	6641 ± 2946
	Control	8165 ± 3130	6499 ± 2683
Tract Length	AWS	65.579 ± 3.707	58.801 ± 6.014
	Control	61.337 ± 5.180	56.014 ± 5.927

Table 3.23 – The Mean ± Standard Deviation of the kurtosis measures in the FAT.

Measure	Group	Hemisphere	
		Left	Right
Tract Volume	AWS	4285 ± 1483	3795 ± 2348
	Control	5730 ± 2302	3891 ± 1614
Tract Length	AWS	72.358 ± 2.664	68.061 ± 5.361
	Control	71.973 ± 6.448	68.254 ± 4.346

Table 3.24 – The Mean ± Standard Deviation of the kurtosis measures in the CST.

Measure	Group	Hemisphere	
		Left	Right
Tract Volume	AWS	5241 ± 1053	5521 ± 2130
	Control	6673 ± 1619	7585 ± 4076
Tract Length	AWS	110.842 ± 3.546	112.758 ± 3.413
	Control	111.304 ± 4.038	109.459 ± 2.542

Table 3.25 – The Mean ± Standard Deviation of the kurtosis measures in the body of corpus callosum.

Measure	Group	
	AWS	Control
Tract Volume	49941 ± 6389	50182 ± 9976
Tract Length	96.915 ± 5.996	93.877 ± 8.979

Table 3.26 – The Mean ± Standard Deviation of the kurtosis measures in the genu of corpus callosum.

Measure	Group	
	AWS	Control
Tract Volume	28806 ± 2673	28007 ± 6111
Tract Length	91.415 ± 9.112	84.169 ± 7.580

Table 3.27 – The Mean ± Standard Deviation of the kurtosis measures in the splenium of corpus callosum.

Measure	Group	
	AWS	Control
Tract Volume	70273 ± 5550	68761 ± 6316
Tract Length	126.308 ± 5.429	125.126 ± 6.185

Table 3.28 – Results of the comparisons on tract morphology measures.

*lAF: long segment of the arcuate fasciculus, aAF: anterior segment of the arcuate fasciculus, pAF: posterior segment of the arcuate fasciculus, CST: corticospinal tract, FAT: frontal aslant tract, n. s.: not significant at the level of the adjusted p-value. *: significant at the adjusted p-value level, p-values without any symbols are not significant at the level of p<.05.*

Tract	Measure	Hemispheric Effect Statistics	Group Effect Statistics	Interaction Statistics
lAF	**Tract Volume**	$p = .004 *$ $F(1, 12) = 12.95$	$p = .532$ $F(1, 12) = 0.415$	$p = .625$ $F(1, 12) = 0.252$
	Tract Length	$p = .147$ $F(1, 12) = 2.400$	$p = .214$ $F(1, 12) = 1.724$	$p = .672$ $F(1, 12) = 0.188$
aAF	**Tract Volume**	$p = .002 *$ $F(1, 14) = 15.001$	$p = .131$ $F(1, 14) = 2.568$	$p = .917$ $F(1, 14) = 0.011$
	Tract Length	$p = .584$ $F(1, 14) = 0.314$	$p = .615$ $F(1, 14) = 0.265$	$p = .254$ $F(1, 14) = 1.417$
pAF	**Tract Volume**	$p = .016\ (n.s.)$ $F(1, 14) = 7.56$	$p = .442$ $F(1, 14) = 0.626$	$p = .396$ $F(1, 14) = 0.768$
	Tract Length	$p = .005\ (n.s.)$ $F(1, 14) = 10.89$	$p = .086$ $F(1, 14) = 3.403$	$p = .697$ $F(1, 14) = 0.158$
FAT	**Tract Volume**	$p = .067$ $F(1, 14) = 3.949$	$p = .349$ $F(1, 14) = 0.938$	$p = .269$ $F(1, 14) = 1.324$
	Tract Length	$p = .02\ (n.s.)$ $F(1, 14) = 6.902$	$p = .961$ $F(1, 14) = 0.003$	$p = .852$ $F(1, 14) = 0.036$
CST	**Tract Volume**	$p = .412$ $F(1, 14) = 0.714$	$p = .111$ $F(1, 14) = 2.892$	$p = .661$ $F(1, 14) = 0.201$
	Tract Length	$p = .975$ $F(1, 14) = 0.001$	$p = .294$ $F(1, 14) = 1.190$	$p = .114$ $F(1, 14) = 2.837$
bCC	**Tract Volume**	N/A	$p = .955$ $t(14) = 0.057$	N/A
	Tract Length	N/A	$p = .439$ $t(14) = -0.796$	N/A

Tract	Measure	Hemispheric Effect Statistics	Group Effect Statistics	Interaction Statistics
gCC	**Tract Volume**	N/A	$p = .740$ $t(14) = -0.339$	N/A
	Tract Length	N/A	$p = .106$ $t(14) = -1.729$	N/A
sCC	**Tract Volume**	N/A	$p = .619$ $t(14) = -0.509$	N/A
	Tract Length	N/A	$p = .691$ $t(14) = -0.406$	N/A

The laterality indices (LI) for the different kurtosis, diffusion and tract morphology based measures showed that the anterior segment of the arcuate fasciculus is a right-lateralized tract based on tract volume ($LI = -0.2$), while the long segment of the arcuate fasciculus is left-lateralized based on the same measure ($LI = 0.3$), all in the combined control and AWS group (Figure 3.3 shows the post-hoc *t*-test results on the mentioned segments of the arcuate fasciculus). Also, the posterior segment of the arcuate fasciculus as well as the FAT were shown to be left-lateralized based on tract volume ($LI = 0.1$). None of the other LI values passed the threshold of 0.1 or -0.1 (Table 3.29).

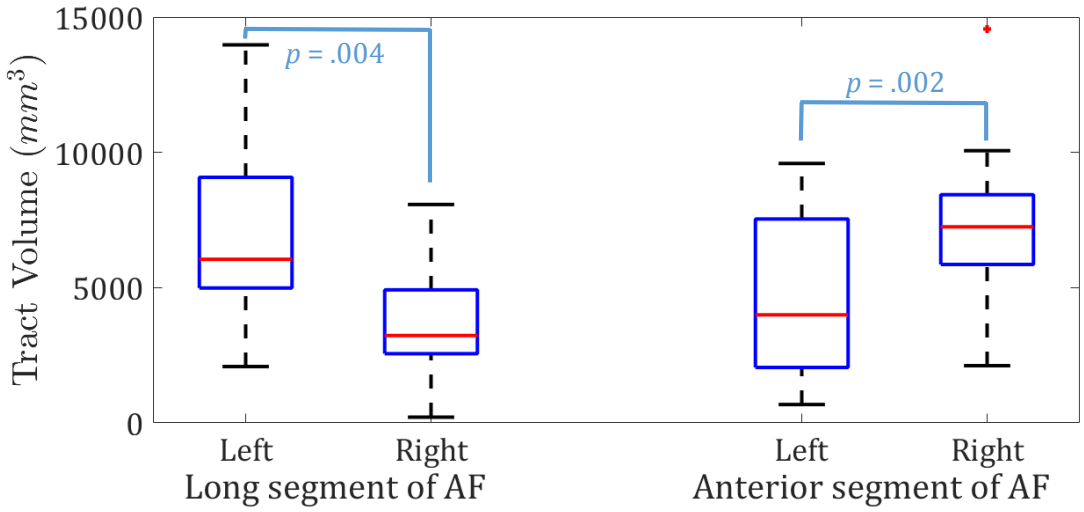

Figure 3.3 – Boxplot indicating the lateralization of the long and anterior segments of arcuate fasciculus.

AF: Arcuate Fasciculus. On each box, the central mark (red) is the median, the edges of the box represent the 25th and 75th percentiles and the whiskers extend to the extreme data points. There is only one outlier here, which is shown using a red data point.

Table 3.29 – Laterality indices for the different tracts based on diffusion tensor-, kurtosis tensor- and tract morphology-based results.

lAF: long segment of arcuate fasciculus, aAF: anterior segment of arcuate fasciculus, pAF: posterior segment of arcuate fasciculus, FAT: frontal aslant tract, CST: corticospinal tract.

Tract	LI Values based on								
	FA	MD	AD	RD	MK	AK	RK	Tract Volume	Tract Length
lAF	0.011	0.027	0.03	0.024	0.019	-0.018	-0.011	0.335	0.024
aAF	-0.007	0.019	0.016	0.024	0.025	-0.015	-0.025	-0.226	0.014
pAF	0.009	0.005	0.009	-0.001	0.005	-0.007	-0.017	0.157	0.05
FAT	0.031	0.002	0.016	-0.014	0.014	0.0003	0.034	0.132	0.029
CST	0.011	0.012	0.018	0.005	-0.008	-0.0004	0.004	-0.048	-0.0002

3.3 Correlations between tractography metrics and behavioural results

Correlational analyses showed that the OASES scores were negatively correlated with RK in only the right FAT ($r = -.74$, $p = .019$, one-tailed, corrected, Figure 3.4). The correlation between the OASES scores and RK in the left FAT was not statistically significant ($r = -.107$, $p = .802$).

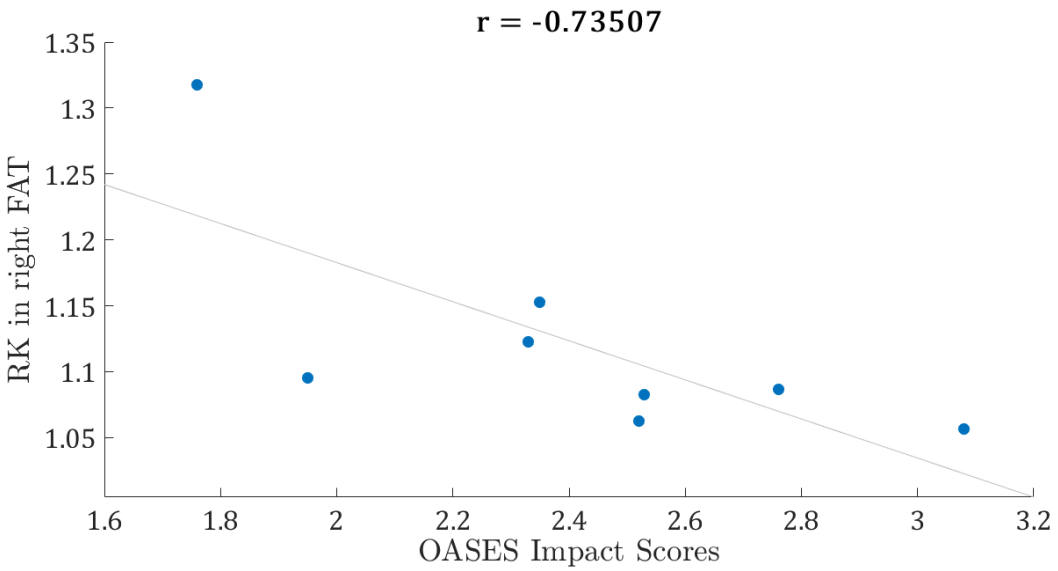

Figure 3.4 – Scatter plot showing the correlation between OASES impact scores and RK in the right FAT in the AWS group.

4 Discussion

In this project, I acquired behavioural (for the purpose of matching the two groups) and DKI data and then, looked into the differences that may be present in the brains of adults who stutter compared to brains of adults who do not stutter. I found that diffusion kurtosis can add useful and important information to the diffusion tensor based analysis of diffusion MRI. The analyses showed that axial kurtosis is higher in the left frontal aslant tract of AWS compared to their right FAT and compared to the left FAT of controls. The OASES impact scores also negatively correlated with the radial kurtosis in the right FAT of AWS. Below, I will discuss the results and their significance in the current literature of speech (disorders) and stuttering and relate them to the previous reports available in the current literature of the field. It is of note that statistical significance is not equal to meaningfulness and/or practical significance. However, the values of the metrics measured in this study are comparable to the previous DKI studies for which raw data is reported (Table 1.2). This study had a small sample size and therefore, it is important to conduct a study with a greater sample size to further corroborate the results obtained here. The study at hand can be used in the calculation of the sample size/power statistics for the said corroboration study.

4.1 AK in the FAT shows a different trend in adults who stutter

While the metrics extracted from the diffusion tensor did not show any major differences between the two groups, the kurtosis metrics showed a hemisphere by group interaction in the AK of the FAT. Further analysis of this result revealed a higher AK in the left FAT of AWS compared to controls. A higher AK in the left FAT of AWS was also observed compared to the right counterpart of this tract in the same group. No between group differences were observed in the right FAT.

The current study was the first to assess kurtosis tensor based measures in developmental stuttering. Examining the literature, at least two DTI studies yielded results that are comparable to those of the current study. A recent DTI study by Kronfeld-Duenias et al. (2016) showed that MD, AD and RD are higher in both the left and right FAT of AWS compared to controls. They concluded that this may mean a reduced tissue density in the connection between the premotor cortex and the Broca's area. A DTI tractography study in

our own lab on CWS showed that FA is higher in the right FAT of CWS compared to the left FAT in the same group and the right FAT of fluent children. The results of the same study also showed that AD is higher in the right FAT of CWS compared to both the left FAT of the same group and the right FAT of fluent controls, while fluent children presented with higher AD values in the left FAT compared to the right FAT in the same group (Misaghi et al., in preparation).

Studies have shown that kurtosis measures (MK, AK and RK) are negatively correlated with diffusion measures (MD, AD and RD) (Falangola et al., 2014; Hui et al., 2008; Pang et al., 2015). The same studies have postulated that neural filament breakdowns, and thus more hindrances in the way of diffusion brought about by the complex cell compartments, is associated with an increase in AK and a decrease in AD (Falangola et al., 2014; Hui et al., 2008; Pang et al., 2015). Increasing AK can also be associated with swelling and 'beading' in the axons causing regions of diffusion dead-zones and decreasing diffusion along the main axis of the axons (Hui et al., 2012; Taoka et al., 2014). Tan et al. (2016) showed that MK, AK and RK increase as the tissue microstructure becomes more complex. However, AK is known to be more sensitive and specific to the restrictions of diffusion than RK and MK (Tan et al., 2015).

As discussed in section 1.1.4.2 of the document, the FAT plays a major role in speech production and connects two important speech areas together (Catani et al., 2012; Catani et al., 2013). Based on the DIVA and GODIVA models, this tract connects the initiation map to the speech sound map (Bohland et al., 2010) and thus the disruption of this tract may imply that the cells in the speech sound map are not being activated in a timely manner by the initiation map. This tract has previously been shown to be deficient in PWS (Kronfeld-Duenias et al., 2016; Misaghi et al., in preparation). This study further corroborates these results using a novel DKI sequence. It also shows that analyses based on DKI are able to show the present differences even in a small sample size, while the diffusion tensor based metrics fail to reach this goal.

4.2 RK in the right FAT is negatively correlated with the impact of stuttering on everyday lives of AWS

The results of this study also indicated that the more severe the impact of stuttering on the everyday lives of individuals who stutter, the lower RK in their right FAT. As mentioned before, the impact of stuttering on the everyday lives of CWS is correlated with stuttering severity (Chun et al., 2010). Stuttering severity has also been shown to be correlated with the deficits in the FAT (Kronfeld-Duenias et al., 2016), such that the severer the stuttering, the more elevated the MD levels in the left FAT. Lower RK is associated with demyelination and/or increased impediments (e.g. broken cell compartments) in the way of the normal diffusion inside the axons (Zhuo et al., 2012) and higher OASES score means a severer impact of stuttering on the person who stutter's everyday life. Therefore, the results of the study at hand show that the more damaged the right FAT of AWS, the more the impact of stuttering on their daily lives and possibly the more the severity of their stuttering. Considering the nature of the results of this study and the Kronfeld-Duenias et al. (2016) study, there is a need for further investigations of the relationship between brain and behaviour in PWS.

4.3 Tract morphology measures predict lateralization of the tracts

I observed many hemispheric effects in the analyses, suggesting that many tracts are lateralized in the combined stuttering and control groups (Please refer to Table 3.10, Table 3.19 and Table 3.28). More specifically, a leftward asymmetry for the long and posterior segments of arcuate fasciculus, the CST and the FAT were observed, while the anterior segment of arcuate fasciculus appeared to be right-lateralized. The LI analysis based on tract volume corroborated the hemispheric effects, except for the CST.

A combined functional-structural study of speech areas (e.g. the arcuate fasciculus) in the brain showed that right-handers present with higher FA, MD and tract volume values in the left hemisphere compared to right hemisphere (James et al., 2015). A recent DTI tractography study also showed higher FA and fiber count in the left arcuate fasciculus

compared to its right counterpart in right-handed people (Shu, Liu, Duan, & Li, 2015). Although these results may tempt us to conclude that the arcuate fasciculus, altogether, is a completely left-lateralized tract, at least in right-handers, we should be careful with that conclusion. Studies have shown that the anterior segment of the arcuate fasciculus is a right-lateralized tract (Catani et al., 2007; Thiebaut de Schotten, Ffytche, et al., 2011), while a portion of the adult population shows bilateral symmetry in the posterior segment of the arcuate fasciculus (Catani et al., 2007). The long segment of the arcuate fasciculus appears to be a left-lateralized tract in most cases (Catani et al., 2007; Catani & Thiebaut de Schotten, 2012; Thiebaut de Schotten, Ffytche, et al., 2011). In the study at hand, I found that RD is greater in the anterior segment of the left arcuate fasciculus compared to its right counterpart. The same tract is more voluminous in the right side compared to the left hemisphere. The laterality index using tract volume in this tract also confirmed that this tract is right-lateralized. The laterality index analysis further confirmed the left-lateralization in the long segment of the arcuate fasciculus. This is in complete agreement with the conclusions made by Catani and Thiebaut de Schotten (2012) and Thiebaut de Schotten, Dell'Acqua, et al. (2011).

I also noticed hemispheric effects in the FAT and the CST. More specifically, I observed a leftward asymmetry based on MK and RK as well as FA, AD, and tract length in the FAT and MD and AD in the CST. Moreover, the LI analysis confirmed the left-lateralization of the FAT based on tract volume. Studies by Angstmann and colleagues and Dubois and colleagues reported a leftward asymmetry in the CST of adolescents (Angstmann et al., 2016) and infants (Dubois et al., 2009). Seizeur et al. (2014) postulated that the CST is left-lateralized in right-handed adults, as well. Catani et al. (2012) also showed that the FAT is a left-lateralized tract. Since the FAT is a recently documented tract, there aren't many studies assessing this tract and thus its lateralization pattern.

In addition to the studies cited above, Caeyenberghs and Leemans (2014) reported a leftward asymmetry for white matter underlying areas such as the precentral gyrus, superior and inferior frontal gyri, and superior temporal gyrus and a rightward asymmetry for white matter underlying the supramarginal and angular gyri. These results are in agreement with the lateralization pattern reported for the arcuate fasciculus discussed above (e.g. the right-

lateralized white matter around Geschwind's territory and the left-lateralized white matter around Broca's and Wernicke's territories) and the patterns observed for the CST (pertaining to the precentral gyrus results in the mentioned study) and the FAT (pertaining to the inferior and superior frontal gyri findings in the mentioned study).

4.4 Remarks about methods and limitations

In this study, I observed a few differences in the metrics that were investigated for the first time in stuttering, while no differences were found in some of the metrics that have been reported previously. This may partly be because of the small sample size in this study, in which case, it shows that DKI is a better and more robust method of assessing the diffusion pattern in the brain white matter, at least in stuttering. The fact that I found group differences based on the kurtosis measures, while no group differences were evident based on the diffusion tensor based measures shows that metrics specific to DKI-only can predict the underlying deficits in PWS, while DTI-only metrics cannot do that at least in small sample sizes.

Differences in the technicalities of methods of imaging (e.g. functional vs. structural, DTI vs. DKI, number of directions in diffusion imaging, image resolution, use of scanners with different field strengths, for more information refer to part 1.2 of the thesis), the method of analysis (e.g. TBSS (Tract-based spatial statistics; Smith et al., 2006) vs. tractography) and the software packages used to analyze the data (e.g. ExploreDTI vs. DKE (Diffusion Kurtosis Estimator; Tabesh, Jensen, Ardekani, & Helpern, 2011) vs. DKIu) are a few important factors contributing to the differences in the results of the studies carried out so far. For example, TBSS identifies focal differences in the white matter between the control and the patient groups (Smith et al., 2006), while using tractography, researchers are able to extract the whole white matter tracts and their diffusion properties (Colby et al., 2012). Furthermore, the TBSS method requires that the images are normalized to a template (e.g. the Montreal Neurological Institute (MNI) template), while tractography can be done without aligning the images to a specific template (Colby et al., 2012). The fact that many histological and virtual dissection (tractography) methods are biased and rater-dependent (e.g. one should have a somewhat clear idea of where the fibers reside before attempting to dissect cadaver brains since the dissection should follow the main fiber orientation to avoid cutting through the

fibers) (Axer et al., 2013) is a limitation of the studies of brain white matter. I have to note that animal studies are not directly relevant to the matter here because even though there have been some improvements in using animal models of speech, we still do not have a generally accepted animal model to study the course of speech production. Yet another reason for the controversies in the studies is that a lesion in a grey and/or white matter area can change the course of development of the brain structure and function (because of the plasticity of the brain) and therefore affect other areas as well, thus when we are looking at the deficits in patient brains we are not sure whether this is the cause of the disorder or it's the result of that disorder and even in terms of the results, is it the initial result or is it secondary to another deficit. Hopefully, further developments in the field will address these issues.

Our participants were scanned using a 4.7T scanner, which theoretically provides a reasonable resolution and number of directions in a DKI sequence. However, the current DKI specific software packages are not able to trace the tracts based on the kurtosis tensor, yet, which is why I used ExploreDTI, which traces the tracts based on the diffusion tensor.

Apart from the methods themselves, the population studied and the number of participants in each group are also important factors. For example, because of the difficulty of recruiting AWS using more robust and conservative inclusion criteria, we were liberal in terms of the languages other than English our participants spoke, their level of stuttering and whether they had family members who stuttered or not. Even with this much liberalism, we could not recruit more than 16 matched participants.

4.5 Conclusions and Suggestions for Future Work

In this project, I studied a group of 8 AWS and 8 controls matched based on age and the level of education. A diffusion kurtosis imaging sequence was used to look into the differences in the white matter connections of the brains of adults who stutter and fluent controls. Using tractography, I delineated tracts important in speech motor control. The results showed that the kurtosis measures in the FAT are different between the groups and that the right FAT is stronger than the left FAT in AWS, while no differences were observed using only diffusion-tensor based measures. I also replicated some of the tract lateralization

results of the previous studies as well as showing that measures in the right FAT is correlated with the impact of stuttering on the daily lives of AWS.

Given the abovementioned results and our previous discussion on the limitations of this study, following are some suggestions for future work:

- Using fMRI and/or structural images will help make the ROI placement more reliable and less rater-dependent. However, this may need co-registration of images, in which case special care should be taken to make sure the image information doesn't change as much.
- Corpus callosum can be divided into more than three parts (e.g. adding anterior midbody, posterior midbody and tapetum to the schema), which can help with being more specific in terms of where it connects and what function it represents and thus ruling out the possibility of contamination of speech-related fibers with other non-speech-related streamlines. The same goes for FAT. A study by Mandelli et al. (2014) has shown that there are various connections in the area where the FAT relies, more specifically, there are connections between the SMA and BA 44, the insula and BA 44, and the SMA and the insula. Future work should also investigate the possible subsections of the FAT.
- As mentioned in section 1.1, the lateral parts of the motor cortex are also involved in speech production. The corticobulbar tract connects those parts to the brainstem nuclei. Thus, tracing the corticobulbar tract and assessing it in a population of people who stutter would be beneficial for the field.
- Basal ganglia and cerebellum also play important roles in speech production. They can be identified in the susceptibility-weighted images (SWI) of the brain. Along with the DKI sequence, we have acquired SWIs during the scanning phase. Therefore, they and their connections to other speech production areas should be studied using a combination of the SWIs and DKI tractography.
- With the development of newer software packages to process DKI data, I suggest using DKI specific tractography methods to make sure we use the DKI data to its highest potential.

- Stuttering severity can be a better measure of a person's level of stuttering and its potential correlation with diffusion/kurtosis metrics can shed more light on the involvement of different white matter connections in stuttering. Therefore, future research should investigate the stuttering severity and its possible correlations with the metrics obtained from neuroimaging.
- As with other studies that have a small sample size, studies with greater number of participants are needed to confirm the results of the study at hand.

* * *

References

Ackermann, H., & Riecker, A. (2004). The contribution of the insula to motor aspects of speech production: a review and a hypothesis. *Brain Lang, 89*(2), 320-328. doi:10.1016/S0093-934X(03)00347-X

Ackermann, H., & Riecker, A. (2010). The contribution(s) of the insula to speech production: a review of the clinical and functional imaging literature. *Brain Struct Funct, 214*(5-6), 419-433. doi:10.1007/s00429-010-0257-x

Ackermann, H., & Ziegler, W. (2010). Brain mechanisms underlying speech motor control. In W. J. Hardcastle, J. Laver, & F. E. Gibbon (Eds.), *The handbook of phonetic sciences* (2nd ed., pp. xi, 870 p.). Chichester, U.K. ; Malden, MA: Wiley-Blackwell.

Alamia, A., Solopchuk, O., D'Ausilio, A., Van Bever, V., Fadiga, L., Olivier, E., & Zenon, A. (2016). Disruption of Broca's Area Alters Higher-order Chunking Processing during Perceptual Sequence Learning. *J Cogn Neurosci, 28*(3), 402-417. doi:10.1162/jocn_a_00911

Alexander, A. L., Hurley, S. A., Samsonov, A. A., Adluru, N., Hosseinbor, A. P., Mossahebi, P., Tromp do, P. M., Zakszewski, E., & Field, A. S. (2011). Characterization of cerebral white matter properties using quantitative magnetic resonance imaging stains. *Brain Connect, 1*(6), 423-446. doi:10.1089/brain.2011.0071

Alexander, A. L., Lee, J. E., Lazar, M., & Field, A. S. (2007). Diffusion tensor imaging of the brain. *Neurotherapeutics, 4*(3), 316-329. doi:10.1016/j.nurt.2007.05.011

Andrade, C. S., Leite, C. C., Otaduy, M. C., Lyra, K. P., Valente, K. D., Yasuda, C. L., Beltramini, G. C., Beaulieu, C., & Gross, D. W. (2014). Diffusion abnormalities of the corpus callosum in patients with malformations of cortical development and epilepsy. *Epilepsy Res, 108*(9), 1533-1542. doi:10.1016/j.eplepsyres.2014.08.023

Angstmann, S., Madsen, K. S., Skimminge, A., Jernigan, T. L., Baare, W. F., & Siebner, H. R. (2016). Microstructural asymmetry of the corticospinal tracts predicts right-left differences in circle drawing skill in right-handed adolescents. *Brain Struct Funct*. doi:10.1007/s00429-015-1178-5

Awad, M., Warren, J. E., Scott, S. K., Turkheimer, F. E., & Wise, R. J. (2007). A common system for the comprehension and production of narrative speech. *J Neurosci, 27*(43), 11455-11464. doi:10.1523/JNEUROSCI.5257-06.2007

Axer, H., Klingner, C. M., & Prescher, A. (2013). Fiber anatomy of dorsal and ventral language streams. *Brain and Language, 127*(2), 192-204. doi:10.1016/j.bandl.2012.04.015

Aziz-Zadeh, L., Cattaneo, L., Rochat, M., & Rizzolatti, G. (2005). Covert speech arrest induced by rTMS over both motor and nonmotor left hemisphere frontal sites. *J Cogn Neurosci, 17*(6), 928-938. doi:10.1162/0898929054021157

Baker, E., Blumstein, S. E., & Goodglass, H. (1981). Interaction between phonological and semantic factors in auditory comprehension. *Neuropsychologia, 19*(1), 1-15.

Banich, M. T., & Belger, A. (1990). Interhemispheric interaction: how do the hemispheres divide and conquer a task? *Cortex, 26*(1), 77-94.

Basser, P. J., Mattiello, J., & LeBihan, D. (1994). MR diffusion tensor spectroscopy and imaging. *Biophys J, 66*(1), 259-267. doi:10.1016/S0006-3495(94)80775-1

Basser, P. J., & Özarslan, E. (2011). Introduction to Diffusion MR. In H. Johansen-Berg & T. E. J. Behrens (Eds.), *Diffusion MRI : from quantitative measurement to in vivo neuroanatomy* (Second edition. ed., pp. 1 online resource.).

Beal, D. S., Gracco, V. L., Brettschneider, J., Kroll, R. M., & De Nil, L. F. (2013). A voxel-based morphometry (VBM) analysis of regional grey and white matter volume abnormalities within the speech production network of children who stutter. *Cortex, 49*(8), 2151-2161. doi:10.1016/j.cortex.2012.08.013

Beal, D. S., Gracco, V. L., Lafaille, S. J., & De Nil, L. F. (2007). Voxel-based morphometry of auditory and speech-related cortex in stutterers. *Neuroreport, 18*(12), 1257-1260. doi:10.1097/WNR.0b013e3282202c4d

Beal, D. S., Lerch, J. P., Cameron, B., Henderson, R., Gracco, V. L., & De Nil, L. F. (2015). The trajectory of gray matter development in Broca's area is abnormal in people who stutter. *Frontiers in Human Neuroscience, 9*(MAR). doi:10.3389/fnhum.2015.00089

Beaulieu, C. (2002). The basis of anisotropic water diffusion in the nervous system - a technical review. *NMR Biomed, 15*(7-8), 435-455. doi:10.1002/nbm.782

Behrens, T. E., Berg, H. J., Jbabdi, S., Rushworth, M. F., & Woolrich, M. W. (2007). Probabilistic diffusion tractography with multiple fibre orientations: What can we gain? *NeuroImage, 34*(1), 144-155. doi:10.1016/j.neuroimage.2006.09.018

Behroozmand, R., Shebek, R., Hansen, D. R., Oya, H., Robin, D. A., Howard, M. A., & Greenlee, J. D. W. (2015). Sensory-motor networks involved in speech production and motor control: An fMRI study. *Neuroimage, 109*, 418-428. doi:10.1016/j.neuroimage.2015.01.040

Belin, P., Zatorre, R. J., Lafaille, P., Ahad, P., & Pike, B. (2000). Voice-selective areas in human auditory cortex. *Nature, 403*(6767), 309-312. doi:10.1038/35002078

Bernal, B., & Altman, N. (2010). The connectivity of the superior longitudinal fasciculus: a tractography DTI study. *Magn Reson Imaging, 28*(2), 217-225. doi:10.1016/j.mri.2009.07.008

Blank, S. C., Scott, S. K., Murphy, K., Warburton, E., & Wise, R. J. (2002). Speech production: Wernicke, Broca and beyond. *Brain, 125*(Pt 8), 1829-1838.

Bloodstein, O., & Ratner, N. B. (2008). *A handbook on stuttering* (6th ed.). Clifton Park, NY: Thomson Delmar Learning.

Bohland, J. W., Bullock, D., & Guenther, F. H. (2010). Neural representations and mechanisms for the performance of simple speech sequences. *J Cogn Neurosci, 22*(7), 1504-1529. doi:10.1162/jocn.2009.21306

Bohland, J. W., & Guenther, F. H. (2006). An fMRI investigation of syllable sequence production. *Neuroimage, 32*(2), 821-841. doi:10.1016/j.neuroimage.2006.04.173

Booth, J. R., Wood, L., Lu, D., Houk, J. C., & Bitan, T. (2007). The role of the basal ganglia and cerebellum in language processing. *Brain Res, 1133*(1), 136-144. doi:10.1016/j.brainres.2006.11.074

Borovsky, A., Saygin, A. P., Bates, E., & Dronkers, N. (2007). Lesion correlates of conversational speech production deficits. *Neuropsychologia, 45*(11), 2525-2533. doi:10.1016/j.neuropsychologia.2007.03.023

Buchsbaum, B. R., Hickok, G., & Humphries, C. (2001). Role of left posterior superior temporal gyrus in phonological processing for speech perception and production. *Cognitive Science, 25*(5), 663-678. doi:DOI 10.1207/s15516709cog2505_2

Caeyenberghs, K., & Leemans, A. (2014). Hemispheric lateralization of topological organization in structural brain networks. *Hum Brain Mapp, 35*(9), 4944-4957. doi:10.1002/hbm.22524

Cai, S., Tourville, J. A., Beal, D. S., Perkell, J. S., Guenther, F. H., & Ghosh, S. S. (2014). Diffusion imaging of cerebral white matter in persons who stutter: Evidence for network-level anomalies. *Frontiers in Human Neuroscience, 8*(1 FEB). doi:10.3389/fnhum.2014.00054

Catani, M., Allin, M. P., Husain, M., Pugliese, L., Mesulam, M. M., Murray, R. M., & Jones, D. K. (2007). Symmetries in human brain language pathways correlate with verbal recall. *Proc Natl Acad Sci U S A, 104*(43), 17163-17168. doi:10.1073/pnas.0702116104

Catani, M., Dell'acqua, F., Vergani, F., Malik, F., Hodge, H., Roy, P., Valabregue, R., & Thiebaut de Schotten, M. (2012). Short frontal lobe connections of the human brain. *Cortex, 48*(2), 273-291. doi:10.1016/j.cortex.2011.12.001

Catani, M., Jones, D. K., & ffytche, D. H. (2005). Perisylvian language networks of the human brain. *Ann Neurol, 57*(1), 8-16. doi:10.1002/ana.20319

Catani, M., Mesulam, M. M., Jakobsen, E., Malik, F., Martersteck, A., Wieneke, C., Thompson, C. K., Thiebaut de Schotten, M., Dell'Acqua, F., Weintraub, S., & Rogalski, E. (2013). A novel frontal pathway underlies verbal fluency in primary progressive aphasia. *Brain, 136*(Pt 8), 2619-2628. doi:10.1093/brain/awt163

Catani, M., & Thiebaut de Schotten, M. (2012). *Atlas of human brain connections*. Oxford ; New York: Oxford University Press.

Chang, S. E., Erickson, K. I., Ambrose, N. G., Hasegawa-Johnson, M. A., & Ludlow, C. L. (2008). Brain anatomy differences in childhood stuttering. *Neuroimage, 39*(3), 1333-1344. doi:10.1016/j.neuroimage.2007.09.067

Chao, Y. P., Cho, K. H., Yeh, C. H., Chou, K. H., Chen, J. H., & Lin, C. P. (2009). Probabilistic topography of human corpus callosum using cytoarchitectural parcellation and high angular resolution diffusion imaging tractography. *Hum Brain Mapp, 30*(10), 3172-3187. doi:10.1002/hbm.20739

Cheyne, D., Kristeva, R., & Deecke, L. (1991). Homuncular organization of human motor cortex as indicated by neuromagnetic recordings. *Neurosci Lett, 122*(1), 17-20.

Choo, A. L., Chang, S. E., Zengin-Bolatkale, H., Ambrose, N. G., & Loucks, T. M. (2012). Corpus callosum morphology in children who stutter. *Journal of Communication Disorders, 45*(4), 279-289. doi:10.1016/j.jcomdis.2012.03.004

Choo, A. L., Kraft, S. J., Olivero, W., Ambrose, N. G., Sharma, H., Chang, S. E., & Loucks, T. M. (2011). Corpus callosum differences associated with persistent stuttering in adults. *J Commun Disord, 44*(4), 470-477. doi:10.1016/j.jcomdis.2011.03.001

Chun, R. Y., Mendes, C. D., Yaruss, J. S., & Quesal, R. W. (2010). The impact of stuttering on quality of life of children and adolescents. *Pro Fono, 22*(4), 567-569.

Civier, O., Kronfeld-Duenias, V., Amir, O., Ezrati-Vinacour, R., & Ben-Shachar, M. (2015). Reduced fractional anisotropy in the anterior corpus callosum is associated with reduced speech fluency in persistent developmental stuttering. *Brain Lang, 143*, 20-31. doi:10.1016/j.bandl.2015.01.012

Clarke, J. M., Lufkin, R. B., & Zaidel, E. (1993). Corpus callosum morphometry and dichotic listening performance: individual differences in functional interhemispheric inhibition? *Neuropsychologia, 31*(6), 547-557.

Cogan, G. B., Thesen, T., Carlson, C., Doyle, W., Devinsky, O., & Pesaran, B. (2014). Sensory-motor transformations for speech occur bilaterally. *Nature, 507*(7490), 94-98. doi:10.1038/nature12935

Cohen, Y., & Assaf, Y. (2002). High b-value q-space analyzed diffusion-weighted MRS and MRI in neuronal tissues - a technical review. *NMR Biomed, 15*(7-8), 516-542. doi:10.1002/nbm.778

Colby, J. B., Soderberg, L., Lebel, C., Dinov, I. D., Thompson, P. M., & Sowell, E. R. (2012). Along-tract statistics allow for enhanced tractography analysis. *Neuroimage, 59*(4), 3227-3242. doi:10.1016/j.neuroimage.2011.11.004

Connally, E. L., Ward, D., Howell, P., & Watkins, K. E. (2014). Disrupted white matter in language and motor tracts in developmental stuttering. *Brain and Language, 131*, 25-35. doi:10.1016/j.bandl.2013.05.013

Cook, N. D. (1984). Callosal inhibition: the key to the brain code. *Behav Sci, 29*(2), 98-110.

Cykowski, M. D., Fox, P. T., Ingham, R. J., Ingham, J. C., & Robin, D. A. (2010). A study of the reproducibility and etiology of diffusion anisotropy differences in developmental

stuttering: a potential role for impaired myelination. *Neuroimage, 52*(4), 1495-1504. doi:10.1016/j.neuroimage.2010.05.011

Das, S. K., Wang, J. L., Bing, L., Bhetuwal, A., & Yang, H. F. (2016). Regional Values of Diffusional Kurtosis Estimates in the Healthy Brain during Normal Aging. *Clin Neuroradiol*. doi:10.1007/s00062-015-0490-z

De Santis, S., Assaf, Y., & Jones, D. K. (2012). Using the biophysical CHARMED model to elucidate the underpinnings of contrast in diffusional kurtosis analysis of diffusion-weighted MRI. *MAGMA, 25*(4), 267-276. doi:10.1007/s10334-011-0292-5

DeCarlo, L. T. (1997). On the meaning and use of kurtosis. *Psychological Methods, 2*(3), 292-307. doi:Doi 10.1037//1082-989x.2.3.292

Dejerine, J. (1895). Anatomie des Centres Nerveux. Tome 1: Rueff et Cie, Paris.

Denenberg, V. H., Gall, J. S., Berrebi, A., & Yutzey, D. A. (1986). Callosal mediation of cortical inhibition in the lateralized rat brain. *Brain Res, 397*(2), 327-332.

Dennis, M. (1976). Impaired sensory and motor differentiation with corpus callosum agenesis: a lack of callosal inhibition during ontogeny? *Neuropsychologia, 14*(4), 455-469.

Dhakar, M. B., Ilyas, M., Jeong, J. W., Behen, M. E., & Chugani, H. T. (2016). Frontal Aslant Tract Abnormality on Diffusion Tensor Imaging in an Aphasic Patient With 49, XXXXY Syndrome. *Pediatr Neurol, 55*, 64-67. doi:10.1016/j.pediatrneurol.2015.10.020

Dhollander, T. (2016). From Diffusion to the Diffusion Tensor. In W. Van Hecke, L. Emsell, & S. Sunaert (Eds.), *Diffusion Tensor Imaging: A Practical Handbook* (pp. 37-63). New York, NY: Springer New York.

Dick, A. S., Bernal, B., & Tremblay, P. (2014). The language connectome: new pathways, new concepts. *Neuroscientist, 20*(5), 453-467. doi:10.1177/1073858413513502

Dronkers, N. F., Plaisant, O., Iba-Zizen, M. T., & Cabanis, E. A. (2007). Paul Broca's historic cases: high resolution MR imaging of the brains of Leborgne and Lelong. *Brain, 130*(Pt 5), 1432-1441. doi:10.1093/brain/awm042

Dubois, J., Hertz-Pannier, L., Cachia, A., Mangin, J. F., Le Bihan, D., & Dehaene-Lambertz, G. (2009). Structural asymmetries in the infant language and sensori-motor networks. *Cereb Cortex, 19*(2), 414-423. doi:10.1093/cercor/bhn097

Duffau, H. (2008). The anatomo-functional connectivity of language revisited. New insights provided by electrostimulation and tractography. *Neuropsychologia, 46*(4), 927-934. doi:10.1016/j.neuropsychologia.2007.10.025

Duffau, H., Capelle, L., Sichez, N., Denvil, D., Lopes, M., Sichez, J. P., Bitar, A., & Fohanno, D. (2002). Intraoperative mapping of the subcortical language pathways using direct stimulations. An anatomo-functional study. *Brain, 125*(Pt 1), 199-214.

Duffau, H., Gatignol, P., Denvil, D., Lopes, M., & Capelle, L. (2003). The articulatory loop: study of the subcortical connectivity by electrostimulation. *Neuroreport, 14*(15), 2005-2008. doi:10.1097/01.wnr.0000094103.16607.9f

Duffau, H., Peggy Gatignol, S. T., Mandonnet, E., Capelle, L., & Taillandier, L. (2008). Intraoperative subcortical stimulation mapping of language pathways in a consecutive series of 115 patients with Grade II glioma in the left dominant hemisphere. *J Neurosurg, 109*(3), 461-471. doi:10.3171/JNS/2008/109/9/0461

Dunn, L. M., & Dunn, D. M. (2007). *PPVT-4 : Peabody picture vocabulary test*. Minneapolis, MN.: Pearson Assessments.

Eling, P., & Whitaker, H. (2010). Chapter 36: history of aphasia: from brain to language. *Handb Clin Neurol, 95*, 571-582. doi:10.1016/S0072-9752(08)02136-2

Elnakib, A., Soliman, A., Nitzken, M., Casanova, M. F., Gimel'farb, G., & El-Baz, A. (2014). Magnetic resonance imaging findings for dyslexia: a review. *J Biomed Nanotechnol, 10*(10), 2778-2805.

Falangola, M. F., Guilfoyle, D. N., Tabesh, A., Hui, E. S., Nie, X., Jensen, J. H., Gerum, S. V., Hu, C., LaFrancois, J., Collins, H. R., & Helpern, J. A. (2014). Histological correlation of diffusional kurtosis and white matter modeling metrics in cuprizone-induced corpus callosum demyelination. *NMR Biomed, 27*(8), 948-957. doi:10.1002/nbm.3140

Feldman, H. M., Yeatman, J. D., Lee, E. S., Barde, L. H., & Gaman-Bean, S. (2010). Diffusion tensor imaging: a review for pediatric researchers and clinicians. *J Dev Behav Pediatr, 31*(4), 346-356. doi:10.1097/DBP.0b013e3181dcaa8b

Fieremans, E., Jensen, J. H., & Helpern, J. A. (2011). White matter characterization with diffusional kurtosis imaging. *NeuroImage, 58*(1), 177-188. doi:10.1016/j.neuroimage.2011.06.006

Fieremans, E., Novikov, D. S., Jensen, J. H., & Helpern, J. A. (2010). Monte Carlo study of a two-compartment exchange model of diffusion. *NMR Biomed, 23*(7), 711-724. doi:10.1002/nbm.1577

Flinker, A., Korzeniewska, A., Shestyuk, A. Y., Franaszczuk, P. J., Dronkers, N. F., Knight, R. T., & Crone, N. E. (2015). Redefining the role of broca's area in speech. *Proceedings of the National Academy of Sciences of the United States of America, 112*(9), 2871-2875. doi:10.1073/pnas.1414491112

Freedman, M., Alexander, M. P., & Naeser, M. A. (1984). Anatomic basis of transcortical motor aphasia. *Neurology, 34*(4), 409-417.

Fridriksson, J., Kjartansson, O., Morgan, P. S., Hjaltason, H., Magnusdottir, S., Bonilha, L., & Rorden, C. (2010). Impaired speech repetition and left parietal lobe damage. *J Neurosci, 30*(33), 11057-11061. doi:10.1523/JNEUROSCI.1120-10.2010

Frost, J. A., Binder, J. R., Springer, J. A., Hammeke, T. A., Bellgowan, P. S., Rao, S. M., & Cox, R. W. (1999). Language processing is strongly left lateralized in both sexes. Evidence from functional MRI. *Brain, 122 (Pt 2)*, 199-208.

Fuertinger, S., Horwitz, B., & Simonyan, K. (2015). The Functional Connectome of Speech Control. *PLoS Biol, 13*(7), e1002209. doi:10.1371/journal.pbio.1002209

Fujii, M., Maesawa, S., Motomura, K., Futamura, M., Hayashi, Y., Koba, I., & Wakabayashi, T. (2015). Intraoperative subcortical mapping of a language-associated deep frontal tract connecting the superior frontal gyrus to Broca's area in the dominant hemisphere of patients with glioma. *J Neurosurg, 122*(6), 1390-1396. doi:10.3171/2014.10.JNS14945

Gatignol, P., Capelle, L., Le Bihan, R., & Duffau, H. (2004). Double dissociation between picture naming and comprehension: an electrostimulation study. *Neuroreport, 15*(1), 191-195.

Geranmayeh, F., Brownsett, S. L., Leech, R., Beckmann, C. F., Woodhead, Z., & Wise, R. J. (2012). The contribution of the inferior parietal cortex to spoken language production. *Brain Lang, 121*(1), 47-57. doi:10.1016/j.bandl.2012.02.005

Geschwind, N. (1965a). Disconnexion syndromes in animals and man. I. *Brain, 88*(2), 237-294.

Geschwind, N. (1965b). Disconnexion syndromes in animals and man. II. *Brain, 88*(3), 585-644.

Geyer, S., Ledberg, A., Schleicher, A., Kinomura, S., Schormann, T., Burgel, U., Klingberg, T., Larsson, J., Zilles, K., & Roland, P. E. (1996). Two different areas within the primary motor cortex of man. *Nature, 382*(6594), 805-807. doi:10.1038/382805a0

Ghosh, S. S., Tourville, J. A., & Guenther, F. H. (2008). A neuroimaging study of premotor lateralization and cerebellar involvement in the production of phonemes and syllables. *J Speech Lang Hear Res, 51*(5), 1183-1202. doi:10.1044/1092-4388(2008/07-0119)

Gibbs, J., Appleton, J., & Appleton, R. (2007). Dyspraxia or developmental coordination disorder? Unravelling the enigma. *Arch Dis Child, 92*(6), 534-539. doi:10.1136/adc.2005.088054

Golfinopoulos, E., Tourville, J. A., & Guenther, F. H. (2010). The integration of large-scale neural network modeling and functional brain imaging in speech motor control. *Neuroimage, 52*(3), 862-874. doi:10.1016/j.neuroimage.2009.10.023

Guenther, F. H. (1994). A neural network model of speech acquisition and motor equivalent speech production. *Biol Cybern, 72*(1), 43-53.

Guenther, F. H. (1995). Speech sound acquisition, coarticulation, and rate effects in a neural network model of speech production. *Psychol Rev, 102*(3), 594-621.

Guenther, F. H. (2006). Cortical interactions underlying the production of speech sounds. *J Commun Disord, 39*(5), 350-365. doi:10.1016/j.jcomdis.2006.06.013

Guenther, F. H. (2008). Neuroimaging of Normal Speech Production. In R. J. Ingham (Ed.), *Neuroimaging in communication sciences and disorders* (pp. xii, 243 p.). San Diego, CA: Plural Pub.

Guenther, F. H., Ghosh, S. S., & Tourville, J. A. (2006). Neural modeling and imaging of the cortical interactions underlying syllable production. *Brain Lang, 96*(3), 280-301. doi:10.1016/j.bandl.2005.06.001

Guenther, F. H., Hampson, M., & Johnson, D. (1998). A theoretical investigation of reference frames for the planning of speech movements. *Psychol Rev, 105*(4), 611-633.

Guenther, F. H., & Vladusich, T. (2012). A Neural Theory of Speech Acquisition and Production. *J Neurolinguistics, 25*(5), 408-422. doi:10.1016/j.jneuroling.2009.08.006

Hagmann, P., Jonasson, L., Maeder, P., Thiran, J. P., Wedeen, V. J., & Meuli, R. (2006). Understanding diffusion MR imaging techniques: from scalar diffusion-weighted imaging to diffusion tensor imaging and beyond. *Radiographics, 26 Suppl 1*, S205-223. doi:10.1148/rg.26si065510

Halsband, U. (1987). Higher Disturbances of Movement in Monkeys (Macaca Fascicularis). In G. N. Gantchev, B. Dimitrov, & P. Gatev (Eds.), *Motor Control* (pp. 1 online resource.). Boston, MA: Springer US,.

Hart, J., Jr., & Gordon, B. (1990). Delineation of single-word semantic comprehension deficits in aphasia, with anatomical correlation. *Ann Neurol, 27*(3), 226-231. doi:10.1002/ana.410270303

Hickok, G. (2010). The Functional Anatomy of Speech Processing: From Auditory Cortex to Speech Recognition and Speech Production. In S. Ulmer & O. Jansen (Eds.), *fMRI Basics and Clinical Applications*. Berlin, Heidelberg: Springer-Verlag Berlin Heidelberg,.

Hickok, G., Erhard, P., Kassubek, J., Helms-Tillery, A. K., Naeve-Velguth, S., Strupp, J. P., Strick, P. L., & Ugurbil, K. (2000). A functional magnetic resonance imaging study of the role of left posterior superior temporal gyrus in speech production: implications for the explanation of conduction aphasia. *Neurosci Lett, 287*(2), 156-160.

Hickok, G., Houde, J., & Rong, F. (2011). Sensorimotor integration in speech processing: computational basis and neural organization. *Neuron, 69*(3), 407-422. doi:10.1016/j.neuron.2011.01.019

Hickok, G., & Poeppel, D. (2000). Towards a functional neuroanatomy of speech perception. *Trends Cogn Sci, 4*(4), 131-138.

Hickok, G., & Poeppel, D. (2004). Dorsal and ventral streams: a framework for understanding aspects of the functional anatomy of language. *Cognition, 92*(1-2), 67-99. doi:10.1016/j.cognition.2003.10.011

Hofer, S., & Frahm, J. (2006). Topography of the human corpus callosum revisited--comprehensive fiber tractography using diffusion tensor magnetic resonance imaging. *Neuroimage, 32*(3), 989-994. doi:10.1016/j.neuroimage.2006.05.044

Hori, M., Fukunaga, I., Masutani, Y., Taoka, T., Kamagata, K., Suzuki, Y., & Aoki, S. (2012). Visualizing non-Gaussian diffusion: clinical application of q-space imaging and diffusional kurtosis imaging of the brain and spine. *Magn Reson Med Sci, 11*(4), 221-233.

Houde, J. F., Nagarajan, S. S., Sekihara, K., & Merzenich, M. M. (2002). Modulation of the auditory cortex during speech: an MEG study. *J Cogn Neurosci, 14*(8), 1125-1138. doi:10.1162/089892902760807140

Huang, H., Zhang, J., van Zijl, P. C., & Mori, S. (2004). Analysis of noise effects on DTI-based tractography using the brute-force and multi-ROI approach. *Magn Reson Med, 52*(3), 559-565. doi:10.1002/mrm.20147

Hui, E. S., Cheung, M. M., Qi, L., & Wu, E. X. (2008). Towards better MR characterization of neural tissues using directional diffusion kurtosis analysis. *NeuroImage, 42*(1), 122-134. doi:10.1016/j.neuroimage.2008.04.237

Hui, E. S., Fieremans, E., Jensen, J. H., Tabesh, A., Feng, W., Bonilha, L., Spampinato, M. V., Adams, R., & Helpern, J. A. (2012). Stroke assessment with diffusional kurtosis imaging. *Stroke, 43*(11), 2968-2973. doi:10.1161/STROKEAHA.112.657742

Hynd, G. W., Hall, J., Novey, E. S., Eliopulos, D., Black, K., Gonzalez, J. J., Edmonds, J. E., Riccio, C., & Cohen, M. (1995). Dyslexia and corpus callosum morphology. *Arch Neurol, 52*(1), 32-38.

Indefrey, P., & Levelt, W. J. (2000). The neural correlates of language production. In M. S. Gazzaniga (Ed.), *The new cognitive neurosciences* (pp. xiv, 1419 p., 1424 p. of plates). Cambridge, Mass.: MIT Press.

James, J. S., Kumari, S. R., Sreedharan, R. M., Thomas, B., Radhkrishnan, A., & Kesavadas, C. (2015). Analyzing functional, structural, and anatomical correlation of hemispheric language lateralization in healthy subjects using functional MRI, diffusion tensor imaging, and voxel-based morphometry. *Neurol India, 63*(1), 49-57. doi:10.4103/0028-3886.152634

Jancke, L., Hanggi, J., & Steinmetz, H. (2004). Morphological brain differences between adult stutterers and non-stutterers. *BMC Neurol, 4*(1), 23. doi:10.1186/1471-2377-4-23

Jansen, A., Menke, R., Sommer, J., Forster, A. F., Bruchmann, S., Hempleman, J., Weber, B., & Knecht, S. (2006). The assessment of hemispheric lateralization in functional MRI--robustness and reproducibility. *Neuroimage, 33*(1), 204-217. doi:10.1016/j.neuroimage.2006.06.019

Jellison, B. J., Field, A. S., Medow, J., Lazar, M., Salamat, M. S., & Alexander, A. L. (2004). Diffusion tensor imaging of cerebral white matter: a pictorial review of physics, fiber tract anatomy, and tumor imaging patterns. *AJNR Am J Neuroradiol, 25*(3), 356-369.

Jenkinson, M., Beckmann, C. F., Behrens, T. E., Woolrich, M. W., & Smith, S. M. (2012). Fsl. *Neuroimage, 62*(2), 782-790. doi:10.1016/j.neuroimage.2011.09.015

Jensen, J. H., & Helpern, J. A. (2010). MRI quantification of non-Gaussian water diffusion by kurtosis analysis. *NMR Biomed, 23*(7), 698-710. doi:10.1002/nbm.1518

Jensen, J. H., Helpern, J. A., Ramani, A., Lu, H., & Kaczynski, K. (2005). Diffusional kurtosis imaging: the quantification of non-gaussian water diffusion by means of magnetic resonance imaging. *Magn Reson Med, 53*(6), 1432-1440. doi:10.1002/mrm.20508

Josephs, K. A., Duffy, J. R., Strand, E. A., Machulda, M. M., Senjem, M. L., Master, A. V., Lowe, V. J., Jack, C. R., Jr., & Whitwell, J. L. (2012). Characterizing a neurodegenerative syndrome: primary progressive apraxia of speech. *Brain, 135*(Pt 5), 1522-1536. doi:10.1093/brain/aws032

Jurgens, U. (2002). Neural pathways underlying vocal control. *Neurosci Biobehav Rev, 26*(2), 235-258.

Kamagata, K., Tomiyama, H., Motoi, Y., Kano, M., Abe, O., Ito, K., Shimoji, K., Suzuki, M., Hori, M., Nakanishi, A., Kuwatsuru, R., Sasai, K., Aoki, S., & Hattori, N. (2013). Diffusional kurtosis imaging of cingulate fibers in Parkinson disease: comparison with conventional diffusion tensor imaging. *Magn Reson Imaging, 31*(9), 1501-1506. doi:10.1016/j.mri.2013.06.009

Kamali, A., Flanders, A. E., Brody, J., Hunter, J. V., & Hasan, K. M. (2014). Tracing superior longitudinal fasciculus connectivity in the human brain using high resolution diffusion tensor tractography. *Brain Struct Funct, 219*(1), 269-281. doi:10.1007/s00429-012-0498-y

Kazumata, K., Tha, K. K., Narita, H., Ito, Y. M., Shichinohe, H., Ito, M., Uchino, H., & Abumiya, T. (2016). Characteristics of Diffusional Kurtosis in Chronic Ischemia of Adult Moyamoya Disease: Comparing Diffusional Kurtosis and Diffusion Tensor Imaging. *AJNR Am J Neuroradiol*. doi:10.3174/ajnr.A4728

Kell, C. A., Neumann, K., von Kriegstein, K., Posenenske, C., von Gudenberg, A. W., Euler, H., & Giraud, A. L. (2009). How the brain repairs stuttering. *Brain, 132*(Pt 10), 2747-2760. doi:10.1093/brain/awp185

Kinoshita, M., de Champfleur, N. M., Deverdun, J., Moritz-Gasser, S., Herbet, G., & Duffau, H. (2015). Role of fronto-striatal tract and frontal aslant tract in movement and speech: an axonal mapping study. *Brain Struct Funct, 220*(6), 3399-3412. doi:10.1007/s00429-014-0863-0

Knecht, S., Deppe, M., Drager, B., Bobe, L., Lohmann, H., Ringelstein, E., & Henningsen, H. (2000). Language lateralization in healthy right-handers. *Brain, 123 (Pt 1)*, 74-81.

Knecht, S., Drager, B., Deppe, M., Bobe, L., Lohmann, H., Floel, A., Ringelstein, E. B., & Henningsen, H. (2000). Handedness and hemispheric language dominance in healthy humans. *Brain, 123 Pt 12*, 2512-2518.

Kohler, E., Keysers, C., Umilta, M. A., Fogassi, L., Gallese, V., & Rizzolatti, G. (2002). Hearing sounds, understanding actions: action representation in mirror neurons. *Science, 297*(5582), 846-848. doi:10.1126/science.1070311

Kronfeld-Duenias, V., Amir, O., Ezrati-Vinacour, R., Civier, O., & Ben-Shachar, M. (2016). The frontal aslant tract underlies speech fluency in persistent developmental stuttering. *Brain Struct Funct, 221*(1), 365-381. doi:10.1007/s00429-014-0912-8

Latt, J., Nilsson, M., Wirestam, R., Stahlberg, F., Karlsson, N., Johansson, M., Sundgren, P. C., & van Westen, D. (2013). Regional values of diffusional kurtosis estimates in the healthy brain. *J Magn Reson Imaging, 37*(3), 610-618. doi:10.1002/jmri.23857

Lazar, M., Jensen, J. H., Xuan, L., & Helpern, J. A. (2008). Estimation of the orientation distribution function from diffusional kurtosis imaging. *Magn Reson Med, 60*(4), 774-781. doi:10.1002/mrm.21725

Le Bihan, D. (2013). Apparent diffusion coefficient and beyond: what diffusion MR imaging can tell us about tissue structure. *Radiology, 268*(2), 318-322. doi:10.1148/radiol.13130420

Le Bihan, D., Breton, E., Lallemand, D., Grenier, P., Cabanis, E., & Laval-Jeantet, M. (1986). MR imaging of intravoxel incoherent motions: application to diffusion and perfusion in neurologic disorders. *Radiology, 161*(2), 401-407. doi:10.1148/radiology.161.2.3763909

Leemans, A., Jeurissen, B., Sijbers, J., & Jones, D. (2009). *ExploreDTI: a graphical toolbox for processing, analyzing, and visualizing diffusion MR data.* Paper presented at the 17th Annual Meeting of Intl Soc Mag Reson Med.

Leh, S. E., Ptito, A., Chakravarty, M. M., & Strafella, A. P. (2007). Fronto-striatal connections in the human brain: a probabilistic diffusion tractography study. *Neurosci Lett, 419*(2), 113-118. doi:10.1016/j.neulet.2007.04.049

Lehericy, S., Ducros, M., Van de Moortele, P. F., Francois, C., Thivard, L., Poupon, C., Swindale, N., Ugurbil, K., & Kim, D. S. (2004). Diffusion tensor fiber tracking shows distinct corticostriatal circuits in humans. *Ann Neurol, 55*(4), 522-529. doi:10.1002/ana.20030

Lerner, Y., Honey, C. J., Silbert, L. J., & Hasson, U. (2011). Topographic mapping of a hierarchy of temporal receptive windows using a narrated story. *J Neurosci, 31*(8), 2906-2915. doi:10.1523/JNEUROSCI.3684-10.2011

Levelt, W. J., Praamstra, P., Meyer, A. S., Helenius, P., & Salmelin, R. (1998). An MEG study of picture naming. *J Cogn Neurosci, 10*(5), 553-567.

Levelt, W. J., Roelofs, A., & Meyer, A. S. (1999). A theory of lexical access in speech production. *Behav Brain Sci, 22*(1), 1-38; discussion 38-75.

Li, S., Sun, X., Bai, Y. M., Qin, H. M., Wu, X. M., Zhang, X., Jolkkonen, J., Boltze, J., & Wang, S. P. (2015). Infarction of the corpus callosum: a retrospective clinical investigation. *PLoS One, 10*(3), e0120409. doi:10.1371/journal.pone.0120409

Lin, X., Tench, C. R., Morgan, P. S., Niepel, G., & Constantinescu, C. S. (2005). 'Importance sampling' in MS: use of diffusion tensor tractography to quantify pathology related to specific impairment. *J Neurol Sci, 237*(1-2), 13-19. doi:10.1016/j.jns.2005.04.019

Liu, M., Concha, L., Beaulieu, C., & Gross, D. W. (2011). Distinct white matter abnormalities in different idiopathic generalized epilepsy syndromes. *Epilepsia, 52*(12), 2267-2275. doi:10.1111/j.1528-1167.2011.03313.x

Ludlow, C. L., & Loucks, T. (2003). Stuttering: a dynamic motor control disorder. *J Fluency Disord, 28*(4), 273-295; quiz 295.

Mandelli, M. L., Caverzasi, E., Binney, R. J., Henry, M. L., Lobach, I., Block, N., Amirbekian, B., Dronkers, N., Miller, B. L., Henry, R. G., & Gorno-Tempini, M. L. (2014). Frontal white matter tracts sustaining speech production in primary progressive aphasia. *J Neurosci, 34*(29), 9754-9767. doi:10.1523/JNEUROSCI.3464-13.2014

Marrale, M., Collura, G., Brai, M., Toschi, N., Midiri, F., la Tona, G., Lo Casto, A., & Gagliardo, C. (2015). Physics, Techniques and Review of Neuroradiological Applications of Diffusion Kurtosis Imaging (DKI). *Clinical Neuroradiology*, 1-13. doi:10.1007/s00062-015-0469-9

Melhem, E. R., Mori, S., Mukundan, G., Kraut, M. A., Pomper, M. G., & van Zijl, P. C. (2002). Diffusion tensor MR imaging of the brain and white matter tractography. *AJR Am J Roentgenol, 178*(1), 3-16. doi:10.2214/ajr.178.1.1780003

Mendoza, J. E. (2011a). Auditory Cortex. In J. S. Kreutzer, J. DeLuca, & B. Caplan (Eds.), *Encyclopedia of Clinical Neuropsychology* (pp. 301-301). New York, NY: Springer New York.

Mendoza, J. E. (2011b). Heschl's Gyrus. In J. S. Kreutzer, J. DeLuca, & B. Caplan (Eds.), *Encyclopedia of Clinical Neuropsychology* (pp. 1243-1243). New York, NY: Springer New York.

Mohammadi, S., Tabelow, K., Ruthotto, L., Feiweier, T., Polzehl, J., & Weiskopf, N. (2014). High-resolution diffusion kurtosis imaging at 3T enabled by advanced post-processing. *Front Neurosci, 8*, 427. doi:10.3389/fnins.2014.00427

Mori, S., Crain, B. J., Chacko, V. P., & van Zijl, P. C. (1999). Three-dimensional tracking of axonal projections in the brain by magnetic resonance imaging. *Ann Neurol, 45*(2), 265-269.

Mori, S., & van Zijl, P. C. (2002). Fiber tracking: principles and strategies - a technical review. *NMR Biomed, 15*(7-8), 468-480. doi:10.1002/nbm.781

Mori, S., & Zhang, J. (2006). Principles of diffusion tensor imaging and its applications to basic neuroscience research. *Neuron, 51*(5), 527-539. doi:10.1016/j.neuron.2006.08.012

Mukherjee, P., Berman, J. I., Chung, S. W., Hess, C. P., & Henry, R. G. (2008). Diffusion tensor MR imaging and fiber tractography: theoretic underpinnings. *AJNR Am J Neuroradiol, 29*(4), 632-641. doi:10.3174/ajnr.A1051

Muller, N. G., & Knight, R. T. (2006). The functional neuroanatomy of working memory: contributions of human brain lesion studies. *Neuroscience, 139*(1), 51-58. doi:10.1016/j.neuroscience.2005.09.018

Murdoch, B. E. (2001). Subcortical brain mechanisms in speech and language. *Folia Phoniatr Logop, 53*(5), 233-251. doi:52679

Neto-Henriques, R., Ferreira, H. A., & Correia, M. M. (2015). *United Diffusion Kurtosis Imaging (UDKI) toolbox.* Paper presented at the ESMRMB 2015, 32nd Annual Scientific Meeting, Edinburgh, UK.

Neto Henriques, R., Correia, M. M., Nunes, R. G., & Ferreira, H. A. (2015). Exploring the 3D geometry of the diffusion kurtosis tensor--impact on the development of robust tractography procedures and novel biomarkers. *Neuroimage, 111*, 85-99. doi:10.1016/j.neuroimage.2015.02.004

Oldfield, R. C. (1971). The assessment and analysis of handedness: the Edinburgh inventory. *Neuropsychologia, 9*(1), 97-113.

Pang, H., Ren, Y., Dang, X., Feng, X., Yao, Z., Wu, J., Yao, C., Di, N., Ghinda, D. C., & Zhang, Y. (2015). Diffusional kurtosis imaging for differentiating between high-grade glioma and primary central nervous system lymphoma. *J Magn Reson Imaging*. doi:10.1002/jmri.25090

Papoutsi, M., de Zwart, J. A., Jansma, J. M., Pickering, M. J., Bednar, J. A., & Horwitz, B. (2009). From phonemes to articulatory codes: an fMRI study of the role of Broca's area in speech production. *Cereb Cortex, 19*(9), 2156-2165. doi:10.1093/cercor/bhn239

Parker, G. J., Luzzi, S., Alexander, D. C., Wheeler-Kingshott, C. A., Ciccarelli, O., & Lambon Ralph, M. A. (2005). Lateralization of ventral and dorsal auditory-language pathways in the human brain. *Neuroimage, 24*(3), 656-666. doi:10.1016/j.neuroimage.2004.08.047

Passingham, R. E. (1987). Two cortical systems for directing movement. In C. Foundation. (Ed.), *Motor areas of the cerebral cortex* (pp. ix, 322 p.). Chichester ; New York: Wiley.

Paus, T., Perry, D. W., Zatorre, R. J., Worsley, K. J., & Evans, A. C. (1996). Modulation of cerebral blood flow in the human auditory cortex during speech: role of motor-to-sensory discharges. *Eur J Neurosci, 8*(11), 2236-2246.

Paydar, A., Fieremans, E., Nwankwo, J. I., Lazar, M., Sheth, H. D., Adisetiyo, V., Helpern, J. A., Jensen, J. H., & Milla, S. S. (2014). Diffusional kurtosis imaging of the developing brain. *AJNR Am J Neuroradiol, 35*(4), 808-814. doi:10.3174/ajnr.A3764

Penfield, W., & Boldrey, E. (1937). Somatic motor and sensory representation in the cerebral cortex of man as studied by electrical stimulation. *Brain, 60*, 389-443. doi:DOI 10.1093/brain/60.4.389

Penfield, W., & Rasmussen, T. (1968). *The cerebral cortex of man; a clinical study of localization of function*. New York,: Hafner Pub. Co.

Penfield, W., & Roberts, L. (2014). *Speech and brain-mechanisms Princeton legacy library* (pp. 1 online resource (1 PDF (xiii, 286 pages))). Retrieved from http://muse.jhu.edu/books/9781400854677/

Penfield, W., & Welch, K. (1951). The supplementary motor area of the cerebral cortex; a clinical and experimental study. *AMA Arch Neurol Psychiatry, 66*(3), 289-317.

Pickett, E. R., Kuniholm, E., Protopapas, A., Friedman, J., & Lieberman, P. (1998). Selective speech motor, syntax and cognitive deficits associated with bilateral damage to the putamen and the head of the caudate nucleus: a case study. *Neuropsychologia, 36*(2), 173-188.

Pietrasanta, M., Restani, L., & Caleo, M. (2012). The corpus callosum and the visual cortex: plasticity is a game for two. *Neural Plast, 2012*, 838672. doi:10.1155/2012/838672

Ploner, M., Schmitz, F., Freund, H. J., & Schnitzler, A. (2000). Differential organization of touch and pain in human primary somatosensory cortex. *J Neurophysiol, 83*(3), 1770-1776.

Preston, J. L., Molfese, P. J., Mencl, W. E., Frost, S. J., Hoeft, F., Fulbright, R. K., Landi, N., Grigorenko, E. L., Seki, A., Felsenfeld, S., & Pugh, K. R. (2014). Structural brain

differences in school-age children with residual speech sound errors. *Brain Lang, 128*(1), 25-33. doi:10.1016/j.bandl.2013.11.001

Qiu, A., Mori, S., & Miller, M. I. (2015). Diffusion tensor imaging for understanding brain development in early life. *Annu Rev Psychol, 66*, 853-876. doi:10.1146/annurev-psych-010814-015340

Ratner, N. B. (1995). Language complexity and stuttering in children. *Topics in Language Disorders, 15*(3), 32-47.

Rinne, T., Alho, K., Alku, P., Holi, M., Sinkkonen, J., Virtanen, J., Bertrand, O., & Naatanen, R. (1999). Analysis of speech sounds is left-hemisphere predominant at 100-150ms after sound onset. *Neuroreport, 10*(5), 1113-1117.

Rizio, A. A., & Diaz, M. T. (2016). Language, aging, and cognition: frontal aslant tract and superior longitudinal fasciculus contribute toward working memory performance in older adults. *Neuroreport, 27*(9), 689-693. doi:10.1097/WNR.0000000000000597

Rogic Vidakovic, M., Jerkovic, A., Juric, T., Vujovic, I., Soda, J., Erceg, N., Bubic, A., Zmajevic Schonwald, M., Lioumis, P., Gabelica, D., & Dogas, Z. (2016). Neurophysiologic markers of primary motor cortex for laryngeal muscles and premotor cortex in caudal opercular part of inferior frontal gyrus investigated in motor speech disorder: a navigated transcranial magnetic stimulation (TMS) study. *Cogn Process*. doi:10.1007/s10339-016-0766-5

Rorden, C., & Karnath, H. O. (2004). Using human brain lesions to infer function: a relic from a past era in the fMRI age? *Nature Reviews Neuroscience, 5*(10), 813-819. doi:10.1038/nrn1521

Schmahmann, J. D., & Pandya, D. N. (2006). *Fiber pathways of the brain*. Oxford ; New York: Oxford University Press.

Seghier, M. L., Hope, T. M., Prejawa, S., Parker, J., Vitkovitch, M., & Price, C. J. (2015). A trade-off between somatosensory and auditory related brain activity during object naming but not reading. *J Neurosci, 35*(11), 4751-4759. doi:10.1523/JNEUROSCI.2292-14.2015

Seizeur, R., Magro, E., Prima, S., Wiest-Daessle, N., Maumet, C., & Morandi, X. (2014). Corticospinal tract asymmetry and handedness in right- and left-handers by diffusion

tensor tractography. *Surg Radiol Anat, 36*(2), 111-124. doi:10.1007/s00276-013-1156-7

Shu, N., Liu, Y., Duan, Y., & Li, K. (2015). Hemispheric Asymmetry of Human Brain Anatomical Network Revealed by Diffusion Tensor Tractography. *Biomed Res Int, 2015*, 908917. doi:10.1155/2015/908917

Sierpowska, J., Gabarros, A., Fernandez-Coello, A., Camins, A., Castaner, S., Juncadella, M., de Diego-Balaguer, R., & Rodriguez-Fornells, A. (2015). Morphological derivation overflow as a result of disruption of the left frontal aslant white matter tract. *Brain Lang, 142*, 54-64. doi:10.1016/j.bandl.2015.01.005

Simonyan, K., & Horwitz, B. (2011). Laryngeal motor cortex and control of speech in humans. *Neuroscientist, 17*(2), 197-208. doi:10.1177/1073858410386727

Sivapatham, T., & Melhem, E. R. (2012). Physical Principles of Diffusion Imaging. In H. S. Faro, B. F. Mohamed, M. Law, & T. J. Ulmer (Eds.), *Functional Neuroradiology: Principles and Clinical Applications* (pp. 3-11). Boston, MA: Springer US.

Smith, S. M. (2002). Fast robust automated brain extraction. *Hum Brain Mapp, 17*(3), 143-155. doi:10.1002/hbm.10062

Smith, S. M., Jenkinson, M., Johansen-Berg, H., Rueckert, D., Nichols, T. E., Mackay, C. E., Watkins, K. E., Ciccarelli, O., Cader, M. Z., Matthews, P. M., & Behrens, T. E. (2006). Tract-based spatial statistics: voxelwise analysis of multi-subject diffusion data. *Neuroimage, 31*(4), 1487-1505. doi:10.1016/j.neuroimage.2006.02.024

Soares, J. M., Marques, P., Alves, V., & Sousa, N. (2013). A hitchhiker's guide to diffusion tensor imaging. *Front Neurosci, 7*, 31. doi:10.3389/fnins.2013.00031

Sommer, M., Koch, M. A., Paulus, W., Weiller, C., & Buchel, C. (2002). Disconnection of speech-relevant brain areas in persistent developmental stuttering. *Lancet, 360*(9330), 380-383. doi:10.1016/S0140-6736(02)09610-1

Soros, P., Sokoloff, L. G., Bose, A., McIntosh, A. R., Graham, S. J., & Stuss, D. T. (2006). Clustered functional MRI of overt speech production. *Neuroimage, 32*(1), 376-387. doi:10.1016/j.neuroimage.2006.02.046

Sreedharan, R. M., Menon, A. C., James, J. S., Kesavadas, C., & Thomas, S. V. (2015). Arcuate fasciculus laterality by diffusion tensor imaging correlates with language

laterality by functional MRI in preadolescent children. *Neuroradiology, 57*(3), 291-297. doi:10.1007/s00234-014-1469-1

Stejskal, E. O., & Tanner, J. E. (1965). Spin Diffusion Measurements: Spin Echoes in the Presence of a Time-Dependent Field Gradient. *Journal of Chemical Physics, 42*(1), 288-+. doi:Doi 10.1063/1.1695690

Steven, A. J., Zhuo, J., & Melhem, E. R. (2014). Diffusion kurtosis imaging: an emerging technique for evaluating the microstructural environment of the brain. *AJR Am J Roentgenol, 202*(1), W26-33. doi:10.2214/AJR.13.11365

Stout, D., & Chaminade, T. (2012). Stone tools, language and the brain in human evolution. *Philos Trans R Soc Lond B Biol Sci, 367*(1585), 75-87. doi:10.1098/rstb.2011.0099

Sussman, H. M. (2015). Why the Left Hemisphere Is Dominant for Speech Production: Connecting the Dots. *Biolinguistics, 9*, 116-131.

Szaflarski, J. P., Holland, S. K., Schmithorst, V. J., & Byars, A. W. (2006). fMRI study of language lateralization in children and adults. *Hum Brain Mapp, 27*(3), 202-212. doi:10.1002/hbm.20177

Tabesh, A., Jensen, J. H., Ardekani, B. A., & Helpern, J. A. (2011). Estimation of tensors and tensor-derived measures in diffusional kurtosis imaging. *Magn Reson Med, 65*(3), 823-836. doi:10.1002/mrm.22655

Takai, O., Brown, S., & Liotti, M. (2010). Representation of the speech effectors in the human motor cortex: somatotopy or overlap? *Brain Lang, 113*(1), 39-44. doi:10.1016/j.bandl.2010.01.008

Tan, Y., Wang, X. C., Zhang, H., Wang, J., Qin, J. B., Wu, X. F., Zhang, L., & Wang, L. (2015). Differentiation of high-grade-astrocytomas from solitary-brain-metastases: Comparing diffusion kurtosis imaging and diffusion tensor imaging. *Eur J Radiol, 84*(12), 2618-2624. doi:10.1016/j.ejrad.2015.10.007

Tan, Y., Zhang, H., Zhao, R. F., Wang, X. C., Qin, J. B., & Wu, X. F. (2016). Comparison of the values of MRI diffusion kurtosis imaging and diffusion tensor imaging in cerebral astrocytoma grading and their association with aquaporin-4. *Neurol India, 64*(2), 265-272. doi:10.4103/0028-3886.177621

Taoka, T., Fujioka, M., Sakamoto, M., Miyasaka, T., Akashi, T., Ochi, T., Hori, S., Uchikoshi, M., Xu, J., & Kichikawa, K. (2014). Time course of axial and radial

diffusion kurtosis of white matter infarctions: period of pseudonormalization. *AJNR Am J Neuroradiol, 35*(8), 1509-1514. doi:10.3174/ajnr.A3908

Tettamanti, M., Moro, A., Messa, C., Moresco, R. M., Rizzo, G., Carpinelli, A., Matarrese, M., Fazio, F., & Perani, D. (2005). Basal ganglia and language: phonology modulates dopaminergic release. *Neuroreport, 16*(4), 397-401.

Thiebaut de Schotten, M., Dell'Acqua, F., Forkel, S. J., Simmons, A., Vergani, F., Murphy, D. G., & Catani, M. (2011). A lateralized brain network for visuospatial attention. *Nat Neurosci, 14*(10), 1245-1246. doi:10.1038/nn.2905

Thiebaut de Schotten, M., Ffytche, D. H., Bizzi, A., Dell'Acqua, F., Allin, M., Walshe, M., Murray, R., Williams, S. C., Murphy, D. G., & Catani, M. (2011). Atlasing location, asymmetry and inter-subject variability of white matter tracts in the human brain with MR diffusion tractography. *Neuroimage, 54*(1), 49-59. doi:10.1016/j.neuroimage.2010.07.055

Tournier, J. D., & Mori, S. (2014). Moving Beyond DTI: High Angular Resolution Diffusion Imaging (HARDI). In J. D. Tournier & S. Mori (Eds.), *Introduction to Diffusion Tensor Imaging (Second Edition)* (pp. 65-78). San Diego: Academic Press.

Tourville, J. A., & Guenther, F. H. (2011). The DIVA model: A neural theory of speech acquisition and production. *Lang Cogn Process, 26*(7), 952-981. doi:10.1080/01690960903498424

Tremblay, P., & Gracco, V. L. (2009). Contribution of the pre-SMA to the production of words and non-speech oral motor gestures, as revealed by repetitive transcranial magnetic stimulation (rTMS). *Brain Res, 1268*, 112-124. doi:10.1016/j.brainres.2009.02.076

Tremblay, P., & Gracco, V. L. (2010). On the selection of words and oral motor responses: evidence of a response-independent fronto-parietal network. *Cortex, 46*(1), 15-28. doi:10.1016/j.cortex.2009.03.003

Tremblay, S., Shiller, D. M., & Ostry, D. J. (2003). Somatosensory basis of speech production. *Nature, 423*(6942), 866-869. doi:10.1038/nature01710

Tuch, D. S., Reese, T. G., Wiegell, M. R., & Wedeen, V. J. (2003). Diffusion MRI of complex neural architecture. *Neuron, 40*(5), 885-895.

Vandermosten, M., Boets, B., Poelmans, H., Sunaert, S., Wouters, J., & Ghesquiere, P. (2012). A tractography study in dyslexia: neuroanatomic correlates of orthographic, phonological and speech processing. *Brain, 135*(Pt 3), 935-948. doi:10.1093/brain/awr363

Vassal, F., Boutet, C., Lemaire, J. J., & Nuti, C. (2014). New insights into the functional significance of the frontal aslant tract: an anatomo-functional study using intraoperative electrical stimulations combined with diffusion tensor imaging-based fiber tracking. *Br J Neurosurg, 28*(5), 685-687. doi:10.3109/02688697.2014.889810

Vergani, F., Lacerda, L., Martino, J., Attems, J., Morris, C., Mitchell, P., Thiebaut de Schotten, M., & Dell'Acqua, F. (2014). White matter connections of the supplementary motor area in humans. *J Neurol Neurosurg Psychiatry, 85*(12), 1377-1385. doi:10.1136/jnnp-2013-307492

Wakana, S., Caprihan, A., Panzenboeck, M. M., Fallon, J. H., Perry, M., Gollub, R. L., Hua, K., Zhang, J., Jiang, H., Dubey, P., Blitz, A., van Zijl, P., & Mori, S. (2007). Reproducibility of quantitative tractography methods applied to cerebral white matter. *NeuroImage, 36*(3), 630-644. doi:10.1016/j.neuroimage.2007.02.049

Wang, J. J., Lin, W. Y., Lu, C. S., Weng, Y. H., Ng, S. H., Wang, C. H., Liu, H. L., Hsieh, R. H., Wan, Y. L., & Wai, Y. Y. (2011). Parkinson disease: diagnostic utility of diffusion kurtosis imaging. *Radiology, 261*(1), 210-217. doi:10.1148/radiol.11102277

Watkins, K. E., Smith, S. M., Davis, S., & Howell, P. (2008). Structural and functional abnormalities of the motor system in developmental stuttering. *Brain, 131*(Pt 1), 50-59. doi:10.1093/brain/awm241

Wechsler, D. (2008). *Wechsler adult intelligence scale-fourth*: San Antonio: Pearson.

Whitwell, J. L., Duffy, J. R., Strand, E. A., Machulda, M. M., Senjem, M. L., Gunter, J. L., Kantarci, K., Eggers, S. D., Jack, C. R., Jr., & Josephs, K. A. (2013). Neuroimaging comparison of primary progressive apraxia of speech and progressive supranuclear palsy. *Eur J Neurol, 20*(4), 629-637. doi:10.1111/ene.12004

Wildgruber, D., Ackermann, H., & Grodd, W. (2001). Differential contributions of motor cortex, basal ganglia, and cerebellum to speech motor control: effects of syllable repetition rate evaluated by fMRI. *Neuroimage, 13*(1), 101-109. doi:10.1006/nimg.2000.0672

Wise, R., Chollet, F., Hadar, U., Friston, K., Hoffner, E., & Frackowiak, R. (1991). Distribution of cortical neural networks involved in word comprehension and word retrieval. *Brain, 114 (Pt 4)*, 1803-1817.

Wise, R. J. S., Scott, S. K., Blank, S. C., Mummery, C. J., Murphy, K., & Warburton, E. A. (2001). Separate neural subsystems within 'Wernicke's area'. *Brain, 124*, 83-95. doi:DOI 10.1093/brain/124.1.83

Wisnowski, J. L., Ceschin, R. C., & Schmithorst, V. J. (2013). Diffusion-Weighted Magnetic Resonance Imaging: Principles and Implementation in Clinical and Research Settings. In B. D. Coley (Ed.), *Caffey's pediatric diagnostic imaging* (Twelfth edition. ed., pp. 2 volumes (xxix, 1616 pages)).

Witelson, S. F. (1989). Hand and sex differences in the isthmus and genu of the human corpus callosum. A postmortem morphological study. *Brain, 112 (Pt 3)*, 799-835.

Xing, S., Lacey, E. H., Skipper-Kallal, L. M., Jiang, X., Harris-Love, M. L., Zeng, J., & Turkeltaub, P. E. (2016). Right hemisphere grey matter structure and language outcomes in chronic left hemisphere stroke. *Brain, 139*(Pt 1), 227-241. doi:10.1093/brain/awv323

Yagmurlu, K., Middlebrooks, E. H., Tanriover, N., & Rhoton, A. L., Jr. (2016). Fiber tracts of the dorsal language stream in the human brain. *J Neurosurg, 124*(5), 1396-1405. doi:10.3171/2015.5.JNS15455

Yaruss, J. S., & Quesal, R. W. (2006). Overall Assessment of the Speaker's Experience of Stuttering (OASES): documenting multiple outcomes in stuttering treatment. *J Fluency Disord, 31*(2), 90-115. doi:10.1016/j.jfludis.2006.02.002

Yaruss, J. S., & Quesal, R. W. (2008). *OASES: Overall Assessment of the Speaker's Experience of Stuttering: Manual*: Pearson.

Zhang, W., Olivi, A., Hertig, S. J., van Zijl, P., & Mori, S. (2008). Automated fiber tracking of human brain white matter using diffusion tensor imaging. *NeuroImage, 42*(2), 771-777. doi:10.1016/j.neuroimage.2008.04.241

Zhuo, J., Xu, S., Proctor, J. L., Mullins, R. J., Simon, J. Z., Fiskum, G., & Gullapalli, R. P. (2012). Diffusion kurtosis as an in vivo imaging marker for reactive astrogliosis in traumatic brain injury. *Neuroimage, 59*(1), 467-477. doi:10.1016/j.neuroimage.2011.07.050

Ziegler, W., Kilian, B., & Deger, K. (1997). The role of the left mesial frontal cortex in fluent speech: evidence from a case of left supplementary motor area hemorrhage. *Neuropsychologia, 35*(9), 1197-1208.

Zipse, L., Norton, A., Marchina, S., & Schlaug, G. (2012). When right is all that is left: plasticity of right-hemisphere tracts in a young aphasic patient. *Ann N Y Acad Sci, 1252*, 237-245. doi:10.1111/j.1749-6632.2012.06454.x

Appendices

A1 – Online Participation Pre-screening Form

Speech Laboratory Research Participant Screening Form

Thank you for your interest in participating in one of our speech studies. Please complete and submit this form. Following our receipt of the form, someone will be in touch with you via email to schedule a set of research appointments.

* Required

Date: *

Please pick the date on which you are completing this form.

mm/dd/yyyy

PERSONAL INFORMATION

Last Name *

First Name *

Date of Birth *

Please pick your date of birth.

mm/dd/yyyy

Gender *

Are you left or right handed? *

Email Address *

Telephone Number *

Alternate Telephone Number

Address *
Apt #, House #, Street, City, Province, Postal Code

What is your current profession? *

What is the highest level of education that you have completed? *
For example, if you are a university senior you have completed 4 years of a Bachelors degree.

How many years of education have you completed? *
For example, if you have completed Grade 12 you have completed 13 years (Kindergarten to Grade 12).

Are you willing to participate in other experiments? *
If you select "yes" you may be contacted by a member of our laboratory to ask if you are interested in participating in a future experiment.

DEVELOPMENTAL & MEDICAL HISTORY INFORMATION

Are you aware of any difficulties that you experienced as a child learning to eat food, drink liquids or to walk? *

Please tell us about your difficulties as a child learning to eat, drink or walk.
Only answer if you responded "yes" to the previous question.

Are you currently taking any medications? *

Please tell us about the medications that you are currently taking.
Only answer if you responded "yes" to the previous question.

Are you seeing a doctor on a regular basis for any type of medical problem? *

Please tell us about your medical problems.

Only answer if you responded "yes" to the previous question.

Have you ever had to consult a doctor, physiotherapist or occupational therapist because of difficulties using your mouth, arms, hands or legs? *

Please tell us about the difficulties for which you consulted a doctor, physiotherapist or occupational therapist.

Only answer if you responded "yes" to the previous question.

Do you use recreational drugs? *

If "yes" please tell us about your recreational drug use.

For example, what drugs do you use? How often do you use them?

Have you ever experienced seizures, epilepsy or fits? *

Have you ever lost consciousness? *

Please tell us about your experiences losing consciousness.
Please describe if you chose "yes" to the previous question.

Have you ever suffered a head or brain injury? *

Please tell us about your head or brain injury.
Please describe only if you selected "yes" for the previous question.

Please tell us if you wear the following. *

- [ ] Eye glasses
- [ ] Contact lenses
- [ ] None of the above, my vision is normal.

Do you have difficulties hearing? *

MRI Compatibility

Do you have any type of metal on your body? *

For example, do you have any kind of metal implant OR have you ever worked with metal as a welder or a grinder?

Do you have body piercings or tattoos? *

Please tell us about your body piercings or tattoos.

Only answer if you responded "yes" to the previous question.

Do you have any type of dental work? *

For example, do you have false teeth, bridges, false fronts or permanent retainers or braces?

Please tell us about your dental work.

Only answer if you responded "yes" to the previous question.

Have you ever had a surgery? *

Please tell us about your surgery.

Only answer if you responded "yes" to the previous question.

SPEECH AND LANGUAGE DEVELOPMENT

To the best of your knowledge, please tell us did you ever have difficulty learning to speak OR to read as a child? *

If you are person who stutters, there is an opportunity to describe your stuttering in detail in a separate section of the form. Please only tell us about speaking or reading difficulties in addition to your stuttering here.

Please tell us about the difficulties that you experienced learning to speak or to read as a child.

Only answer if you responded "yes" to the previous question.

Do you have any speech, language or reading difficulties now? *

If you are a person who stutters, we mean only in addition to stuttering here.

Please tell us about your current speech, language or reading difficulties.

Only answer if you responded "yes" to the previous question.

Have you ever received special instruction or therapy for speech or reading difficulties from a speech-language pathologist, speech teacher or other professional? *

If you are a person who stutters, we mean therapy for problems in addition to stuttering here.

Please tell us about the therapy that you received for your speech, language or reading difficulties.

Only answer if you responded "yes" to the previous question.

Were you born in Canada? *

Were you raised in Canada? *

Is ENGLISH your first and native language? *

Please answer "yes" only if English was the first language that you learned from birth.

If English is not your first and native language, how old were you when you mastered English?

Only answer if you responded "No" to the previous question.

Do you speak any other languages proficiently in addition to English? *

Please tell us what other languages you speak proficiently.

Only answer if you responded "yes" to the previous question.

Does anyone in your family stutter? *

Stuttering is characterized by whole or part-word (sound) repetitions, prolongations and silent blocks that impede the fluent production of speech.

Do you feel that you currently stutter? *

In other words, are you a person who stutters?

STUTTERING PROFILE

Questions in this section are only to be answered by people who stutter.

If you are a person who DOES NOT stutter you have finished the questionnaire. Please check your responses for accuracy and then submit the form.

If you are a PERSON WHO STUTTERS please respond to the following questions, check your responses for accuracy and then submit the form.

How old were you when you started to stutter?

In other words, how old were you at the onset of your stuttering OR how old do your parents tell you that you were?

Please tell us about, if any, the situations in which you feel that you speak more fluently.

Please tell us about, if any, the sounds that you find easier to say fluently than others.

Conversely, please tell us about, if any, the sounds that you find more difficult to say fluently than others.

Have you ever received therapy or special instruction for stuttering from a speech-language pathologist, speech teacher or other professionals?

Please briefly describe each course of therapy.

For example, if you have had therapy at multiple times in your life you might respond as follows: 1. Preschool - treatment once a week with a speech-language pathologist for one year 2. School age - treatment once a month with a speech-language pathologist off and on for 3 years 3. College - attended an intensive program

In total, how many years have you had stuttering therapy?

How many total hours of stuttering therapy do you think you have had in your lifetime?

When did your most recent therapy end?

How does your stuttering today compare to your typical day? Is your stuttering today (please choose one):

Please tell us who also stutters, if anyone, in your immediate family?

Check all that apply.

- ☐ Mother
- ☐ Father
- ☐ Sister(s)
- ☐ Brother(s)

Please tell us who also stutters, if anyone, on your father's side of the family.

Check all that apply.

- ☐ Grandfather
- ☐ Grandmother
- ☐ Aunt
- ☐ Uncle
- ☐ Niece
- ☐ Nephew
- ☐ Cousin

Please tell us who also stutters, if anyone, on your mother's side of the family.

Check all that apply.

- ☐ Grandfather
- ☐ Grandmother

- [ ] Aunt
- [ ] Uncle
- [ ] Niece
- [ ] Nephew
- [ ] Cousin

Is there anything else that you would like to tell us about your stuttering that we have not asked?

Submit

Never submit passwords through Google Forms.

100%: You made it.

Powered by Google Forms

This form was created inside of University of Alberta.

Report Abuse - Terms of Service - Additional Terms

A2 – Study Consent Form (Control)

UNIVERSITY OF ALBERTA

PARTICIPANT CONSENT FORM (CONTROL)

Title of Study: Magnetic resonance imaging of the neural network for speech production

Investigators: *Jacqueline Cummine, PhD (jcummine@ualberta.ca)*
Deryk Beal, PhD (dbeal@hollandbloorview.ca)

Research/Study Coordinator: *Ehsan Misaghi (780-492-7895, misaghi@ualberta.ca)*

Why am I being asked to take part in this research study?
You are being asked to be in this study because you are a healthy adult with normal speech production. The study aims to understand the brain network for speech production. Before you make a decision one of the researchers will go over this form with you. You are encouraged to ask questions if you feel anything needs to be made clearer. You will be given a copy of this form for your records.

What is the reason for doing the study?
We are trying to understand the brain network for speech production. We plan to compare normal control data with data from people with speech disorders. The information that we collect will help us understand the causes of speech disorders in the brain and potentially improve treatments for people with these disorders.

What will I be asked to do?
You will participate in a research experiment that takes less than 3 hours to complete.

We will administer a routine screening to assess your health history, receptive vocabulary, cognitive abilities, motor skills and speech fluency. The screening involves answering questions about your health and development and playing simple games on a computer as well as identifying pictures on a page in response to verbal prompts from the researcher. You will also be speaking and reading aloud while being audio and video recorded.

You will then undergo a magnetic resonance imaging (MRI) examination. You will rest lying down on your back inside the central tube (or bore) of the MRI. It is very important that you lie still while the MRI is operating, as moving will render the images of your brain unusable. We will supply earplugs and ear protectors to muffle the loud noises produced by the scanner. The scan will take about an hour.

What are the risks and discomforts?
A potential risk of participation in this study is that the routine screening may detect speech, language, or hearing concerns that may require further clinical investigation. If the routine screening reveals clinically significant speech, language or hearing concerns, Dr. Beal will discuss the concerns with you and advise you on the necessary next steps for pursuing a formal clinical assessment.

The MRI exam has no known harmful effects assuming that you have none of the risk factors

listed on the MRI screening form. *Great care should be taken in reviewing the MRI screening form since items on that list could be hazardous to your safety in the MRI room.* There is the possibility that you might feel claustrophobic in the scanner. However, if you wish to leave the scanner at any time all you have to do is squeeze the ball/button that we provide for you. The MRI will be quite loud during scanning, but if it is uncomfortably loud, tell us right away and we will stop the scan.

There are no other known risks or discomforts associated with this research study. It is not possible to know all of the risks that may happen in a study, but the researchers have taken all reasonable safeguards to minimize any known risks to a study participant.

What are the benefits to me?
There may be no immediate benefit to you for participating. The results of this study may benefit people with stuttering in the future, as this research aims to advance knowledge in the area of stuttering and improve treatment outcomes.

Do I have to take part in the study?
Participating in this study is your choice. If you change your mind about participating once the study has started you can stop being in the study at any time, and it will in no way affect the care or treatment that you are entitled to.

Can my participation in the study end early?
In addition to you being able to stop the study at any time, the research coordinator may withdraw you from this study if you do not meet the criteria for further participation.

Will I be paid to be in the research?
All participants will be given a $25.00 gift certificate as compensation for parking and other expenses incurred while participating in this study.

Will my information be kept private?
All personal information will remain confidential. The study data will be securely stored in a locked cabinet in Dr. Cummine's locked laboratory at the University of Alberta, to which only the study team will have access. Digital data will be encrypted and password-protected and stored on a password-protected computer to which only study team members will have access. All data, save for consent forms and the master list, will contain only a unique identifier that can only be traced back to the participants via the encrypted and password protected master list accessible only to the study team members. We will keep the data indefinitely. We may use the anonymized data for future research projects. At the time that the data is no longer required, it will be securely destroyed. Published study results will only involve unidentifiable numerical data.

What if I have questions?
If you have any questions about the research now or later, please contact Dr. Jacqueline Cummine (jcummine@ualberta.ca) or Ehsan Misaghi (780-492-7895, misaghi@ualberta.ca).

If you have any questions regarding your rights as a research participant, you may contact the Health Research Ethics Board at 780-492-2615. This office has no affiliation with the study investigators.

The study is being sponsored by the Faculty of Rehabilitation Medicine at the University of Alberta. The institution and researchers are getting money from the study sponsor to cover the costs of doing this study. You are entitled to request any details concerning this compensation from the Principal Investigator.

UNIVERSITY OF ALBERTA

CONSENT

Title of Study: Magnetic resonance imaging of the neural network for speech production

Principal Investigator(s): Dr. Jacqueline Cummine, PhD **Phone Number(s): 780-492-7895**
Study Coordinator: Ehsan Misaghi **misaghi@ualberta.ca**

	Yes	No
Do you understand that you have been asked to be in a research study?	☐	☐
Have you read and received a copy of the attached Information Sheet?	☐	☐
Do you understand the benefits and risks involved in taking part in this research study?	☐	☐
Have you had an opportunity to ask questions and discuss this study?	☐	☐
Do you understand that you are free to leave the study at any time, without having to give a reason and without affecting your future medical care?	☐	☐
Has the issue of confidentiality been explained to you?	☐	☐
Do you understand who will have access to the information that you provide?	☐	☐
Do you understand that you will be audio and video recorded while reading aloud?	☐	☐
Do you agree to allow your recorded speech sample to be used by the principal investigator for teaching purposes, such as training students and scientists about speech disorders?	☐	☐
Do you agree to be contacted in the future for the purpose of determining your willingness to participate in follow-up research to the current study?	☐	☐

Who explained this study to you? _____

I agree to take part in this study:

Signature of Research Participant _____

(Printed Name) _____

Date _____

I believe that the person signing this form understands what is involved in the study and voluntarily agrees to participate.

Signature of Investigator or Designee _____ Date _____

THE INFORMATION SHEET MUST BE ATTACHED TO THIS CONSENT FORM AND A COPY GIVEN TO THE RESEARCH PARTICIPANT

A3 – Study Consent Form (AWS)

UNIVERSITY OF ALBERTA

PARTICIPANT CONSENT FORM (PATIENT)

Title of Study: Magnetic resonance imaging of the neural network for speech production

Investigators: *Jacqueline Cummine, PhD (jcummine@ualberta.ca)*
Deryk Beal, PhD (dbeal@hollandbloorview.ca)

Research/Study Coordinator: *Ehsan Misaghi (780-492-7895, misaghi@ualberta.ca)*

Why am I being asked to take part in this research study?
You are being asked to be in this study because you are a person who stutters. The study aims to understand the brain network for speech production and if it differs in people who stutter. Before you make a decision one of the researchers will go over this form with you. You are encouraged to ask questions if you feel anything needs to be made clearer. You will be given a copy of this form for your records.

What is the reason for doing the study?
We are trying to understand the brain network for speech production and how it may differ in people who stutter. We plan to compare control data from people with typical speech with data from people with speech disorders. The information that we collect will help us understand the causes of speech disorders in the brain and potentially improve treatments for people with these disorders.

What will I be asked to do?
You will participate in a research experiment that takes less than 3 hours to complete.

We will administer a routine screening to assess your health history, receptive vocabulary, cognitive abilities, motor skills and speech fluency. The screening involves answering questions about your health and development and playing simple games on a computer as well as identifying pictures on a page in response to verbal prompts from the researcher. You will also be speaking and reading aloud while being audio and video recorded.

You will then undergo a magnetic resonance imaging (MRI) examination. You will rest lying down on your back inside the central tube (or bore) of the MRI. It is very important that you lie still while the MRI is operating, as moving will render the images of your brain unusable. We will supply earplugs and ear protectors to muffle the loud noises produced by the scanner. The scan will take about an hour.

What are the risks and discomforts?
A potential risk of participation in this study is that the routine screening may detect speech, language, or hearing concerns that may require further clinical investigation. If the routine screening reveals clinically significant speech, language or hearing concerns, Dr. Beal will discuss the concerns with you and advise you on the necessary next steps for pursuing a formal clinical assessment.

The MRI exam has no known harmful effects assuming that you have none of the risk factors listed on the MRI screening form. *Great care should be taken in reviewing the MRI screening form since items on that list could be hazardous to your safety in the MRI room.* There is the possibility that you might feel claustrophobic in the scanner. However, if you wish to leave the scanner at any time all you have to do is squeeze the ball/button that we provide for you. The MRI will be quite loud during scanning but, if it is uncomfortably loud, tell us right away and we will stop the scan.

There are no other known risks or discomforts associated with this research study. It is not possible to know all of the risks that may happen in a study, but the researchers have taken all reasonable safeguards to minimize any known risks to a study participant.

What are the benefits to me?
There may be no immediate benefit to you for participating. The results of this study may benefit people with stuttering in the future, as this research aims to advance knowledge in the area of stuttering and improve treatment outcomes.

Do I have to take part in the study?
Participating in this study is your choice. If you change your mind about participating once the study has started you can stop being in the study at any time, and it will in no way affect the care or treatment that you are entitled to.

Can my participation in the study end early?
In addition to you being able to stop the study at any time, the research coordinator may withdraw you from this study if you do not meet the criteria for further participation.

Will I be paid to be in the research?
All participants will be given a $25.00 gift certificate as compensation for parking and other expenses incurred while participating in this study.

Will my information be kept private?
All personal information will remain confidential. The study data will be securely stored in a locked cabinet in Dr. Cummine's locked laboratory at the University of Alberta, to which only the study team will have access. Digital data will be encrypted and password-protected and stored on a password-protected computer to which only study team members will have access. All data, save for consent forms and the master list, will contain only a unique identifier that can only be traced back to the participants via the encrypted and password protected master list accessible only to the study team members. We will keep the data indefinitely. We may use the anonymized data for future research projects. At the time that the data is no longer required, it will be securely destroyed. Published study results will only involve unidentifiable numerical data.

What if I have questions?
If you have any questions about the research now or later, please contact Dr. Jacqueline Cummine (jcummine@ualberta.ca) or Ehsan Misaghi (780-492-7895, misaghi@ualberta.ca).

If you have any questions regarding your rights as a research participant, you may contact the Health Research Ethics Board at 780-492-2615. This office has no affiliation with the study investigators.

The study is being sponsored by the Faculty of Rehabilitation Medicine at the University of Alberta. The institution and researchers are getting money from the study sponsor to cover the costs of doing this study. You are entitled to request any details concerning this compensation from the Principal Investigator.

UNIVERSITY OF ALBERTA

CONSENT

Title of Study: Magnetic resonance imaging of the neural network for speech production

Principal Investigator(s): Dr. Jacqueline Cummine, PhD **Phone Number(s): 780-492-7895**
Study Coordinator: Ehsan Misaghi **misaghi@ualberta.ca**

	Yes	No
Do you understand that you have been asked to be in a research study?	☐	☐
Have you read and received a copy of the attached Information Sheet?	☐	☐
Do you understand the benefits and risks involved in taking part in this research study?	☐	☐
Have you had an opportunity to ask questions and discuss this study?	☐	☐
Do you understand that you are free to leave the study at any time, without having to give a reason and without affecting your future medical care?	☐	☐
Has the issue of confidentiality been explained to you?	☐	☐
Do you understand who will have access to the information that you provide?	☐	☐
Do you understand that you will be audio and video recorded while reading and speaking aloud?	☐	☐
Do you agree to allow your recorded speech sample to be used by the principal investigator for teaching purposes, such as training students and scientists about speech disorders?	☐	☐
Do you agree to be contacted in the future for the purpose of determining your willingness to participate in follow-up research to the current study?	☐	☐

Who explained this study to you? _____

I agree to take part in this study:

Signature of Research Participant _____

(Printed Name) _____

Date _____

I believe that the person signing this form understands what is involved in the study and voluntarily agrees to participate.

Signature of Investigator or Designee _____ Date _____

THE INFORMATION SHEET MUST BE ATTACHED TO THIS CONSENT FORM AND A COPY GIVEN TO THE RESEARCH PARTICIPANT

A4 – MRI Screening Form (both AWS and Control)

Alberta Health Services

Patient History and MRI Screening (Male)

Covenant Health

Name: _____ Hospital #: _____

The following items may interfere with your Magnetic Resonance Imaging examination, and some can be potentially hazardous.
Please Indicate if you have the following:

Section 1

Yes	No	
☐	☐	Cardiac Pacemaker / Automatic Defibrillator
☐	☐	Aneurysm Clip(s)
☐	☐	Implanted Insulin Pump
☐	☐	Implanted Drug Infusion Device
☐	☐	Bone Growth or Bio Stimulator
☐	☐	Neurostimulator
☐	☐	Epicardial Leads
☐	☐	Cochlear Implant
☐	☐	Intra-vascular Coils
☐	☐	Swan-Ganz Catheter

Section 2

Yes	No	
☐	☐	Stents
☐	☐	Any type of surgical clip or staple(s)
☐	☐	Heart Valve Prosthesis
☐	☐	Vena Cava Filter
☐	☐	Middle Ear Implant
☐	☐	Penile Prosthesis
☐	☐	Eye Prosthesis
☐	☐	Shrapnel or Bullet
☐	☐	Magnetically operated devices
☐	☐	Wire Sutures
☐	☐	Silver impregnated dressing (Acticoat, Actisorb Plus, Aquacel)

Section 3

Yes	No	
☐	☐	Intraventricular Shunt
☐	☐	Intracranial Pressure Monitor
☐	☐	Wire Mesh
☐	☐	Artificial Limb or Joint
☐	☐	Any orthopedic item(s) (i.e. pins, rods, screws, nails, clips, plates, wire, etc.)
☐	☐	Dentures or any type of removable dental item
☐	☐	Hearing Aid
☐	☐	Tattoos
☐	☐	Body Piercings
☐	☐	Transdermal Patches (i.e. nicotine, nitroglycerine, etc.)

Yes	No	
☐	☐	**Worked as welder, lathe operator, sheet metal worker or any similar occupation that may result in a metallic foreign object in your eyes.**
☐	☐	Have you ever had an endoscopy (gastroscopy/colonoscopy) procedure in 2011 or later and is there any possibility that you have a Metallic Clip

Have you ever had any surgical procedure or operation? ☐ Yes ☐ No

Type _____ Year _____

Type _____ Year _____

Type _____ Year _____

Have you **EVER** had any metal fragments in your eyes, or had an injury to your eyes with metal? ☐ Yes ☐ No

Do you have a history of kidney failure or are you on kidney dialysis? ☐ Yes ☐ No

Patient Weight _____ lb / kg Patient Height _____ in / cm

I have answered the above questions to the best of my ability.
The MRI examination has been explained to me and I have had my questions answered to my satisfaction.

Signature of Patient or Guardian _____ Date _____

Witness / Technologist _____

CH-0186 Aug 2007 **PAGE 1 OF 1**

A5 – Edinburgh Handedness Inventory

Your Initials:_____

Please indicate with a check (✓) your preference in using your left or right hand in the following tasks.

Where the preference is so strong you would never use the other hand, unless absolutely forced to, put two checks (✓✓).

If you are indifferent, put one check in each column (✓ | ✓).

Some of the activities require both hands. In these cases, the part of the task or object for which hand preference is wanted is indicated in parentheses.

Task / Object	Left Hand	Right Hand
1. Writing		
2. Drawing		
3. Throwing		
4. Scissors		
5. Toothbrush		
6. Knife (without fork)		
7. Spoon		
8. Broom (upper hand)		
9. Striking a Match (match)		
10. Opening a Box (lid)		
11. Holding a computer mouse		
12. Holding a Hammer		
Total checks:	LH =	RH =
Cumulative Total	CT = LH + RH =	
Difference	D = RH – LH =	
Result	R = (D / CT) × 100 =	
Interpretation: (Left Handed: R < -40) (Ambidextrous: -40 ≤ R ≤ +40) (Right Handed: R > +40)		